Control of Reactive Batch Distillation Columns via Extents Transformation

Carlos Samuel Méndez Blanco





Control of Reactive Batch Distillation Columns via Extents Transformation

MASTER OF SCIENCE THESIS

For the degree of Master of Science in Systems and Control at Delft University of Technology

Carlos Samuel Méndez Blanco

June 13, 2017

Faculty of Mechanical, Maritime and Materials Engineering (3mE) \cdot Delft University of Technology



The work in this literature survey was done jointly with the Eindhoven University of Technology Control Systems Department. Their cooperation is hereby gratefully acknowledged.





Copyright \odot Delft Center for Systems and Control (DCSC) All rights reserved.

Table of Contents

	Ack	nowledgements	vii
1	Intro	oduction	1
2	Rea	active and Distillation Processes	5
	2-1	Distillation and Reactive Processes	5
	2-2	Reactive Distillation Process	7
3	Exte	ents Transformation for Reaction Systems	17
	3-1	Extents of Reaction	17
	3-2	Variant and Invariant Spaces of Chemical Processes	20
		3-2-1 Inclusion of Energy Balance	24
		3-2-2 Sensitivity Analysis	27
	3-3	Limitations of the extent transformation approach	29
		3-3-1 Span of the chemical species space	30
		3-3-2 Rank deficiency of $[N^\intercal \ W_{in} \ n_0]$	31
	3-4	Linear Parameter-Varying (LPV) state space model	32
		3-4-1 First Approach: Model with Disturbance	33
		3-4-2 Second Approach: Change of variable Z	35
	3-5	Control based on the LPV models	38
		3-5-1 Case 1: Control based on model with external disturbance	38
		3-5-2 Case 2: Control with change of variable Z	42
4	Exte	ension of the Extent Transformations to Multiphase Reaction Systems	49
	4-1	Continuous Gas-Liquid Reaction Systems	49
	4-2	Batch Gas-Liquid Reaction Systems	52
	4-3	Case study	55

Table of Contents

5		Acronyms	79 85
	4-3-4	Nonlinear Model Predictive Control for the Reactive Batch Distillation Process	74
	4-3-3	Linear Model Predictive Control for the Reactive Batch Distillation Process	64
	4-3-2	State-feedback linearization	61
	4-3-1	Development of the model for control	58

List of Figures

1-1	Thesis structuring flowchart	3
2-1	Schematic diagram of a continuous distillation column. (Skogestad, 2008)	6
2-2	Different types of reactors. (Skogestad, 2008)	7
2-3	Traveling concentration fronts in a nonreactive distillation column after a stepwise increase of the reflux. (Grüner and Kienle, 2004)	8
2-4	Stage equilibrium model (Perry and Green, 2008)	9
3-1	Three-way decomposition (linear transformation) (Amrhein et al., 2010)	23
3-2	Evolution of number of moles per species in the CSTR	24
3-3	Extents of reactions in the CSTR	25
3-4	Extents of inlet in the CSTR	26
3-5	Evolution of number of moles per species in the CSTR	27
3-6	Evolution of internal temperature in the CSTR	28
3-7	Extents of reactions in the CSTR	29
3-8	Extents of inlet in the CSTR	30
3-9	$\frac{\partial f}{\partial x_r}$ gradient surface to changes in T and $x_{in,b}$ with $x_r=1$ kmol and $x_{in,a}=1$ kg	31
3-10	$\frac{\partial f}{\partial x_r}$ gradient surface to changes in T and $x_{in,b}$ with $x_r=1$ kmol and $x_{in,a}=20~\mathrm{kg}$	32
3-11	Extents of inlet	33
3-12	Reconstructed moles	34
3-13	Extents of inlet	35
3-14	Reconstructed moles	36
3-15	Comparison of nonlinear model and LPV system response to reference changes .	37
3-16	Control based on model with external disturbance	40
3-17	LPV-model-based LQR controllers for reference tracking	42
3-18	LPV-model-based LQR controllers control actions	43

iv List of Figures

3-19	LPV-model-based LQR controllers for reference tracking	45
3-20	LPV-model-based LQR controllers control actions	46
3-21	LPV-model-based LQR controllers for reference tracking	48
3-22	LPV-model-based LQR controllers control actions	48
4-1	Representation of the gas-liquid reaction system (Bhatt et al., 2010)	50
4-2	Representation of the reactive distillation column (Shah et al., 2011)	56
4-3	Comparision between the formulations of Z	60
4-4	Comparision between the nonlinear plant dynamics and the reproduction done by the LPV model	63
4-5	Reference trajectories of the distillate composition and reactor temperature	68
4-6	Block diagram of the reactive batch distillation column control loop	70
4-7	Controlled response of the distilled water composition at the accumulator stage (blue solid line) vs. Distilled water composition reference trajectory (red dashed line). Left to right: 1. Full view, 2. Transient response, 3. Tracking over optimal reference composition, 4. Final composition	70
4-8	Controlled response of the reactor temperature (blue solid line) vs. Temperature reference trajectory (red dashed line). Left to right: 1. Full view, 2. Transient response, 3. Tracking over optimal reference temperature, 4. Final temperature.	71
4-9	Control actions generated by the linear model-predictive controller. Left side of the dashed line: P controller action. Right side of the dashed line: MPC controller action.	71
4-10	Moles of water and propylene glycol in the distillate accumulator	72
4-11	Moles of reactants and products in the reactor	73
4-12	Scheme of nonlinear optimization procedure assuming piecewise constant inputs .	75
4-13	Controlled response of the distilled water composition at the accumulator stage (blue solid line) vs. Distilled water composition reference trajectory (red dashed line)	76
4-14	Controlled response of the reactor temperature (blue solid line) vs. Temperature reference trajectory (red dashed line)	77
4-15	Control actions generated by the nonlinear model-predictive controller	77
4-16	Moles of water and propylene glycol in the distillate accumulator	78
4-17	Moles of reactants and products in the reactor	78

List of Tables

2-1	Most common equilibrium models	10
2-2	Summary of control of reactive distillation of Poly(polypropylene/hexylene) -terephthalate	11
2-3	Summary of control of reactive distillation of Methyl Tert-Butyl Ether (MTBE)	11
2-4	Summary of control of reactive distillation of Ethyl Acetate	12
2-5	Summary of control of reactive distillation of Ethyl Tert-Butyl Ether (ETBE) .	13
2-6	Summary of control of reactive distillation of Methyl Acetate	14
2-7	Summary of control of reactive distillation of Ethylene Glycol	14
2-8	Summary of control of reactive distillation of Methacrylic Anhydride	15
4-1	Change of input bound with respect to the parameters of the plant	67

vi List of Tables

Acknowledgements

I would like to thank to Dr. L. Özkan for giving me the opportunity to come to TU Eindhoven to work on this project. For her interest and valuable input throughout the development of this thesis.

I would also would like to thank Dr. A. Márquez, my daily supervisor, for his unconditional support and help with his advice and encouraging attitude; for having shown me the beauty of control engineering and awaken in me the taste for research and innovative ideas.

To parents and my sister, who always stood by me, pushing me to follow my passion. To my family, who was always there supporting me along the way. To my best friend Camila, with whom I had several interesting debates about the content of this thesis. And to all of those who remained by my side knowing I was pursuing my dream.

Gracias totales.

Delft, University of Technology June 13, 2017 Carlos Samuel Méndez Blanco

viii Acknowledgements

Chapter 1

Introduction

Nowadays in large-scale process industry, high purity of products is not only desired but crucial. Products must meet high-purity standards to conform with market and customers' requirements. Attaining such quality standards, and at the same time, produce sufficiently to satisfy the demand, are typical challenges chemical industry faces. These processes allow the manufacturing of new materials in timely and efficient manner.

In process industry, reaction and distillation processes are essential to achieve these objectives. The former transforms raw material into added-value products that can serve a myriad of purposes. The latter, on the other hand, separates and purifies the products obtained through reaction to conform to the quality requirements.

Generally, these two processes are carried out in different units. However, there are production schemes where it is convenient and possible to combine both of them. This is done to overcome certain disadvantages and/or limitations that each operation unit possess. The combination of a reactor and a distillation column results in a reactive distillation (RD) column. This unit operation has many advantages that motivate its implementation in industry. They are:

- 1. For consecutive reactions in which the desired product is formed in an intermediate step, excess reactant can be used to suppress additional series reactions.
- 2. By Le Chatelier's principle, the reaction can be driven to completion by removal of one or more of the products as they are formed.
- 3. Azeotrope breakage by altering or eliminating the condition for azeotrope formation in the reaction zone.
- 4. Reactants can be kept much closer to stoichiometric proportions in a reactive distillation.
- 5. Reaction is used to convert the species to components that are more easily distilled.
- 6. Conversion and selectivity often can be improved significantly with much lower reactant inventories.

2 Introduction

- 7. In a reactive batch distillation specifications can be achieved more tightly.
- 8. It has the potential to lower the capital and energy cost of the operation.

Despite these advantages, reactive batch distillation processes are complex, nonlinear and due to interaction of reaction and separation processes in one unit, they have limited operational flexibility. Therefore, achieving tight composition control is a challenge and requires good understanding of the process and the right control strategy.

Modeling reactive batch distillation column has been very well studied topic. These models are generally have a set of differential algebraic equations which are in turn very complex and highly nonlinear models, described in terms of differential and algebraic equations, which can yield a very accurate description of the process dynamics. Nevertheless, this kind of models are inconvenient when it comes to process monitoring and model-based control implementation; controllers and estimators require simpler models to perform reliably and efficiently.

The simplest proposed control methods rely on very simplified models that lead to suboptimal operation (use of PID controllers), with many parameters in the model fixed around an operating point or calculated via some unrealistic model assumption. Additionally, more accurate model-based controllers are normally not implementable in real processes, mainly due to the fact that these are designed on much more complex models. This results in unfeasible techniques that are computationally expensive. This situation poses a trade-off problem between model accuracy and control efficiency and implementability.

This trade-off problem needs to be tackled because rigorous models describe a wider range of process operation and large amount of process knowledge which is very valuable for real-time model-based operations. The (batch) reactive distillation control and monitoring is currently an open topic in industry processes and it still has a lot of room for improvement and development. The aforementioned trade-off brings forward the question:

can we find a way to have the information improved by the rigorous model, at the same time, develop simple model-based controllers for these complex models?

This problem poses a real challenge, which is to find a way to obtain both of these good features.

This thesis work is organized with the following structure. A flowchart of the structure of the thesis is also presented in figure 1-1.

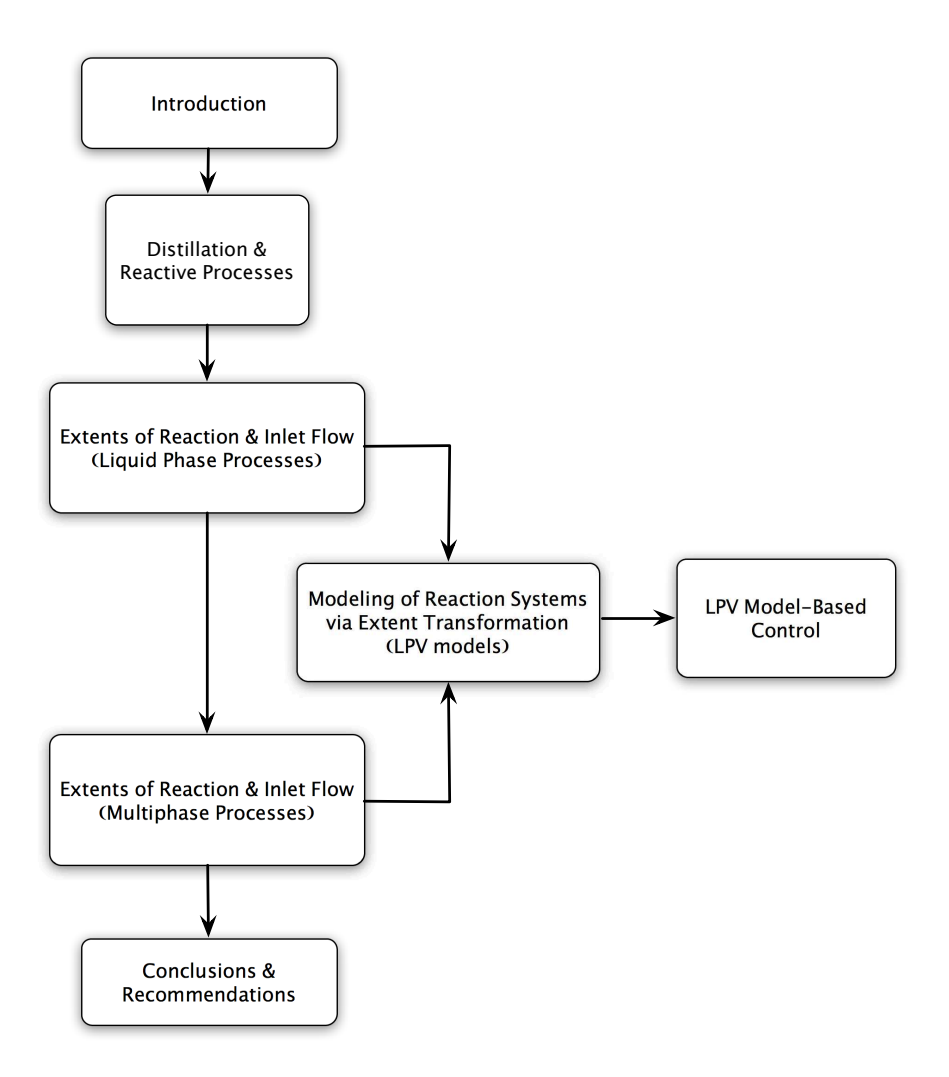


Figure 1-1: Thesis structuring flowchart

- Chapter 2 gives brief overview and explanation of the distillation and reactive processes, its fundamental mathematical description in terms of partial differential equations as well as the standard simplifications for modeling and simulation of these two.
- Chapter 3 introduces the concept of extent reaction for liquid-phase batch reactors. It also develops the existing concept of variants, invariants and extents of reaction and inlet flow for reaction systems with inlet streams of material (semi-batch and continuous stirred-tank (CSTR) reactors). Additionally, it presents two basic case studies: isothermal and temperature-varying CSTR's, where the extent transformation approach is utilized to simplify their rigorous modeling. The advantages and limitations of this transformation are also discussed in detail. Finally, it is shown that control models obtained via this approach result in linear parameter-varying systems.
- Chapter 4 extends the underlying mathematical approach to continuous multiphase reaction system and to the more complicated batch case. Conditions for existence, advantages and limitations are explained. Ultimately, the extent transformation for

4 Introduction

multiphase reaction system is used to develop a model-based control strategy for a reactive batch distillation column on a polyesterification process.

• Chapter 5 presents the conclusions of this thesis, as well as recommendations and possible future work that could complement the results obtained in this work.

Reactive and Distillation Processes

Distillation and chemical reactive processes are standard unit operations in process industry. They are governed by complex dynamics that are normally expressed in terms of partial differential equations with many parameters involved in the evolution of the system. The infinite nature of its dimensionality along with its mathematical complexity makes of these processes difficult to deal with. Nevertheless, there exists approaches where this infinite-dimensionality issue can be tackled; equilibrium models help reduce the system to a finite-dimension problem in terms of algebraic differential equations. In this chapter, a brief introduction to the reaction and distillation process will be addressed as well as its governing dynamics, parameters and models. This is also explained for the intensified version, the reactive distillation column.

2-1 Distillation and Reactive Processes

The distillation process is a well-known industrial separation process. As a general principle, separation operations achieve their objectives by the creation of two or more zones with different operating conditions, such as temperature, pressure, composition and/or phase (Perry and Green, 2008). In the vast majority of cases, the chemical species involved in the separation behave differently to these conditions, hence the separation is performed as the system approaches its equilibrium. In the case of distillation, the process of separating chemical components from a mixture (or feed F) into a "light" product (distillate D) and a "heavy" product (bottom product B), is performed through selective evaporation and condensation of the liquid and vapor phases; hence, exploiting differences in the volatility of components (Skogestad, 2008). In figure 2-1, a schematic representation of a distillation column is shown.

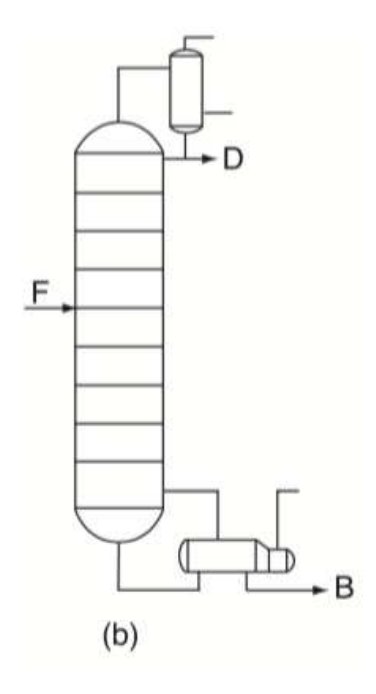


Figure 2-1: Schematic diagram of a continuous distillation column. (Skogestad, 2008)

Normally, this process is carried in a distillation column and can be operated continuously or in batch mode. The mode of operation depends on many factors and constraints like scale, target compositions or physical characteristic of the feed (Perry and Green, 2008).

- Batch Distillation: The feed or mixture is charged at the bottom of the column as a batch and heated; the distillate is obtained at the top of the column as the process progresses. The remaining liquid or residue in the bottom at the end of the operation is the "heavy" product (Skogestad, 2008).
- Continuous Distillation: The feed is continuous and there is withdrawal from both top and bottom section of the column. Generally, it consists of the following sub-units: Two trayed or packed column sections with the feed entering between them, two heat exchangers (reboiler and condenser), two holdup vessels (condenser drum and reboiler sump) and a splitter for the reflux. The upward vapor flow is generated by heating the bottom section at high temperature with the reboiler, which evaporates parts of the liquid; the less volatile components do not vaporize and are drawn out continuously. The downward liquid flow is generated by cooling the top section with the condenser, and returning a fraction of the condensed liquid as reflux to improve mass and heat transfer between the phases; the rest of the condensed liquid is drawn out as distillate (Skogestad, 2008).

On the other hand, a chemical reactor is a controlled volume in which a chemical conversion occurs in a safe and controllable manner (Perry and Green, 2008). These chemical reactions are responsible for the generation of desired products and some by-products. The latter are usually separated from the former by means of, for example, the distillation process. There

are various types of reactors: continuous-stirred tank reactor, plug-flow reactor and batch reactor, etc. The schematic representations of each case are shown in figure 2-2.

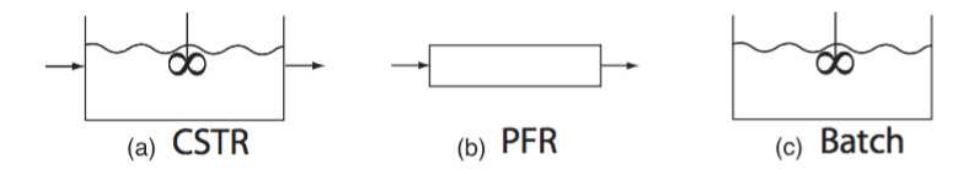


Figure 2-2: Different types of reactors. (Skogestad, 2008)

2-2 Reactive Distillation Process

"Reactive distillation (RD) is a process in which a chemical reaction and distillation (fractionation of reactants and products) occur simultaneously in one single apparatus. Reactive distillation belongs to the so-called process-intensification technologies" (Sakuth et al., 2008).

Additionally, a typical implementation of reactive distillation columns (just like in non-reactive distillation or reaction alone) is under batch regime: Batch distillation is used in the chemical industry for the production of small amounts of products with high added value (Sørensen and Skogestad, 1996). Batch reactors, on the other hand, allow for tightly controlled reaction conditions and scaling of the operation more easily than continuous-time operations, and thus, obtaining desired products with high purity and adjusting to market demands (Bonvin, 2006). The combination of a batch reactor with a distillation column is denominated reactive batch distillation column (RBD).

Reactive distillation is a complex process where many physical phenomena occur. Concentration rates evolve not only in time but also in space and it is heavily dependent on mass transfer and reaction kinetics, which are described by nonlinear functions. A general and rigorous model that describe the dynamic behavior of this process can be in the following form:

$$\frac{\partial x_i}{\partial t} - \frac{\partial x_i}{\partial z} - D_x \frac{\partial^2 x_i}{\partial z^2} = -\mathcal{J}(x_i, y_i) + r(x_i, T)$$
 (2-1)

$$\varrho \frac{\partial y_i}{\partial t} - \frac{1}{A} \frac{\partial y_i}{\partial z} - D_y \frac{\partial^2 y_i}{\partial z^2} = \mathcal{J}(x_i, y_i)$$
(2-2)

$$\alpha \frac{\partial^2 T}{\partial z^2} - \bar{v} \frac{\partial T}{\partial z} - (-\Delta H_{rxn} r(x_i, T)) + Q_{in} = \rho C_p \frac{\partial T}{\partial t}$$
(2-3)

where, t is the time coordinate and z is the spatial coordinate; x_i and y_i are the liquid and vapor concentration of the i-th chemical component in the process respectively; D_x and D_y diffusion coefficients; $\mathcal{J}(x_i, y_i)$ is the mass transfer rate; $r(x_i, T)$ is the reaction rate; T is the mixture temperature, α is the thermal diffusivity and \bar{v} the average velocity that the quantity is moving with; ΔH_{rxn} is the reaction heat; Q_{in} is the heat flow; ρ and C_p are the mixture density and the mixture heat capacity, respectively.

With $\varrho = \frac{y_i}{x_i}$ and $A = \frac{L}{V}$ where L and V are liquid phase and vapor phase molar flows respectively. L can be calculated with the knowledge of the column internal design hydraulics; however, V is generally much more complicated to calculate. The terms accounting for reaction rates $r(x_i, T)$ and reaction heat ΔH_{rxn} , are set to zero in case of a non-reactive distillation process.

As seen in (2-1), (2-2) and (2-3), the rigorous model is described by a set of partial differential equations which are nonlinear and have a high computational cost. This set of equations describe the profiles in terms of a propagating wave as depicted in figure 2-3.

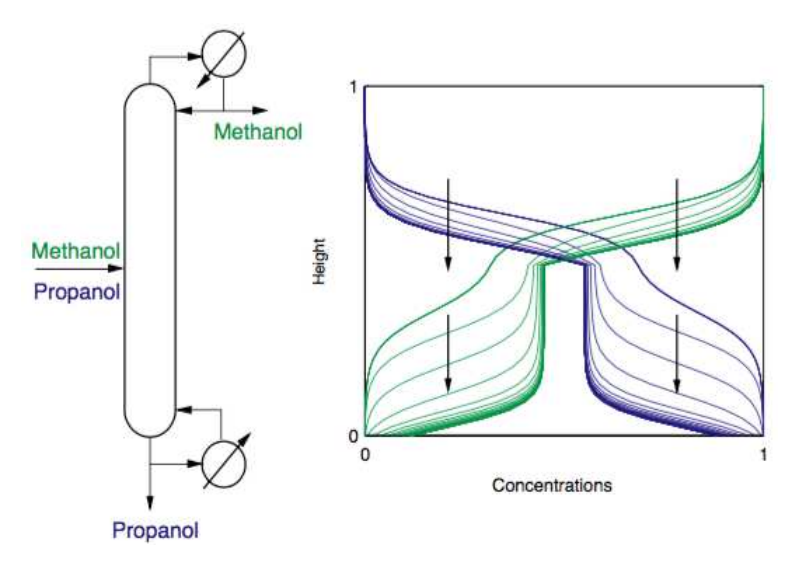


Figure 2-3: Traveling concentration fronts in a nonreactive distillation column after a stepwise increase of the reflux. (Grüner and Kienle, 2004)

Thus, to simplify the model several assumptions are introduced. These simplifications serve to discretrize the spatial-coordinate in the model, allowing the reduction of an infinite-dimension system to one of finite-dimension. Some of these are:

• Reactive dynamics: Mole balance

$$\dot{n} = \mathcal{V}(t)N^{\mathsf{T}}r(t) + W_{in,l}u_{in}(t) - \frac{u_{out}(t)}{m(t)}n(t)$$
(2-4)

where \cdot represents the derivative with respect to time, n is the number of moles, \mathcal{V} is the reaction mixture volume; u_{in} and u_{out} are the inlet and outlet mass flows; m is the reacting mixture mass; N is the stoichiometric coefficient matrix and $W_{in,l}$ is the inlet composition matrix.

• Distillation dynamics: Molar flow balance (feed tray) assuming stages in equilibrium

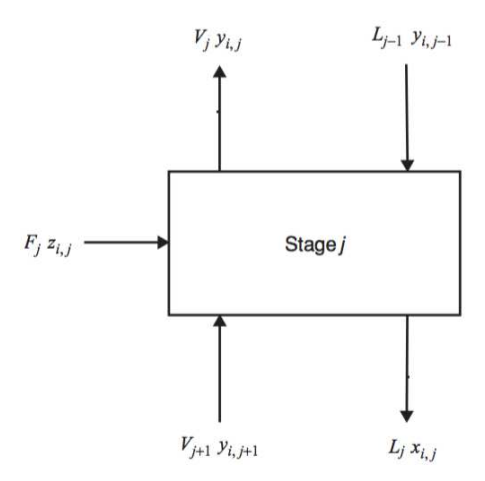


Figure 2-4: Stage equilibrium model (Perry and Green, 2008)

$$\frac{dM_j x_{j,i}}{dt} = F_j f_{j,i} + L_{j-1} x_{j-1,i} + V_{j+1} y_{j+1,i} - (L_j x_{j,i} + V_j y_{j,i})$$

where M is the total molar holdup, F, L and V are the total molar flow going into the column, the liquid molar flow and the vapor molar flow respectively, f_i , x_i and y_i are the compositions in the feed, in the liquid phase and in the gas phase respectively for the i-th component of the mixture at the j-th stage.

• Mass transfer

$$\begin{cases} \mathcal{J} = K_l(x - x^*) \\ \mathcal{J} = K_g(y^* - y) \end{cases}$$

where K_l and K_g are the overall mass transfer coefficient based on the liquid and gas phase concentrations respectively. x and y are the bulk concentrations in liquid and gas phase; and x^* and y^* are the liquid and gas equilibrium concentrations respectively as well.

• Equilibrium models

The bulk concentrations can be measured but equilibrium concentrations are calculated from mixture phase equilibrium theories or laws, generally called vapor-liquid equilibrium (VLE). Some of the most used are presented in table 2-1

Model	Equation
Henry's Law (Ideal mixtures)	$yP = \sum_{i}^{N} \mathcal{H}_{i} x_{i}$
Raoult's Law (Ideal mixture)	$yP = \sum_{i}^{N} P_{sat_i} x_i$
Raoult's Law $\phi - \gamma$ model (Non-ideal mixtures)	$y\phi P = \sum_{i}^{N} P_{sat_i} \gamma_i x_i$

Table 2-1: Most common equilibrium models

Where \mathcal{H} is the Henry's coefficient, P is the total pressure of the system, P_{sat_i} is the saturation pressure of the *i*-th component. ϕ is the gas fugacity coefficient, and γ , the liquid activity coefficient.

For the activity coefficient γ calculation, there exists many models to calculate it such as Van Laar's model, Wilson's model, Non-random Two-liquid (NRTL) model, UNIversal QUAChemical (UNIQUAC) model, etc., which all are described by algebraic equations.

As seen, even the simplifications done on the rigorous model of the reactive distillation column yield many ordinary differential and algebraic equations which still results in a very complex system. Therefore, it becomes of great relevance to revise the modeling approaches available in literature to obtain process models suitable for online implementation of control and model-based operation technology.

Several approaches have been studied in modeling, and control of the reactive distillation process. They are presented in tables (2-2)–(2-8). Additionally, they have been organized by the product to be synthesized:

Master of Science Thesis

Table 2-2: Summary of control of reactive distillation of Poly(polypropylene/hexylene)-terephthalate

Controller Used	Parameters Controlled	Achievements	References
Conventional SISO PI controllers using linearization of operating trajectory and RGA analysis	Distillate composition and reactor temperature	Investigate the possible difficulties in controlling a batch reactive distillation process and present simple alternatives for control.	Sørensen and Skogestad (1996)
Sequential Quadratic Programming optimization of set points and conventional single-input/single-output (SISO) proportional-integral (PI) controllers	Product purity, temperature with optimal heat duty	Improve online performance of reactive batch distillation column control by implementation on optimal policies and simple feedback control loops.	Sørensen et al. (1996)

Table 2-3: Summary of control of reactive distillation of **Methyl Tert-Butyl Ether** (MTBE)

Controller Used	Parameters Controlled	Achievements	References
PI controller	Feed composition	Control over feed stoichiometry to avoid an excess of methanol	Bartlett and Wahnschafft (1999)
PI controller with relay feed- back test	Product purity and reactant conversion	99% purity of distillate product	Wang et al. (2003)
PI controller with relay feed- back test	Top and bottom product purity	94.36% conversion, 94% purity (top product), 94% purity (bottom product)	Wang et al. (2003)

12

Table 2-4: Summary of control of reactive distillation of Ethyl Acetate

Controller Used	Parameters Controlled	Achievements	References
Output feedback linearization with PID controllers and anti- reset windup scheme	Distillate composition	Circumvent the lack of robustness in model-dependent optimal policies and exploit the advantages of output feedback linearization.	Monroy- Loperena and Álvarez Ramírez (2000)
Reduced order nonlinear model-based control	Product purity and reactor temperature	Minimize the computational complexity by using a reduced order fundamental model	Balasubramhanya and Doyle III (2000)
Model-based linear and non- linear state feedback con- trollers along with conven- tional SISO PI controllers	Reactant conversion, product purity	Performance of the nonlinear controller is superior over both the linear controller and the conventional PI controller	Vora and Daoutidis (2001)
Nonlinear model predictive control (NMPC)	Overhead and bottoms composition	NLMPC was found to provide signifi- cantly better control performance than PI controller	Kawathekar and Riggs (2007)
Proportional-Integral- Derivative (PID) controller	Product purity	Introduce alternatives to improve control of an ethyl acetate (EtAc) reactive distillation process. (99.78 wt% purity)	Lee et al. (2007)
Decentralized PI controller with Tyreus-Luyben tuning method	Pressure, temperature, product purity	Design of side reactor configuration to facilitate maintenance compared to conventional RD. (99% purity)	Tsai et al. (2008)
PID controller	EtAc purity in the distillate	99.78 mol% EtAc purity	Chien et al. (2008)
Adaptive control	Product purity	Control strategy of a batch reactive rectifier using an adaptive observer. (93.44 mol % purity)	Jana and Adari (2009)
Inferential control	Product purity	Control strategy of a batch reactive rectifier using an artificial neural network (ANN) observer. (97.96% purity)	Prakash et al. (2011)

Master of Science Thesis

 Table 2-5:
 Summary of control of reactive distillation of Ethyl Tert-Butyl Ether (ETBE)

Controller Used	Parameters Controlled	Achievements	References
Inferential controller	Product purity and conversion	Conversion 97.7%, distillate product purity 96.6%	Sneesby et al. (1997)
Linear (PI) controller	Product purity and conversion	Conversion 96.6%, distillate product purity 96.9%	Sneesby et al. (1999)
PI controllers tuned using the Tyreus-Luyben tuning method	Product composition	Double-feed system requires internal composition control to balance the stoichiometry, along with temperature control to maintain product purity. 85% product purity	Al-Arfaj and Luyben (2000)
PI controller and linear model predictive controller	Product purity and reactant conversion	The model predictive controller was able to handle the process interactions well and was found to be very efficient for disturbance rejection and set-point tracking.	(Khaledi and Young, 2005)
Pattern-based predictive control incorporated with conventional PI control	Distillate product purity	98% conversion, 90% purity	Tian et al. (2003)
Decentralized PI controller and constrained MPC	Isobutene conversion and ETBE purity	The control performance was discussed to handle the nonlinearity and reduce the unwanted variability. (97.87% Isobutylene conversion, 93.96% product purity	Athimathi and Rad- hakrishnan (2006)
Adaptive PI control strategies: Nonlinear PI (NPI) and model gain scheduling (MGS) control	One point control (product purity)	Recommended model-based controller for the control of a reactive distillation pro- cess, as it is effective for both set point and load disturbance rejection.	Bisowarno et al. (2003)

Table 2-6: Summary of control of reactive distillation of Methyl Acetate

Controller Used	Parameters Controlled	Achievements	References
PI controllers tuned using the Tyreus-Luyben tuning method	Tray temperature and distillate product purity	99.2% distillate purity	Al-Arfaj and Luyben (2002a)
Nonlinear predictive control using a neural network model	Distillate product purity	Neural network-based nonlinear controller obtain better results than conventional strategies	Engell and Fernholz (2003)
Ratio-control-based temperature controller	Product purity	Tighter product purity control is achieved for a throughput change when the two feeds are fed in ratio.	Kumar and Kaistha (2009)

Table 2-7: Summary of control of reactive distillation of Ethylene Glycol

Controller Used	Parameters Controlled	Achievements	References
Nonlinear inversion based controller	Distillate product purity	Analysis of a non-minimum phase behavior and addressed in the design of a non-linear inversion based controller	Kumar and Daoutidis (1999)
PI controller	Product purity	Proposal of a new concept for robust stabilization	Monroy- Loperena et al. (2000)
PI controller	Distillate product purity	A simple single temperature PI structure provides effective control. (94.8% distillate purity)	Al-Arfaj and Luyben (2002)

Carlos Samuel Méndez Blanco

Master of Science Thesis

Table 2-8: Summary of control of reactive distillation of Methacrylic Anhydride

Controller Used	Parameters Controlled	Achievements	References
		Introduction of a learning technique to overcome uncertainties in the model and achieve perfect tracking in the process	Ahn et al. (2013)

Extents Transformation for Reaction Systems

Chemical reaction is probably the corner stone of industrial chemical processes. Chemical reaction is key to convert raw material into added value products that are important and beneficial for all commercial sectors. However, chemical reaction kinetics are subject to nonlinear behavior commonly described by products of exponential and power functions. Additionally, industrial processes exhibit a wide variety of phenomena, where reaction, flow and phase change dynamics are strongly coupled. In light of this complexity, the extent of reaction is a very useful tool to deal with the nonlinear behavior of the reaction dynamics. Furthermore, the extent approach can be even extended to other process variables to achieve decoupling in the model. This last property is especially attractive for the development of a decoupled structure in models for control. This chapter will introduce the main definitions behind the extent of reaction and the general extent transformation approach as a tool for decoupling process dynamics.

3-1 **Extents of Reaction**

The extents of reaction, denoted with the Greek letter ξ , is a measure of the degree of completion of any reaction. In other words, they quantify the progress of a reaction while it consumes the reactants (Vandezande et al., 2013). It is more precisely defined as:

$$\xi_r = \frac{\text{mol of component s generated or consumed in reaction r}}{\text{stoichiometric coefficient for component s in reaction r}}$$
(3-1)

Consider a reactive system with S species and R_I independent reactions, the extents of reaction are defined mathematically by, as presented in (Amrhein et al., 2010):

$$d\xi_r := \frac{dn_{s,r}}{\nu_{s,r}}, \ \forall s = 1, \dots, S, \ \forall r = 1, \dots, R_I$$
 $\xi_r(0) = 0$ (3-2)

Master of Science Thesis

Carlos Samuel Méndez Blanco

Hence:

$$\nu_{s,r} \int d\xi_r = \int dn_{s,r} \Longrightarrow \nu_{s,r} \xi_r = n_{s,r} \tag{3-3}$$

where $dn_{s,r}$ is the variation of the number of moles of the s-th species involved in the r-th reaction and $\nu_{s,r}$ is the corresponding stoichiometric coefficient. Note that $\nu_{s,r} < 0$ for reactants and $\nu_{s,r} > 0$ for products.

As an example, take the following irreversible reaction for which S=6 and $R_I=1$:

$$2\,\mathrm{NaIO_3} + 3\,\mathrm{Na_2SO_3} + 2\,\mathrm{NaHSO_3} \longrightarrow \mathrm{I_2} + 5\,\mathrm{Na_2SO_4} + \mathrm{H_2O}$$

with initial conditions:

$$n_{0_{\text{NaIO}_3}} = 5 \text{ moles}$$
 $n_{0_{\text{I}_2}} = 0 \text{ moles}$ $n_{0_{\text{Na}_2\text{SO}_3}} = 8 \text{ moles}$ $n_{0_{\text{Na}_2\text{SO}_4}} = 0 \text{ moles}$ $n_{0_{\text{Na}_2\text{SO}_4}} = 0 \text{ moles}$ $n_{0_{\text{H}_2\text{O}}} = 0 \text{ moles}$

Based on the extent definition presented in (3-1), the extent of reaction (ξ_r) only represents the change in the number of moles of a species s in the reaction r; thus, initial conditions n_0 are independent from all the reactions. The evolution of moles in the system defined in terms of the extent of reaction is:

$$n_{\text{NaIO}_3} = 5 - 2\xi_r$$
 $n_{\text{I}_2} = \xi_r$
 $n_{\text{Na}_2\text{SO}_3} = 8 - 3\xi_r$ $n_{\text{Na}_2\text{SO}_4} = 5\xi_r$
 $n_{\text{NaHSO}_3} = 4 - 2\xi_r$ $n_{\text{H}_2\text{O}} = \xi_r$

To find the extent of reaction, we must find the value of ξ_r at which the reactants are entirely consumed. This will give us three different extents of reactions depending of the species. Nonetheless, since there is only one reaction, there is only one extent of reaction as well; ξ_r then corresponds to the lowest value, at which the limiting reactant has consumed entirely and the reaction cannot progress any further.

$$n_{\mathrm{NaIO_3}} = 0 \implies 5 - 2\xi_r = 0 \implies \xi_r = 2,50$$

 $n_{\mathrm{Na_2SO_3}} = 0 \implies 8 - 3\xi_r = 0 \implies \xi_r = 2,66$
 $n_{\mathrm{NaHSO_3}} = 0 \implies 4 - 2\xi_r = 0 \implies \xi_r = 2,00$

We conclude that the limiting reactant is NaHSO₃ as ξ_r obtained its lowest value for that component ($\xi_r = 2$). Substituting this value of the extent of reaction in expressions of the evolution of moles:

3-1 Extents of Reaction 19

$$n_{
m NaIO_3} = 1 \
m mol$$
 $n_{
m I_2} = 2 \
m moles$ $n_{
m Na_2SO_3} = 2 \
m moles$ $n_{
m Na_1SO_3} = 0 \
m mol$ $n_{
m H_2O} = 2 \
m moles$

As seen, the extent of reaction approach can be applied to chemically reactive systems. Hence, we can exploit its potentiality and utilize it in reactor models to simplify their representation. Cases of batch and semibatch reactors are presented next:

For batch reactors, where there is neither inlet nor outlet streams (u_{out}) , the mole balance is only driven by the reaction and hence:

$$\dot{n}_{s,r} = \nu_{s,r} \mathcal{V}(t) r_r(t) \tag{3-4}$$

Making use of equation (3-2) and remembering that $\xi_{r_0} = 0$, we transform (3-4) into:

$$\nu_{s,r}\dot{\xi}_r = \nu_{s,r}\mathcal{V}(t)r_r(t) \tag{3-5}$$

$$\Longrightarrow \dot{\xi}_r = \mathcal{V}(t)r_r(t) \qquad \qquad \xi_r(0) = 0 \qquad (3-6)$$

On the other hand, when reactions take place in a semibatch reactor with an outlet stream (u_{out}) . The outlet stream removes products and reactants as the reaction progresses. In this case, we can write the mole balance of the s-th species of the r-th reaction as:

$$\dot{n}_{s,r} = \nu_{s,r} \mathcal{V}(t) r_r(t) - \frac{u_{out}(t)}{m(t)} n_{s,r} \qquad n_{s,r}(0) = n_{s,r_0}$$
(3-7)

Combining equations (3-2) with (3-7), we obtain:

$$\nu_{s,r}\dot{\xi}_r = \nu_{s,r}\mathcal{V}(t)r_r(t) - \frac{u_{out}(t)}{m(t)}\nu_{s,r}\xi_r \tag{3-8}$$

$$\Longrightarrow \dot{\xi}_r = \mathcal{V}(t)r_r(t) - \frac{u_{out}(t)}{m(t)}\xi_r \qquad \xi_r(0) = 0$$
 (3-9)

In (3-6) and (3-9), it was shown how the extent of reaction can be directly applied where the evolution of moles in the system is reaction-dependent for a batch and a semibatch reactor, respectively. In the case of a batch reactor, only reaction occurs in the process, then it is straightforward to apply the extent transformation. For a semibatch reactor with outlet stream and no inlet stream, the change in time of material in the process depends on the reaction but also on the fraction of reacting mixture leaving the reactor through the outlet stream. The leaving fraction can be written in terms of the moles in the reactor, which allows to apply extent of reaction directly.

The continuous stirred-tank reactor case was not considered, because the inlet stream is independent of the reaction, thus, the representation in terms of extents of reaction cannot be directly applied. The resulting variable from the transformation would lack physical meaning. This particular case will be addressed in section 3-2.

3-2 Variant and Invariant Spaces of Chemical Processes

Reaction Variants and Invariants

As mentioned in the previous section, the extent of reaction can be applied directly to chemical reaction process where the evolution of moles in time is solely related to the reaction and the amount of reacting mixture. Under this circumstances, system is uniquely driven by the chemical reaction; hence, the dynamic space can be split in two subspaces, namely the reaction variant and reaction invariant. These subspaces are defined next:

Reaction Variant: "Any set \mathcal{R} of R_I linearly independent variables that evolve in the reaction space constitutes a reaction variant space" (Amrhein et al., 2010).

Reaction Invariant: "Any set \mathcal{I} of $S - R_I$ linearly independent variables that evolve in the space orthogonal to the reaction space constitutes a reaction invariant space." (Amrhein et al., 2010)

The reaction variants coincide with the extent of reaction if and only if the initial conditions of the former are strictly zero.

Moreover, if the process contains an inlet stream, then the change in time of moles is affected by two independent dynamics, reaction and inlet flow. Under this situation, the reactor dynamics cannot be expressed in terms of the extent of reaction directly. To circumvent this situation, the concept of extent is extended to extents of reaction and inlet flows

Reaction and Inlet Flow Variants and Invariants

Consider the mole balance equation for a continuous-stirred tank reactor CSTR with S species, R_I independent reactions, p independent inlet flows and one outlet flow, given by:

$$\dot{n} = \mathcal{V}(t)N^{\mathsf{T}}r(t) + W_{in}u_{in}(t) - \frac{u_{out}(t)}{m(t)}n(t) \quad n(0) = n_0$$
 (3-10)

where n is the number of moles, \mathcal{V} is the reaction mixture volume; r is the $R_I \times 1$ reaction kinetics vector; u_{in} and u_{out} are the inlet and outlet mass flows; m is the reacting mixture mass; N is the $R_I \times S$ stoichiometric coefficient matrix and W_{in} is the $S \times p$ inlet composition matrix defined as $W_{in} = M_w^{-1}W_{in}$; M_w is the $S \times S$ diagonal molecular weight matrix and w_{in} the $S \times p$ matrix of weight fraction.

Equation 3-10 is nonlinear due to the reaction kinetics contained in the vector r(t). One could find a linear transformation \mathcal{T} such that the system can be re-expressed in terms of new states that each of them only evolves with respect to the reaction and the inlet flow as follows:

$$n \longmapsto \begin{bmatrix} z_r \\ z_{in} \\ z_{inv} \end{bmatrix} = \underbrace{\begin{bmatrix} \mathcal{T}_1^{\mathsf{T}} \\ \mathcal{T}_2^{\mathsf{T}} \\ \mathcal{T}_3^{\mathsf{T}} \end{bmatrix}}_{\mathcal{T}} n \tag{3-11}$$

This transformation leads to the reaction and inlet flow variants $(z_r \text{ and } z_{in})$ and invariants (z_{inv}) as:

$$\dot{z}_r = \underbrace{\mathcal{T}_1^{\mathsf{T}} N^{\mathsf{T}}}_{I_R} \mathcal{V}(t) r(t) + \underbrace{\mathcal{T}_1^{\mathsf{T}} W_{in}}_{0_{R \times p}} u_{in}(t) - \frac{u_{out}(t)}{m(t)} z_r \qquad z_r(0) = \mathcal{T}_1^{\mathsf{T}} n_0 \qquad (3-12)$$

$$\dot{z}_{in} = \underbrace{\mathcal{T}_{0_{R\times R}}^{\intercal} \mathcal{V}(t) r(t) + \underbrace{\mathcal{T}_{2}^{\intercal} W_{in}}_{I_{R}} u_{in}(t) - \frac{u_{out}(t)}{m(t)} z_{in}}_{z_{in}} z_{in} \qquad z_{in}(0) = \mathcal{T}_{2}^{\intercal} n_{0} \qquad (3-13)$$

$$\dot{z}_{inv} = \underbrace{\mathcal{T}_{3}^{\mathsf{T}} N^{\mathsf{T}}}_{0_{(S-R-p)\times R}} \mathcal{V}(t) r(t) + \underbrace{\mathcal{T}_{3}^{\mathsf{T}} W_{in}}_{0_{(S-R-p)\times p}} u_{in}(t) - \frac{u_{out}(t)}{m(t)} z_{inv} \ z_{inv}(0) = \mathcal{T}_{3}^{\mathsf{T}} n_{0} \quad (3-14)$$

where $\mathcal{T}_1^{\mathsf{T}}$ transformation matrix of the reaction space, $\mathcal{T}_2^{\mathsf{T}}$ is the transformation matrix of the inlet space and $\mathcal{T}_3^{\mathsf{T}}$ transformation matrix of the reaction and the inlet invariant space.

Note that we want to make $\mathcal{T}_1^{\mathsf{T}}W_{in} = 0$, otherwise z_r would not represent a true variant of reaction. Likewise, we want to make $\mathcal{T}_2^{\mathsf{T}}N^{\mathsf{T}} = 0$ to allow z_{in} express a true variant of inlet.

If the initial conditions $n_0 \neq 0$, then the reaction and inlet flow variants cannot be interpreted as the true extents. The variants of reaction and inlets would have initial conditions different from zero, even when there is no reaction or material flowing in to the reactor. Hence, these initial conditions must be discounted to obtain the true extents (Amrhein *et al.*, 2010). Then, a new transformation matrix \mathcal{T}_0 is found, which is dependent of the original transformation matrix \mathcal{T} such that:

$$\begin{bmatrix} z_r \\ z_{in} \\ z_{inv} \end{bmatrix} \longmapsto \begin{bmatrix} x_r \\ x_{in} \\ x_{inv} \end{bmatrix} = \begin{bmatrix} z_r \\ z_{in} \\ z_{inv} \end{bmatrix} - \lambda \begin{bmatrix} z_{r_0} \\ z_{in_0} \\ z_{inv_0} \end{bmatrix}$$
(3-15)

where x_r is the extent of reaction, x_{in} is the extent of inlet flow, x_{inv} is the extent of reaction and inlet flow invariants and λ is the initial conditions discounting factor.

Finally, the true extents of reaction and inlet flow are calculated as:

$$n \longmapsto \begin{bmatrix} x_r \\ x_{in} \\ x_{inv} \\ \lambda \end{bmatrix} = \underbrace{\begin{bmatrix} \mathcal{T}_{1_0}^{\mathsf{T}} \\ \mathcal{T}_{2_0}^{\mathsf{T}} \\ \mathcal{T}_{3_0}^{\mathsf{T}} \\ \tau_{0} \end{bmatrix}}_{T_0} n \tag{3-16}$$

with

$$\mathcal{T}_{1_0}^{\mathsf{T}} = \mathcal{T}_1^{\mathsf{T}} (I_S - n_0 \tau_{3_0}^{\mathsf{T}}), \quad \mathcal{T}_{2_0}^{\mathsf{T}} = \mathcal{T}_2^{\mathsf{T}} (I_S - n_0 \tau_{3_0}^{\mathsf{T}}) \text{ and } \tau_{3_0}^{\mathsf{T}} = \frac{1_{S-R-p}^{\mathsf{T}} \mathcal{T}_3^{\mathsf{T}}}{1_{S-R-p}^{\mathsf{T}} \mathcal{T}_3^{\mathsf{T}} n_0}$$
(3-17)

where \mathcal{T}_{1_0} is the transformation matrix of the reaction space, \mathcal{T}_{2_0} is the transformation matrix of the inlet space, \mathcal{T}_{3_0} is the transformation matrix of the reaction and inlet flow invariant

space, all with discounted initial conditions n_0 and τ_{3_0} portion of the reaction and inlet invariant spaces occupied by the initial conditions n_0 .

The aforementioned transformation requires two conditions:

- $\operatorname{rank}([N^{\intercal} W_{in}]) = R_I + p < S$
- $\operatorname{rank}([N^{\intercal} \ W_{in} \ n_0]) = R_I + p + 1.$

The nonlinear differential equation for the mole balance is transformed to:

$$\dot{x}_r = \underbrace{\mathcal{T}_{1_0}^{\mathsf{T}} N^{\mathsf{T}}}_{I_R} \mathcal{V}(t) r(t) + \underbrace{\mathcal{T}_{1_0}^{\mathsf{T}} W_{in}}_{0_{R \times p}} u_{in}(t) - \frac{u_{out}(t)}{m(t)} x_r \qquad x_r(0) = \mathcal{T}_{1_0}^{\mathsf{T}} n_0 = 0 \qquad (3-18)$$

$$\dot{x}_{in} = \underbrace{\mathcal{T}_{20}^{\mathsf{T}} N^{\mathsf{T}}}_{0_{p \times R}} \mathcal{V}(t) r(t) + \underbrace{\mathcal{T}_{20}^{\mathsf{T}} W_{in}}_{I_p} u_{in}(t) - \frac{u_{out}(t)}{m(t)} x_{in} \qquad x_{in}(0) = \mathcal{T}_{20}^{\mathsf{T}} n_0 = 0 \qquad (3-19)$$

$$\dot{x}_{inv} = \underbrace{\mathcal{T}_{3_0}^{\mathsf{T}} N^{\mathsf{T}}}_{0_{(S-R-p)\times R}} \mathcal{V}(t) r(t) + \underbrace{\mathcal{T}_{3_0}^{\mathsf{T}} W_{in}}_{0_{(S-R-p)\times p}} u_{in}(t) - \frac{u_{out}(t)}{m(t)} x_{inv} \quad x_{inv}(0) = \mathcal{T}_{3_0}^{\mathsf{T}} n_0 = 0 \quad (3-20)$$

$$\dot{\lambda} = \underbrace{\tau_{3_0}^{\mathsf{T}} N^{\mathsf{T}}}_{0_{1 \times R}} \mathcal{V}(t) r(t) + \underbrace{\tau_{3_0}^{\mathsf{T}} W_{in}}_{0_{1 \times p}} u_{in}(t) - \frac{u_{out}(t)}{m(t)} \lambda \qquad \lambda(0) = \tau_{3_0}^{\mathsf{T}} n_0 = 1$$
 (3-21)

Since $x_{inv}(0) = 0 \Longrightarrow x_{inv}(t) = 0 \ \forall t \ge 0$, therefore it can be dropped out. The model of the CSTR in terms of extents is:

$$\dot{x}_r = \mathcal{V}(t)r(t) - \frac{u_{out}(t)}{m(t)}x_r \qquad x_r(0) = 0$$
(3-22)

$$\dot{x}_{in} = u_{in}(t) - \frac{u_{out}(t)}{m(t)} x_{in} \qquad x_{in}(0) = 0$$
 (3-23)

$$\dot{\lambda} = -\frac{u_{out}(t)}{m(t)}\lambda \qquad \lambda(0) = 1 \qquad (3-24)$$

Based on this representation, the extent of outlet x_{out} can be obtained with the value of λ as:

$$x_{out} = 1 - \lambda \tag{3-25}$$

Notice the decoupling effect that the extent of reaction and inlet has on the system dynamics. Under this representation, the independent evolution of the reaction, the inlet and outlet can be easily observed.

The moles can be calculated using the extents from the following equation:

$$n(t) = N^{\mathsf{T}} x_r + W_{in} x_{in} + n_0 \lambda \tag{3-26}$$

This transformation is schemed in figure 3-1:

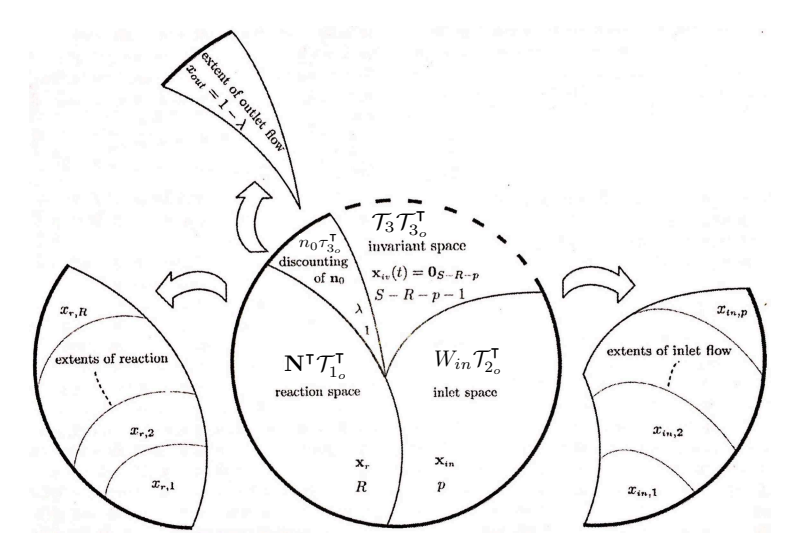


Figure 3-1: Three-way decomposition (linear transformation) (Amrhein et al., 2010)

Example: Isothermal CSTR

We consider the isothermal CSTR model as presented by (Amrhein et al., 2010) with the following characteristics:

- Seven species (S=7)
- Three independent reactions $(R_I = 3)$

$$r_1 : A + B \longrightarrow C + D$$

 $r_2 : C + B \longrightarrow E + D$
 $r_3 : D + B \Longrightarrow F + G$

hence

$$N = \begin{bmatrix} -1 & -1 & 1 & 1 & 0 & 0 & 0 \\ 0 & -1 & -1 & 1 & 1 & 0 & 0 \\ 0 & -1 & 0 & -1 & 0 & 1 & 1 \end{bmatrix}$$

• Reaction rates obey the mass-action principle:

$$r_1 = k_1 C_A C_B$$

$$r_2 = k_2 C_B C_C$$

$$r_3 = k_3 C_B C_C - k_4 C_F C_G$$

with $k_1 = 0.127$, $k_2 = 0.023$, $k_3 = 11.97$ and $k_4 = 8.01$ (m³ kmol⁻¹ h⁻¹) where k

• Two constant and independent inlets (p=2) of A and B, i.e. $u_{in} = [7.8 \ 5.3]^{\dagger}$ (kg h⁻¹)

- $W_{in} = [0.00049 \ 0 \ 0 \ 0 \ 0 \ 0]^{\mathsf{T}} \ (\text{kmol kg}^{-1})$
- $n_0 = [n_{A_0} \ n_{B_0} \ n_{C_0} \ n_{D_0} \ n_{E_0} \ n_{F_0} \ n_{G_0}]^{\mathsf{T}} = [0 \ 0 \ 0 \ 0 \ 1.5 \ 0]^{\mathsf{T}} \ (\mathrm{kmol})$
- A is fed from t = 0 h while B is fed at t = 5 h

The evolution of the number of moles in the CSTR is shown in figure 3-2 while the extents of reaction and extents of inlet are displayed in figures 3-3 and 3-4, respectively.

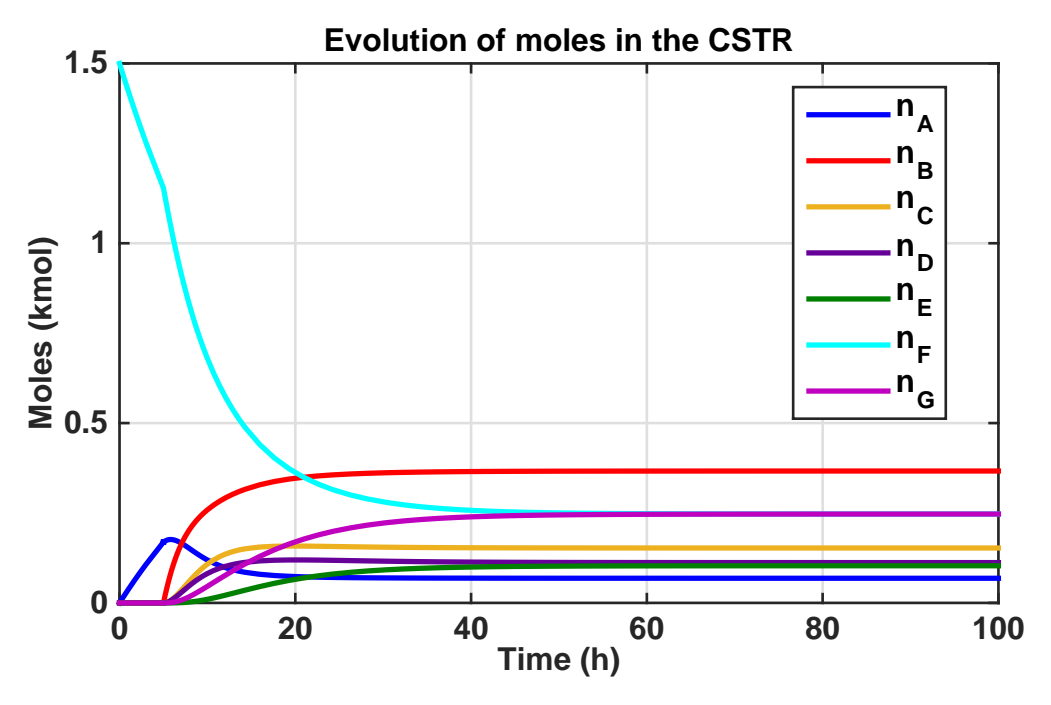


Figure 3-2: Evolution of number of moles per species in the CSTR

3-2-1 Inclusion of Energy Balance

So far it has been shown how the extents of reaction and inlet are used in isothermal systems. Let us make the system description more realistic including the energy balance:

where $\Delta H_f^\ominus\!\!\in\mathbb{R}^{1\times S}$ is the vector of standard enthalpy of formation

with
$$n(0) = n_0$$
, $T(0) = T_0$ and $T_{ref} = 25^{\circ}$ C.

Now consider the equilibrium reactive system $A + B \rightleftharpoons C + D$. In this case we assume again that we have two independent inlets (p = 2) of A and B. The reaction for this example

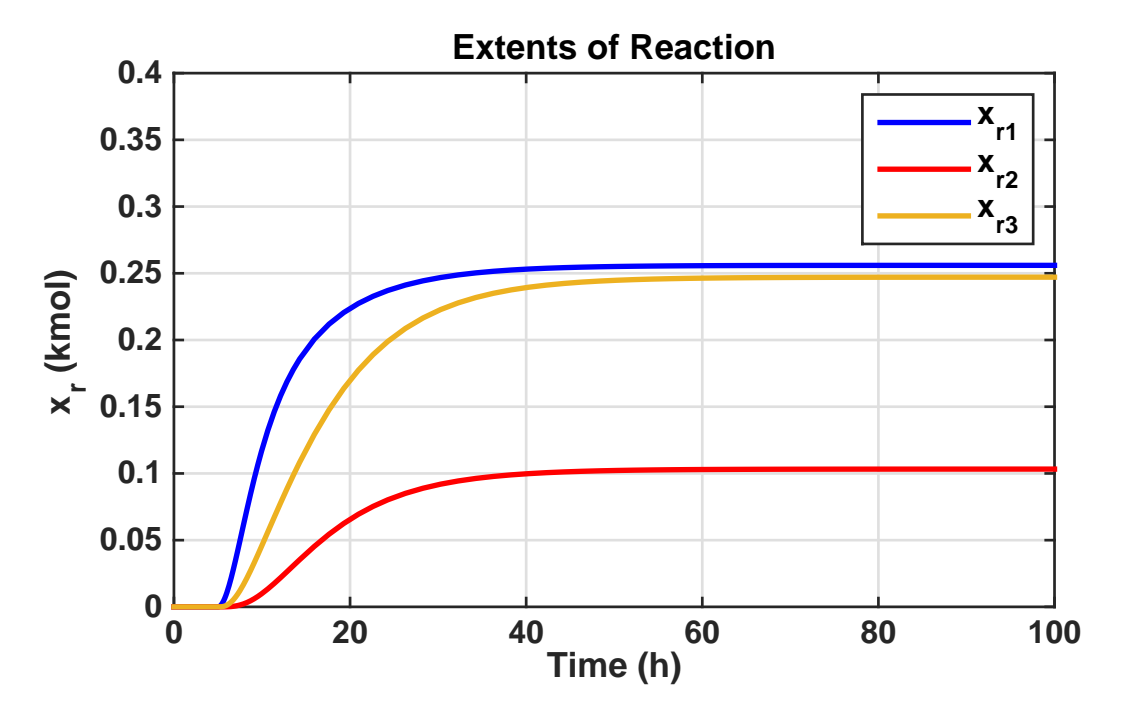


Figure 3-3: Extents of reactions in the CSTR

was changed from the isothermal case because temperature-dependent chemical kinetic data of the species was not available in the literature.

Assuming the reaction kinetics follow the Arrhenius law and the mass-action principle, by means of the linear transformation the mole balance equation can be brought to:

$$\dot{x}_{r,i} = \mathcal{V}(t) \left(k_o \sum_{i=1}^{R} e^{\frac{-E_{a_i}}{RT}} \prod_{k=1}^{S} C_k^{\nu_k} \right) - \frac{u_{out}}{m} x_{r,i}$$
 (3-27)

$$\dot{x}_{in,j} = u_{in,j} - \frac{u_{out}}{m} x_{in,j}$$

$$\dot{\lambda} = -\frac{u_{out}}{m} \lambda$$
(3-28)

$$\dot{\lambda} = -\frac{u_{out}}{m}\lambda \tag{3-29}$$

$$\dot{T}(t) = \frac{u_{in}C_{p_{in}}T_{in} - u_{out}C_{p_{mix}}T(t) - \mathcal{V}(t)\Delta H_f^{\ominus}N^{\dagger}r(C,T) + Q_{in}}{m(t)C_{p_{mix}(t)}}$$
(3-30)

Recall that the concentration C_i is $\frac{n_i}{\mathcal{V}}$ and according to (3-26) we can write:

$$C(t) = \frac{n(t)}{\mathcal{V}} = \frac{N^{\mathsf{T}} x_r(t) + W_{in} x_{in}(t) + n_0 \lambda}{\mathcal{V}}$$
(3-31)

Define $\tau = \frac{m}{u_{out}}$. Substituting (3-31) in (3-27), let us write x_r as:

$$\dot{x}_r = f(x_r, x_{in}, T) - \frac{1}{\tau} x_r$$

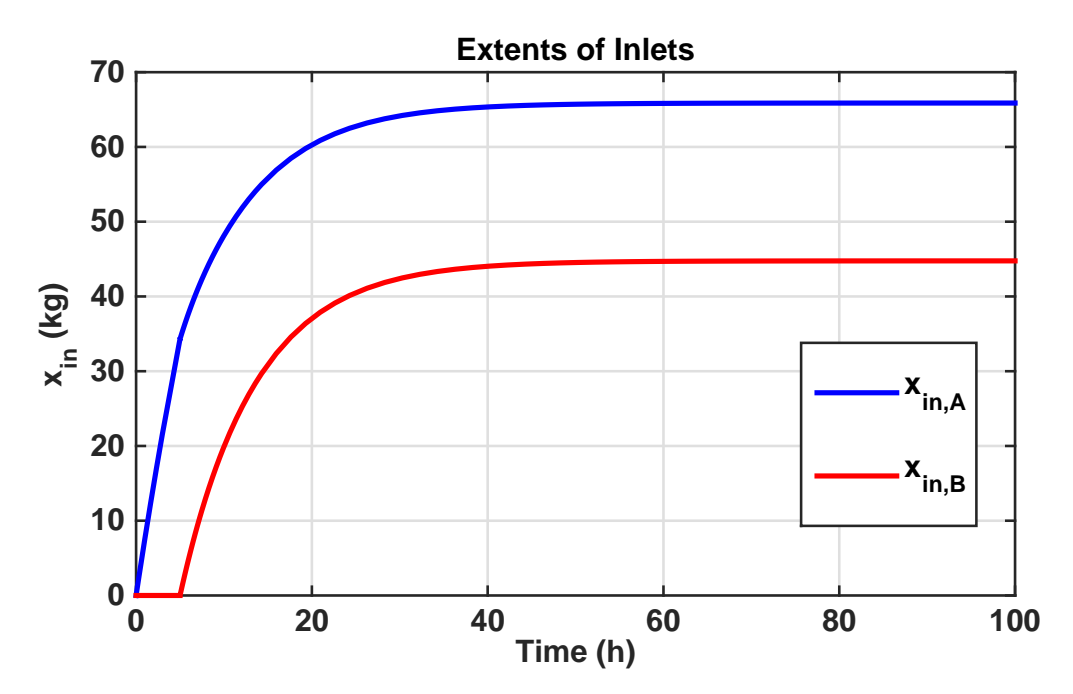


Figure 3-4: Extents of inlet in the CSTR

Example: Non-isothermal CSTR

We now consider the non-isothermal CSTR model with the following characteristics:

- Four species (S=4)
- One independent reaction $(R_I = 1)$

$$r_1: A + B \Longrightarrow C + D$$

hence

$$N = \begin{bmatrix} -1 & -1 & 1 & 1 \end{bmatrix}$$

• Reaction rates obey the mass-action principle and the Arrhenius law:

$$r_1 = k_f C_A C_B - k_r C_C C_D \Longrightarrow (k_{o_f} e^{\frac{-E_{a_f}}{RT}}) C_A C_B - (k_{o_r} e^{\frac{-E_{a_r}}{RT}}) C_C C_D$$

with $k_{o_f}=6.06\times 10^5$ and $k_{o_{rev}}=9.84\times 10^6$ in m³ kmol⁻¹ h⁻¹, $-E_{a_f}$ and $-E_{a_{rev}}$ in kJ kmol⁻¹ and the universal gas constant R=8.314 kJ kmol⁻¹ K⁻¹, where k_o is the preexponential factor in the Arrhenius law, E_a is the activation energy of the reaction, in the forward reaction and reverse reaction.

- Two constant and independent inlets (p=2) of A and B, i.e. $u_{in} = [10 \ 8]^{\mathsf{T}} \ (\text{kg h}^{-1})$
- $W_{in} = [0.01665 \ 0 \ 0 \ 0; \ 0 \ 0.03121 \ 0 \ 0]^{\mathsf{T}} \ (\text{kmol kg}^{-1})$

- $n_0 = [n_{A_0} \ n_{B_0} \ n_{C_0} \ n_{D_0}]^{\mathsf{T}} = [0.5 \ 1 \ 0 \ 0.0001]^{\mathsf{T}} \text{ (kmol)}$
- The heat duty $Q_{in} = -200 \text{ kJ}$ (removing heat from the system)

The evolution of the number of moles and the temperature in the CSTR are shown in figures 3-5 and 3-6, while the extent of reaction and extents of inlet are displayed in figures 3-7 and 3-8, respectively.

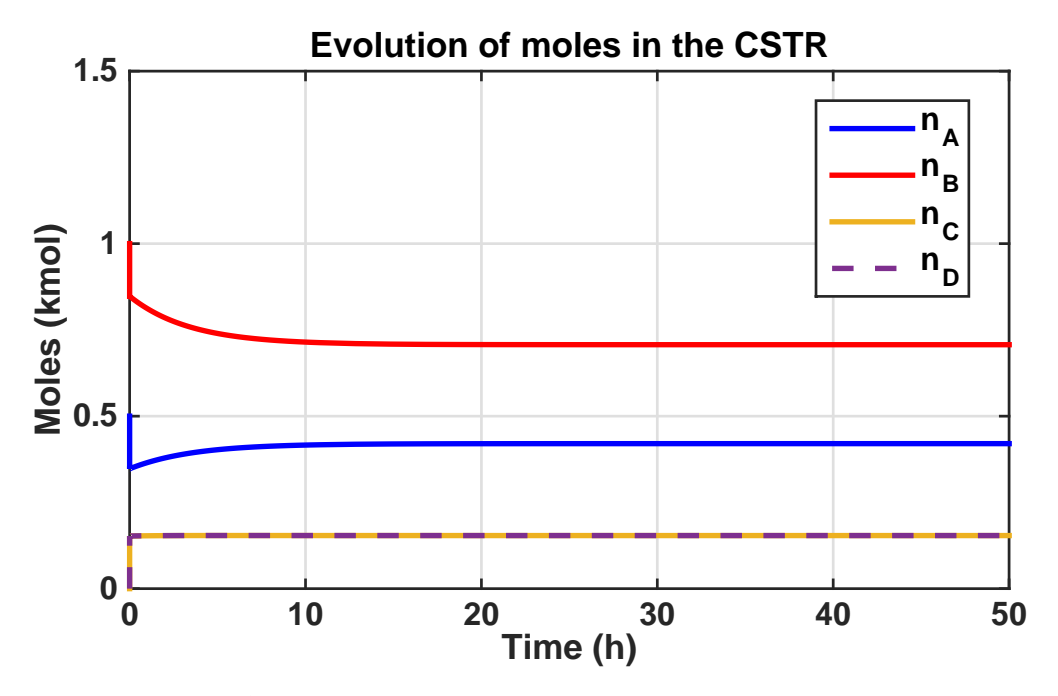


Figure 3-5: Evolution of number of moles per species in the CSTR

3-2-2 Sensitivity Analysis

The extent of reaction and inlet concept can be useful for sensitivity analysis and time scale assessment exploiting its decoupling effect on the system's dynamics. One could manipulate each variable separately to test its influence on the system, or even neglect very fast and less dominant dynamics. This interesting property is helpful for process monitoring, optimization and design purposes.

Taking the same system from the non-isothermal CSTR example, an assessment on time scales in x_r , can be performed. We then write:

$$\delta \dot{x}_r = \left(\frac{\partial f}{\partial x_r} - \frac{1}{\tau}\right) \delta x_r + \frac{\partial f}{\partial x_{in}} \delta x_{in} + \frac{\partial f}{\partial T} \delta T$$
 (3-32)

This allows for a comparison of the speed of the x_r transients as shown in figures 3-9 and 3-10. In figure 3-9 we see the gradient surface of $\frac{\partial f}{\partial x_r}$ to changes in the extent of inlet x_{in_b} and temperature T, while fixing x_r to 1 kmol and $x_{in_a}=1$ kg. Figure 3-10 shows the same but changing $x_{in_a}=20$ kg.

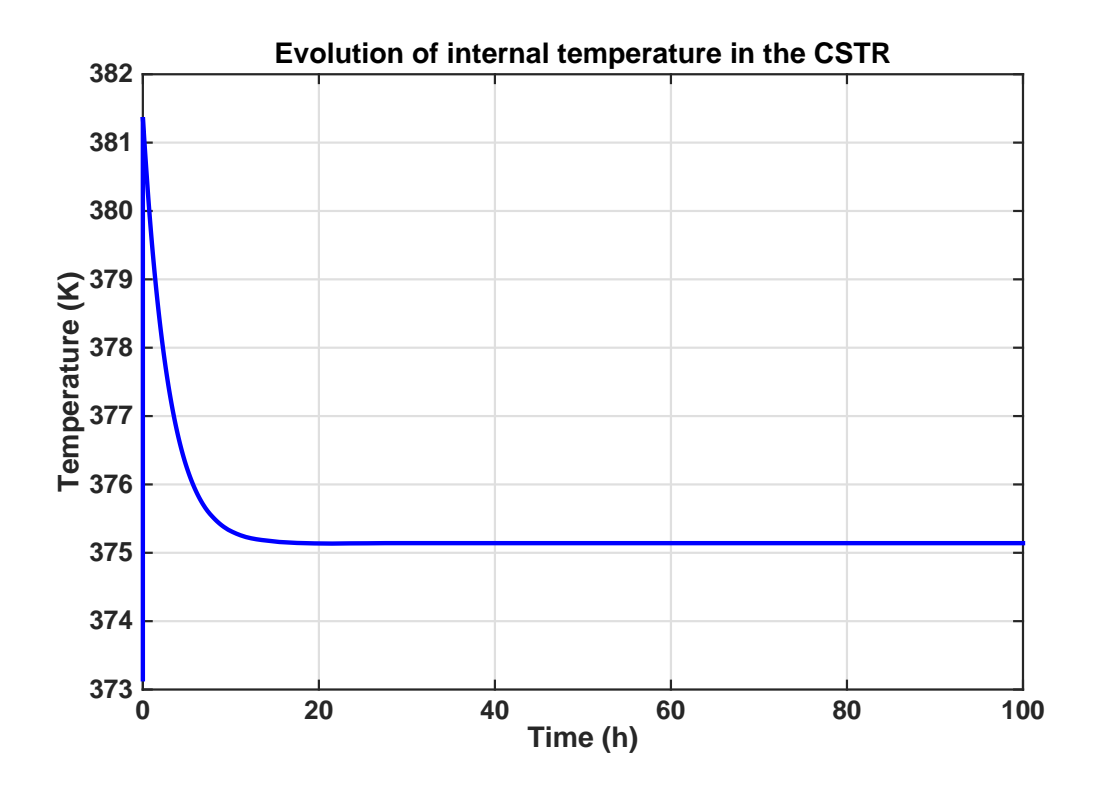


Figure 3-6: Evolution of internal temperature in the CSTR

We show a particular case where the system is linearized around an operating point o^* . This operating point corresponds to the steady-state values of the open-loop plant. Hence o^* is:

- $x_r = 0.31 \text{ kmol}$
- $x_{in_a} = 41.338 \text{ kg}$
- $x_{in_b} = 21.669 \text{ kg}$
- T = 226.28 K
- $\lambda = 0$
- $V = 0.0654 \ m^3$
- m = 62.065 kg
- $u_{out} = 5 \text{ kg h}^{-1}$

Applying Laplace transform:

$$sX_r(s) = \underbrace{\left(\frac{\partial f}{\partial x_r}\Big|_{o^*} - \frac{1}{\tau}\right)}_{\omega_r} X_r(s) + \underbrace{\frac{\partial f}{\partial x_{in}}\Big|_{o^*}}_{\omega_{in}} X_{in}(s) + \underbrace{\frac{\partial f}{\partial T}\Big|_{o^*}}_{\omega_T} T(s)$$
(3-33)

Carlos Samuel Méndez Blanco

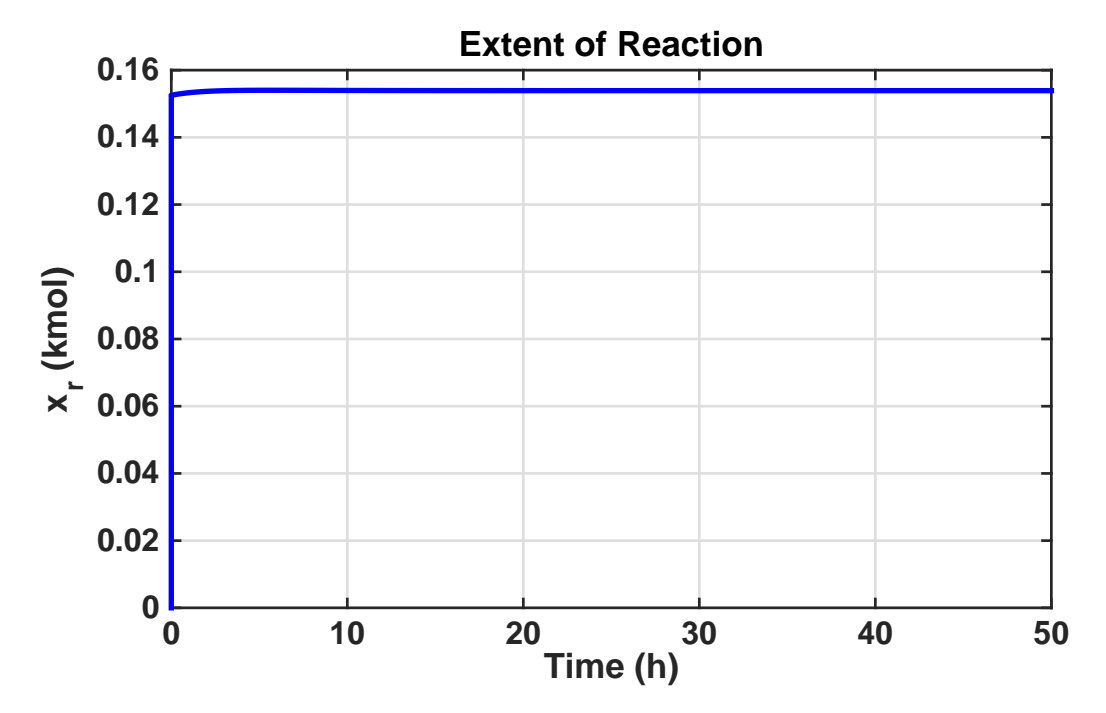


Figure 3-7: Extents of reactions in the CSTR

$$X_r(s) = \frac{\omega_{in}}{s - \omega_r} X_{in}(s) + \frac{\omega_T}{s - \omega_r} T(s)$$
(3-34)

The system is guaranteed to be stable if the $\omega_r < 0$ i.e. $\frac{\partial f}{\partial x_r} < \frac{1}{\tau}$

In figure 3-9 it can be seen that the system is more sensitive to changes in flow than to changes in the chosen temperature range. $x_{in_a}=1$ kg and for x_{in_b} close to zero the system is not stable, whereas increasing x_{in_b} makes the gradient more negative. Decreasing the temperature moves the pole of the linearized system closer to zero but more slowly. Analogously, in figure 3-10, we can see the same behavior, but in the case the gradient is always negative, thus the system is always stable, because $x_{in_a}=20$ kg, which is sufficiently large to keep the system stable despite changes in x_{in_b} and T.

3-3 Limitations of the extent transformation approach

Despite the advantages offered by the extent of reaction and inlet representation, it relies on a matrix linear transformation. This linear transformation is based on the computation of left nullspaces of the system matrices. However, under certain conditions the transformation \mathcal{T} is not directly applicable or, in the worst case scenario, it does not exist. This situation poses some limitations to this mathematical approach. Two conditioning cases are discussed: Span of the chemical species space and the rank deficiency of the matrix $[N^{\dagger} \ W_{in} \ n_0]$.

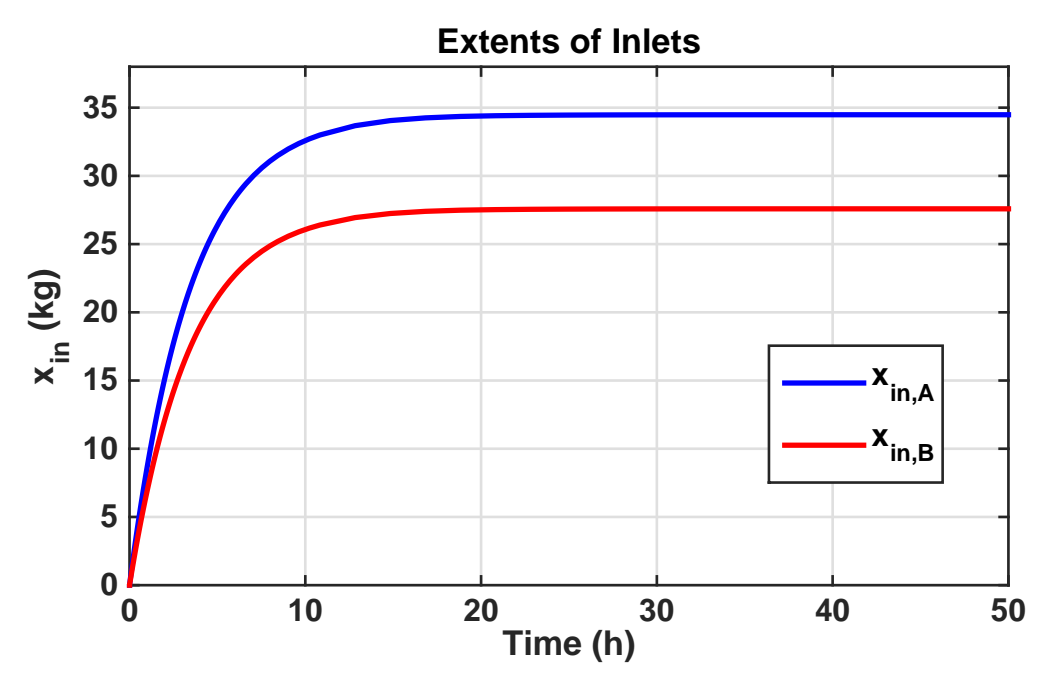


Figure 3-8: Extents of inlet in the CSTR

3-3-1 Span of the chemical species space

Recall the mapping described in (3-16) and (3-17). The first condition for this mapping to exist is that $rank([N^{\dagger} W_{in}]) = R_I + p < S$. Based on this premise, let us explore the other two possible scenarios:

- Case a: rank($[N^{\dagger} W_{in}]$) = $R_I + p > S$
- Case b: rank($[N^{\intercal} W_{in}]$) = $R_I + p = S$

Case a. It is never possible because it is physically inconsistent. If a reactive system contains S species, it might have more reactions than chemical species. However, since there are more chemical reactions than species, then, there must be at least one species present in more than one of these reactions. In other words, not every reaction is linearly independent. Hence, $\mathbf{Col}(N^{\intercal}) = R_I$, which is at most equal to S.

Likewise, the same reasoning can be used to ascertain that $Col(W_{in}) = p$ is at most S; it is not possible to feed more species relevant to the process than a number of species S.

Case b. It is physically consistent and may occur in certain systems. Under this scenario the matrix $[N^{\intercal} W_{in}] \in \mathbb{R}^{S \times S}$ and its rank is S. Since $[N^{\intercal} W_{in}]$ is full-rank then it does not have neither right nor left null space. This means that the invariant space does not exist and all the dynamics evolve in the reaction and inlet spaces. Moreover, one can then find a transformation matrix \mathcal{T} such that:

$$n \longmapsto \begin{bmatrix} z_r \\ z_{in} \end{bmatrix} = \underbrace{\begin{bmatrix} \mathcal{T}_1^{\mathsf{T}} \\ \mathcal{T}_2^{\mathsf{T}} \end{bmatrix}}_{\mathcal{T}} n \tag{3-35}$$

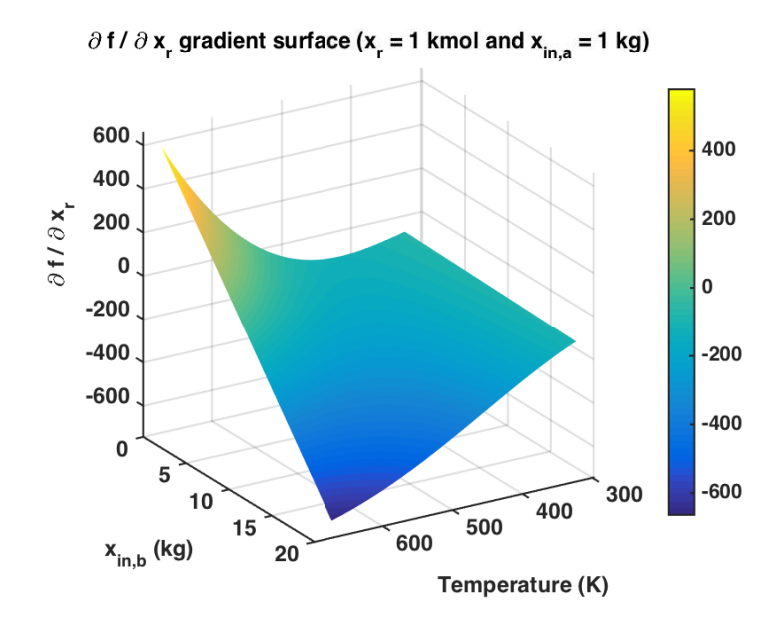


Figure 3-9: $\frac{\partial f}{\partial x_r}$ gradient surface to changes in T and $x_{in,b}$ with $x_r = 1$ kmol and $x_{in,a} = 1$

Then the CSTR equation is recast by means of \mathcal{T} as:

$$\dot{z}_{r} = \underbrace{\mathcal{T}_{1}^{\mathsf{T}} N^{\mathsf{T}}}_{I_{R}} \mathcal{V}(t) r(t) + \underbrace{\mathcal{T}_{0_{R \times p}}^{\mathsf{T}} W_{in}}_{0_{R \times p}} u_{in}(t) - \frac{u_{out}(t)}{m(t)} z_{r} \qquad z_{r}(0) = \mathcal{T}_{1}^{\mathsf{T}} n_{0} \qquad (3-36)$$

$$\dot{z}_{in} = \underbrace{\mathcal{T}_{2}^{\mathsf{T}} N^{\mathsf{T}}}_{0_{p \times R}} \mathcal{V}(t) r(t) + \underbrace{\mathcal{T}_{2}^{\mathsf{T}} W_{in}}_{I_{p}} u_{in}(t) - \frac{u_{out}(t)}{m(t)} z_{in} \qquad z_{in}(0) = \mathcal{T}_{2}^{\mathsf{T}} n_{0} \qquad (3-37)$$

$$\dot{z}_{in} = \underbrace{\mathcal{T}_2^{\mathsf{T}} N^{\mathsf{T}}}_{0_{p \times R}} \mathcal{V}(t) r(t) + \underbrace{\mathcal{T}_2^{\mathsf{T}} W_{in}}_{I_p} u_{in}(t) - \frac{u_{out}(t)}{m(t)} z_{in} \qquad z_{in}(0) = \mathcal{T}_2^{\mathsf{T}} n_0 \qquad (3-37)$$

However, under this scenario $[N^{\intercal} \ W_{in} \ n_0] \in \mathbb{R}^{S \times S + 1}$ and rank $([N^{\intercal} \ W_{in} \ n_0]) < R + p + 1$. This latter result shows the initial conditions cannot be discounted of. Finally, for this case, the variants of reaction z_r and inlet z_{in} only possess physical meaning when $n_0 = 0$, and they would exactly represent the extents of reaction x_r and inlet x_{in} . This situation clearly poses an inconvenient, as many industrial chemical processes have initial conditions different from zero.

3-3-2 Rank deficiency of $[N^{\intercal} \ W_{in} \ n_0]$

The second condition required for the transformation is rank($[N^{\dagger} W_{in} n_0]$) = R + p + 1. This equation means that the initial condition n_0 adds information to the system. Moreover, mathematically, the matrix \mathcal{T}_{3_0} spans the nullspace of $[N^{\intercal} \ W_{in}]^{\intercal}$.

If $\operatorname{rank}([N^{\intercal} \ W_{in} \ n_0]) = R + p$ then the vector $n_0 \subset \operatorname{Col}([N^{\intercal} \ W_{in}])$ and since $\operatorname{Null}([N^{\intercal} \ W_{in}]^{\intercal}) =$ \mathcal{T}_{30} , we obtain:

$$\tau_{3_0}^{\mathsf{T}} = \frac{1_{S-R-p}^{\mathsf{T}} \mathcal{T}_{3_0}^{\mathsf{T}}}{1_{S-R-p}^{\mathsf{T}} \mathcal{T}_{3_0}^{\mathsf{T}} n_0} \longrightarrow \infty$$

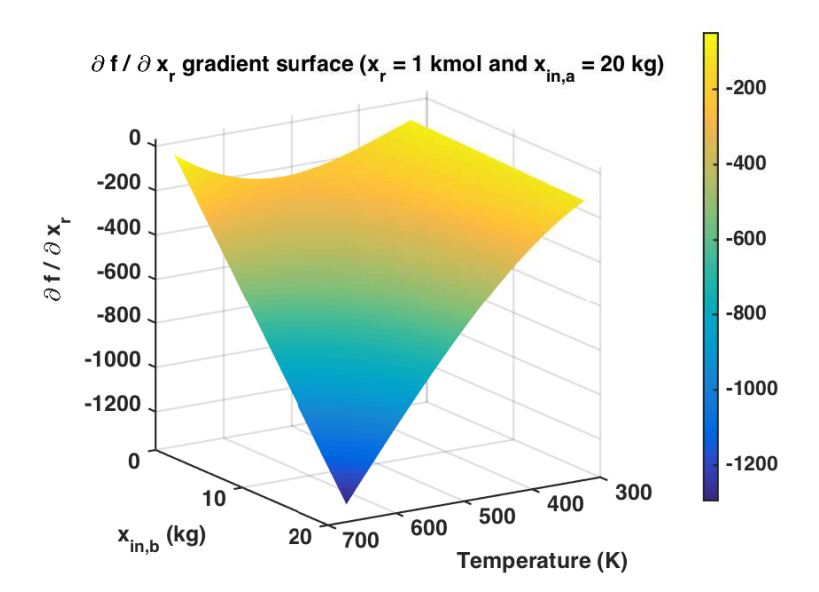


Figure 3-10: $\frac{\partial f}{\partial x_r}$ gradient surface to changes in T and $x_{in,b}$ with $x_r = 1$ kmol and $x_{in,a} = 20$ kg

• When $n_0 = [0.5 \ 1 \ 0 \ 0]^{\intercal} \longrightarrow \operatorname{rank}([N^{\intercal} \ W_{in} \ n_0]) = p$

In figure 3-11 the extent of inlets is badly scaled because of the rank deficiency of $[N^{\dagger} \ W_{in} \ n_0]$. It is observed that the extents of inlet grow to extremely large numbers or result in negative values. The extents of inlet are physical variables that represent the amount of mass being utilized in the reaction, hence it cannot be negative or grow infinitely.

Because of the bad scaling, the moles reconstruction performed with equation (3-26) is wrong. This is shown in figure 3-12

To circumvent this problem, assume that in the reactor at t = 0, there is a very small quantity ε of product D. This enforces full-column rank of $[W_{in} \ n_0]$

• When
$$n_0 = [0.5 \ 1 \ 0 \ \varepsilon]^{\mathsf{T}} \longrightarrow \operatorname{rank}([W_{in} \ n_0]) = p + 1 \text{ with } \varepsilon = 0.0001$$

In figure 3-13 the extent of inlets is correctly calculated because $[W_{in} \ n_0]$ is full-column rank. The figure shows that the inlet increases in time as reaction progresses until it reaches chemical equilibrium, where the mass consumption is constant. Values of the extents of inlet are physical and bounded within reasonable process values.

Since the calculation of x_{in} is correct, the moles reconstruction performed with equation (3-26) results in the real number of moles per species. This is shown in figure 3-14

3-4 Linear Parameter-Varying (LPV) state space model

The system of differential equations described by (3-27), (3-28), (3-29) and (3-30) represents the evolution in time of the extents of reaction, the extents of inlet and the discounting factor, respectively:

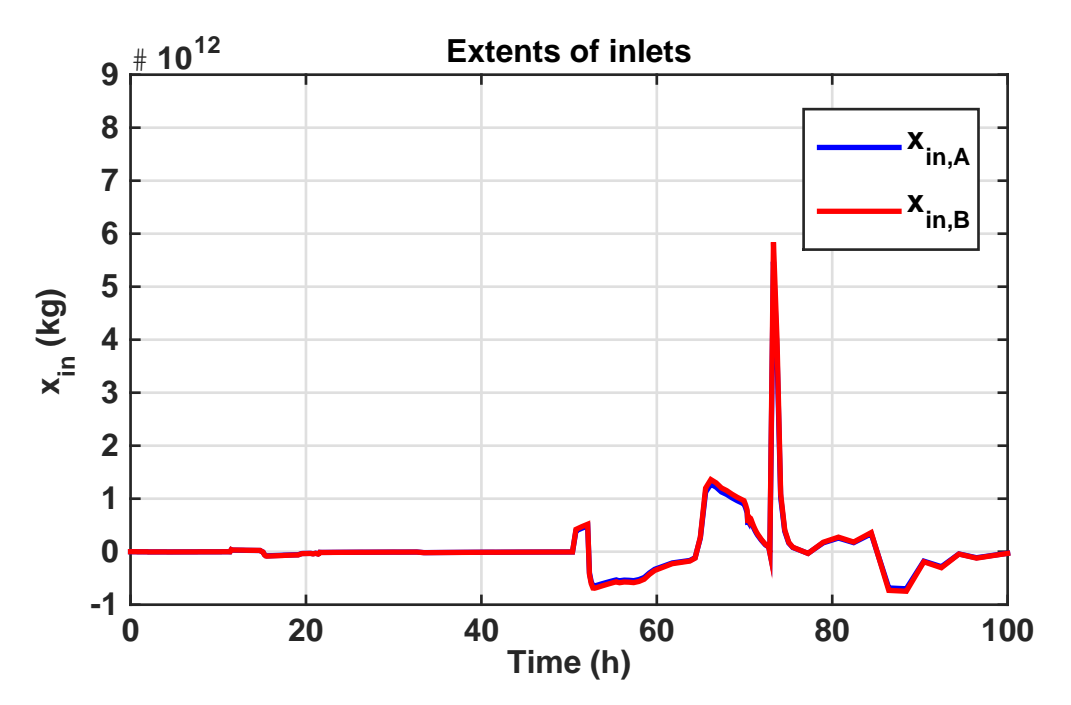


Figure 3-11: Extents of inlet

$$\dot{x}_{r,i} = f(x_r, x_{in}, T) - \frac{u_{out}}{m} x_{r,i}
\dot{x}_{in,j} = u_{in,j} - \frac{u_{out}}{m} x_{in,j}
\dot{\lambda} = -\frac{u_{out}}{m} \lambda
\dot{T}(t) = \frac{u_{in} C_{p_{in}} T_{in} - u_{out} C_{p_{mix}} T(t) - \mathcal{V}(t) \Delta H_f^{\ominus} N^{\dagger} r(C, T) + Q_{in}}{m C_{p_{mix}}}$$

Another advantage of this extent representation is that linear parameter-varying models can be derived based on it, which are suitable for control purposes. The two developed approaches are present as follows:

3-4-1 First Approach: Model with Disturbance

For the CSTR dynamics in terms of the extent representation, the following characteristics are known:

- The dynamics of the discounting factor behave like an autonomous system. The pole (eigenvalue) is located at $-\frac{u_{out}}{m}$ (hence $\tau = \frac{m}{u_{out}}$).
- The dynamics of the extents of inlets x_{in} form a linear system with control input (u_{in}) . The pole (eigenvalue) is located at $-\frac{u_{out}}{m}$ (hence $\tau = \frac{m}{u_{out}}$).

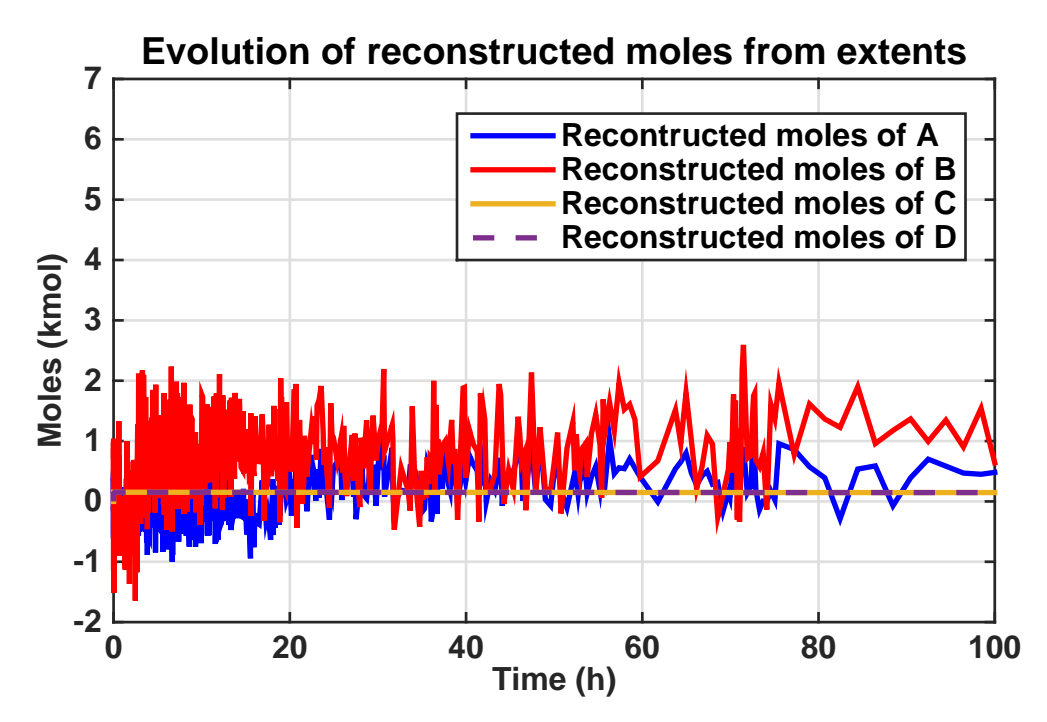


Figure 3-12: Reconstructed moles

• The dynamics of the extent of reaction x_r is nonlinear and depends on the extents of reaction itself and extents of inlets.

In case that the dynamics of x_r is much faster than that of x_{in} ($\tau_{x_r} \ll \tau$), $\dot{x_r} = 0$ with respect to \dot{x}_{in}

$$\dot{x}_{r} = f(x_{r}, x_{in}, T) - \frac{1}{\tau} x_{r}(t)$$
(3-38)

From 3-38 we know that $f(x_r, x_{in}, T) = \frac{1}{\tau} x_r$ and replacing in 3-30:

$$\dot{T} = \frac{u_{in}(t)C_{p_{in}}T_{in} - u_{out}(t)C_{p_{mix}}(t)T(t) + Q_{in} + \frac{\Delta H_f^{\ominus}N^{\dagger}x_r}{\tau}}{m(t)C_{p_{mix}}(t)}$$

Rearranging, we obtain the LPV system

$$\begin{bmatrix} \dot{x}_{in} \\ \dot{T} \end{bmatrix} = \begin{bmatrix} -\frac{u_{out}(t)}{m(t)} \cdot I_{p \times p} & 0 \\ 0 & -\frac{u_{out}(t)}{m(t)} \end{bmatrix} \begin{bmatrix} x_{in} \\ T \end{bmatrix} + \begin{bmatrix} I_{p \times p} & 0 \\ \frac{C_{p_{in}}T_{in}}{m(t)C_{p_{mix}}(t)} & \frac{1}{m(t)C_{p_{mix}}(t)} \end{bmatrix} \begin{bmatrix} u_{in} \\ Q_{in} \end{bmatrix} + \underbrace{\begin{bmatrix} 0 \\ -\Delta H_f^{\ominus}N^{\intercal} \\ \overline{\tau(t)m(t)C_{p_{mix}}(t)} \end{bmatrix}}_{B_{ra}} x_{ra}$$

Under this representation, the matrix B_r acts as a disturbance to the dynamics of the state T.

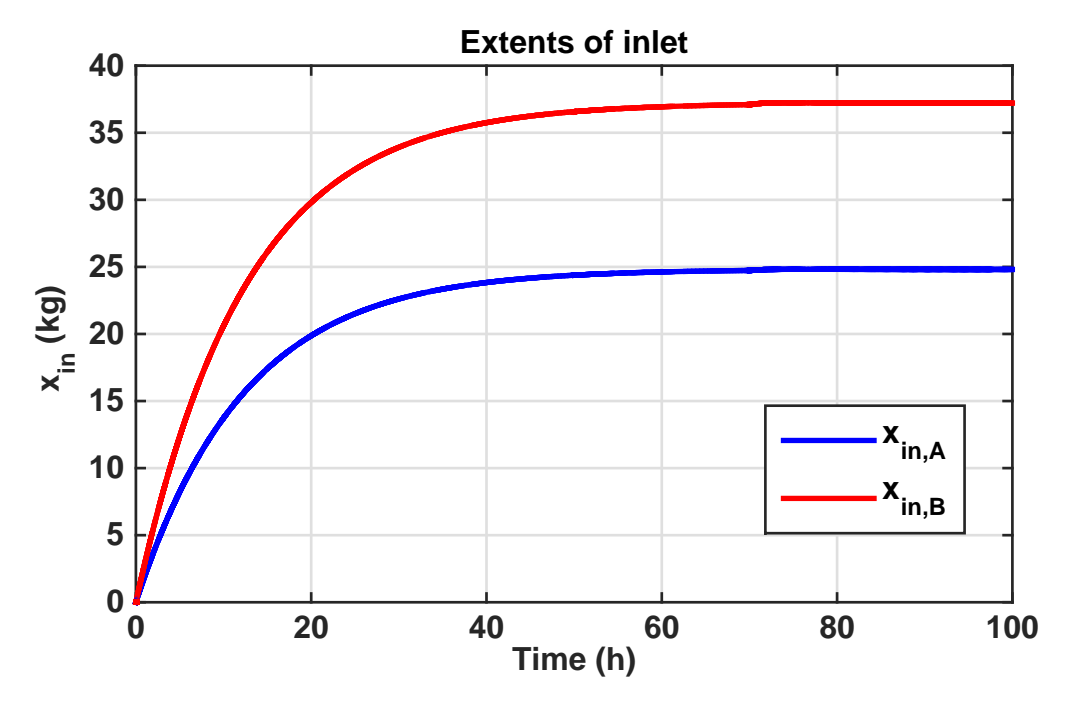


Figure 3-13: Extents of inlet

To assess if the LPV system captures the dynamics of the nonlinear system, reference changes of large magnitude have been performed. Assuming that the system has initial conditions that satisfy $n_0 \not\subset \mathbf{Col}(W_{in})$. The inputs steps:

$$u_{in,a}=2~{\rm kg~h^{-1}}\longrightarrow 20~{\rm kg~h^{-1}}$$

$$u_{in,b}=3~{\rm kg~h^{-1}}\longrightarrow 30~{\rm kg~h^{-1}}$$

$$Q_{in}=-800~{\rm kJ~h^{-1}}\longrightarrow -200~{\rm kJ~h^{-1}}$$

The responses of the nonlinear plant and the LPV system are presented in figure 3-15. It can be seen that the LPV system mimics the dynamics of the nonlinear system with good fidelity.

3-4-2 Second Approach: Change of variable Z

When \dot{x}_r cannot be neglected in the model, the nonlinear reaction kinetics function $f(x_r, x_{in}, T)$ plays an important role in the plant's behavior, thus we want to find a transformation such that x_r can be expressed linearly in terms of a new variable.

Define a change of variable Z as:

$$Z = \frac{\Delta H_f^{\ominus} N^{\mathsf{T}}}{m(t) C_{p_{mix}}(t)} x_r + T = \underbrace{\left[\frac{\Delta H_f^{\ominus} N^{\mathsf{T}}}{m(t) C_{p_{mix}}(t)} \ 1\right]}_{\mathcal{Z}} \begin{bmatrix} x_r \\ T \end{bmatrix}$$
(3-39)

Master of Science Thesis

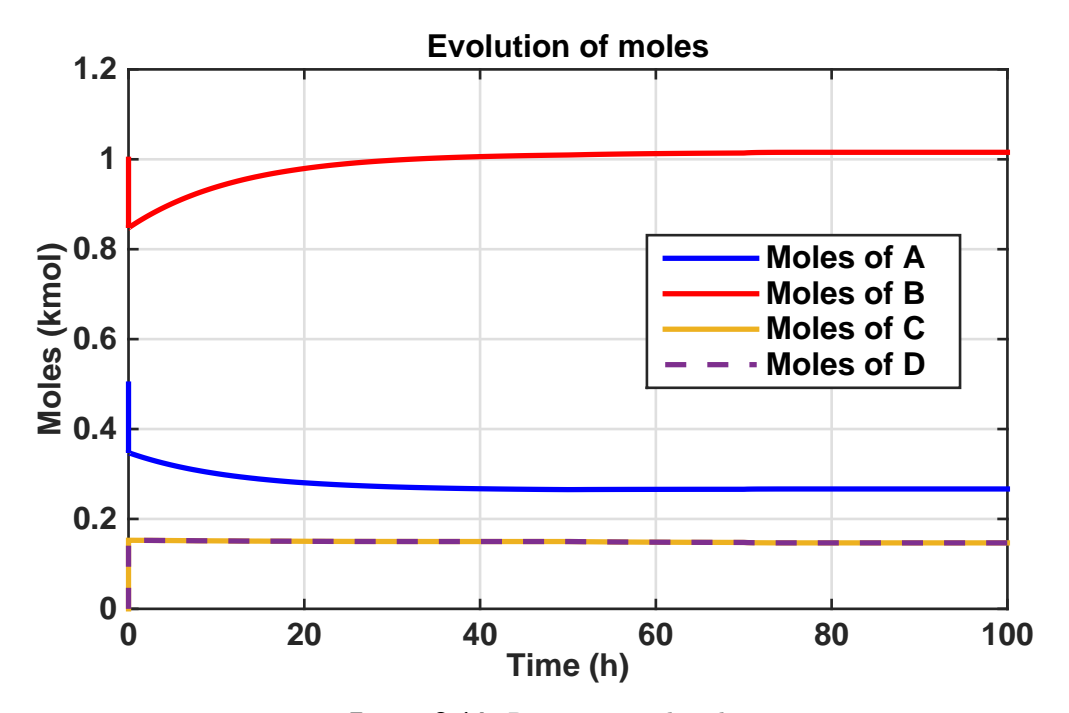


Figure 3-14: Reconstructed moles

During differentiation, the parameters m and $C_{p_{mix}}$ are constant because the term $m(t)C_{p_{mix}}(t)$ does not vary significantly during the operation. Hence, the change of variable Z can be differentiated with respect to time, only considering time-varying the states x_r and T.

$$\dot{Z} = \frac{\Delta H_f^{\ominus} N^{\dagger}}{m(t) C_{p_{mix}}(t)} \dot{x}_r + \dot{T}$$
(3-40)

And substituting (3-27) and (3-30) in (3-40), we obtain:

$$\dot{Z} = -\frac{u_{out}(t)}{m(t)}Z + \frac{C_{p_{in}}T_{in}}{m(t)C_{p_{mix}}(t)}u_{in} + \frac{1}{m(t)C_{p_{mix}}(t)}Q_{in}$$
(3-41)

Stacking the dynamics in a vector x_{in} , λ and Z, we obtain the model:

$$\begin{bmatrix} \dot{x}_{in} \\ \dot{\lambda} \\ \dot{Z} \end{bmatrix} \ = \ \begin{bmatrix} -\frac{u_{out}(t)}{m(t)} \cdot I_{p \times p} & 0 & 0 \\ 0 & -\frac{u_{out}(t)}{m(t)} & 0 \\ 0 & 0 & -\frac{u_{out}(t)}{m(t)} \end{bmatrix} \begin{bmatrix} x_{in} \\ \lambda \\ Z \end{bmatrix} + \begin{bmatrix} I_{p \times p} & 0 \\ 0 & 0 \\ \frac{C_{p_{in}}T_{in}}{m(t)C_{p_{mix}}(t)} & \frac{1}{m(t)C_{p_{mix}}(t)} \end{bmatrix} \begin{bmatrix} u_{in} \\ Q_{in} \end{bmatrix}$$

$$y = \begin{bmatrix} n \\ T \end{bmatrix} \ = \ \underbrace{\begin{bmatrix} W_{in} & n_0 \\ 0 & 0 \end{bmatrix}}_{C_1} \begin{bmatrix} x_{in} \\ \lambda \end{bmatrix} + \underbrace{\begin{bmatrix} \nu_{i,r} & 0 \\ 0 & 1 \end{bmatrix}}_{C_2} \begin{bmatrix} x_r \\ T \end{bmatrix}$$

Using equation 3-39, we can find an expression for $[x_r \ T]^{\intercal}$ in terms of Z. However, \mathcal{Z} cannot be set to 1 by means of its pseudo-inverse. \mathcal{Z} is full row-rank, thus it has a right pseudo-

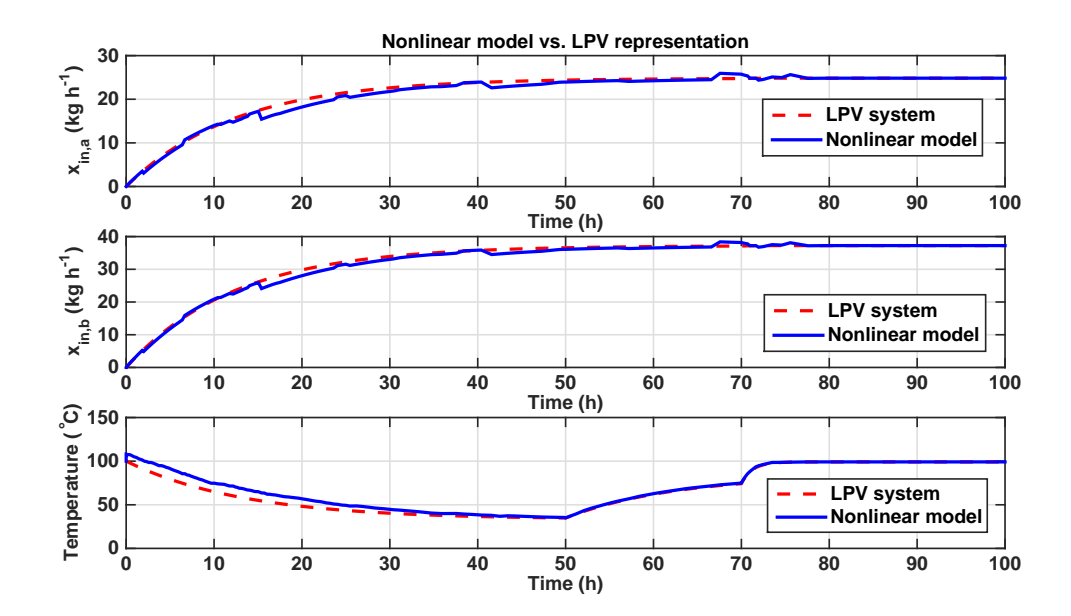


Figure 3-15: Comparison of nonlinear model and LPV system response to reference changes

inverse, i.e. $\mathcal{Z}\mathcal{Z}^{\dagger}=1$ (represents the Moore-Penrose psedoinverse). Therefore, we need to solve an underdetermined equation to obtain an approximate value of Z.

Consider the QR factorization of \mathcal{Z}^{\intercal}

$$\mathcal{Z}^{\mathsf{T}} = Q \cdot R = \begin{bmatrix} \hat{Q} & Q_N \end{bmatrix} \begin{bmatrix} \hat{R} \\ 0 \end{bmatrix} = \hat{Q} \cdot \hat{R}$$
 (3-42)

where Q is an orthogonal matrix, \hat{Q} and Q_N span the range and right null spaces of \mathcal{Z}^{\intercal} , respectively, R is an upper triangular matrix and \hat{R} spans left the null space of \mathcal{Z} .

Let us write the vector $[x_r \ T]^{\intercal}$ as a linear combination of the matrix Q as:

$$\begin{bmatrix} x_r \\ T \end{bmatrix} = \hat{Q}\mathfrak{u} + Q_N\mathfrak{v}$$
 (3-43)

where $\mathfrak u$ and $\mathfrak v$ are arbitrary vectors of corresponding dimensions to $\hat Q$ and Q_N Plugging (3-42) and (3-43) in (3-39):

$$Z = \hat{R}^{\mathsf{T}} \hat{Q}^{\mathsf{T}} (\hat{Q} \mathfrak{u} + Q_N \mathfrak{v}) = \hat{R}^{\mathsf{T}} \mathfrak{u} \Longrightarrow \mathfrak{u} = \hat{R}^{-\mathsf{T}} Z$$
 (3-44)

Replacing (3-44) in (3-43):

$$\begin{bmatrix} x_r \\ T \end{bmatrix} = \hat{Q}\hat{R}^{-\dagger}Z + Q_N \mathfrak{v}$$
 (3-45)

Master of Science Thesis

Since we are solving an underdetermined equation, it can have infinite many solutions. With the QR factorization, we are trying to find the sparsest or minimal length solution. As \mathfrak{v} can take any value, we set it $\mathfrak{v}=0$ to obtain the aforementioned minimal length solution. Then $[x_r \ T]^{\mathsf{T}}$ can be computed in terms of Z as:

$$\begin{bmatrix} x_r \\ T \end{bmatrix} = \hat{Q}\hat{R}^{-\dagger}Z$$
 (3-46)

Replacing (3-46) in the system's output, we arrive to:

$$\begin{bmatrix} \dot{x}_{in} \\ \dot{\lambda} \\ \dot{Z} \end{bmatrix} \ = \ \begin{bmatrix} -\frac{u_{out}(t)}{m(t)} \cdot I_{p \times p} & 0 & 0 \\ 0 & -\frac{u_{out}(t)}{m(t)} & 0 \\ 0 & 0 & -\frac{u_{out}(t)}{m(t)} \end{bmatrix} \begin{bmatrix} x_{in} \\ \lambda \\ Z \end{bmatrix} + \begin{bmatrix} I_{p \times p} & 0 \\ 0 & 0 \\ \frac{C_{p_{in}}(T_{in} - T_{ref})}{m(t)C_{p_{mix}}(t)} & \frac{1}{m(t)C_{p_{mix}}(t)} \end{bmatrix} \begin{bmatrix} u_{in} \\ Q_{in} \end{bmatrix}$$

$$y = \begin{bmatrix} n \\ T \end{bmatrix} \ = \ \mathcal{C}_1 \begin{bmatrix} x_{in} \\ \lambda \end{bmatrix} + \mathcal{C}_2 \hat{Q} \hat{R}^{-\intercal} Z = \begin{bmatrix} \mathcal{C}_1 & | & \mathcal{C}_2 \hat{Q} \hat{R}^{-\intercal} \end{bmatrix} \begin{bmatrix} x_{in} \\ \lambda \\ Z \end{bmatrix}$$

3-5 Control based on the LPV models

It has been shown that the transformation of the system to a extent representation has served as a foundation for the development of two possible models for control. Each model is tested to check its closed-loop performance. The first model requires a feedforward scheme to get rid of the influence of a disturbance matrix. The second model on the other hand, takes care of the reaction kinetics nonlinearity by means of the variable Z. The performance of both models in controlling the number of moles and temperature in the process are shown and compared in respective case studies.

3-5-1 Case 1: Control based on model with external disturbance

Assume that we want to control the number of moles of A and B in the reactor. We establish:

$$\underbrace{\begin{bmatrix} \dot{x}_{in} \\ \dot{T} \end{bmatrix}}_{\hat{\bar{x}}} = \begin{bmatrix} -\frac{u_{out}(t)}{m(t)} & 0 \\ 0 & -\frac{u_{out}(t)}{m(t)} \end{bmatrix} \underbrace{\begin{bmatrix} x_{in} \\ T \end{bmatrix}}_{\hat{x}} + \begin{bmatrix} 1 & 0 \\ \frac{C_{p_{in}}(T_{in} - T_{ref})}{m(t)C_{p_{mix}}(t)} & \frac{1}{m(t)C_{p_{mix}}(t)} \end{bmatrix} \underbrace{\begin{bmatrix} u_{in} \\ Q_{in} \end{bmatrix}}_{\hat{u}} + \underbrace{\begin{bmatrix} 0 \\ -\Delta H_{\ominus}^{\ominus}N^{\dagger} \\ \overline{\tau(t)m(t)C_{p_{mix}}(t)} \end{bmatrix}}_{\mathcal{B}_{r}} x_{r}$$

$$y = \begin{bmatrix} n_{a} \\ n_{b} \\ T \end{bmatrix} = \mathcal{C}barx + \mathcal{C}_{r}(\theta)x_{r} + \mathcal{C}_{\lambda}\lambda$$

Let us rewrite the previous system as:

$$\dot{\bar{x}} = \mathcal{A}(\theta)\bar{x} + \mathcal{B}(\theta)\bar{u} + \mathcal{B}_r(\theta)x_r \tag{3-47a}$$

$$y = C\bar{x} + C_r(\theta)x_r + C_{\lambda}\lambda \tag{3-47b}$$

(3-47c)

with θ is the parameter vector of the LPV system

Applying Laplace transform and assuming that the function is zero at its initial conditions (dropping θ for simplicity):

$$\mathcal{L}[\dot{\bar{x}}] \longrightarrow s\bar{X} = \mathcal{A}\bar{X} + \mathcal{B}\bar{U} + \mathcal{B}_r X_r \tag{3-48}$$

$$\bar{X} = (sI - \mathcal{A})^{-1} (\mathcal{B}\bar{U} + \mathcal{B}_r X_r) \tag{3-49}$$

Substituting in the output equation and rearranging:

$$y = \mathcal{C}(sI - \mathcal{A})^{-1}\mathcal{B}\bar{U} + (\mathcal{C}(sI - \mathcal{A})^{-1}\mathcal{B}_r + \mathcal{C}_r)X_r + \mathcal{C}_\lambda\lambda$$
(3-50)

The output is:

$$y = \underbrace{\mathcal{C}(sI - \mathcal{A})^{-1}\mathcal{B}}_{G} \bar{U} + \underbrace{(\mathcal{C}(sI - \mathcal{A})^{-1}\mathcal{B}_r + \mathcal{C}_r)}_{G_r} X_r + \underbrace{\mathcal{C}_{\lambda}}_{G_{\lambda}} \lambda$$
(3-51)

If we split the input accordingly as:

$$\bar{U} = \bar{U}_1 + \bar{U}_2 + \bar{U}_3 \tag{3-52}$$

We obtain:

$$y = G(\bar{U}_1 + \bar{U}_2 + \bar{U}_3) + G_r X_r + G_{\lambda} \lambda \tag{3-53}$$

By choosing $\bar{U}_2 = -G^{\dagger}G_rX_r$ and $\bar{U}_3 = -G^{\dagger}G_{\lambda}\lambda$ we can cancel the effect of X_r and λ . These are feedforward transfer functions. U_1 can be calculated with any suitable control strategy. In figure 3-16, a block diagram of the control loop is shown

We develop state-feedback linear quadratic regulator (LQR) control scheme. The system has two independent inlets flows $(u_{in,a} \text{ and } u_{in,b})$ which implies that there are two extents of inlets $(x_{in,a} \text{ and } x_{in,b})$. We want to control the moles of reactants A and B and the temperature in the reactor.

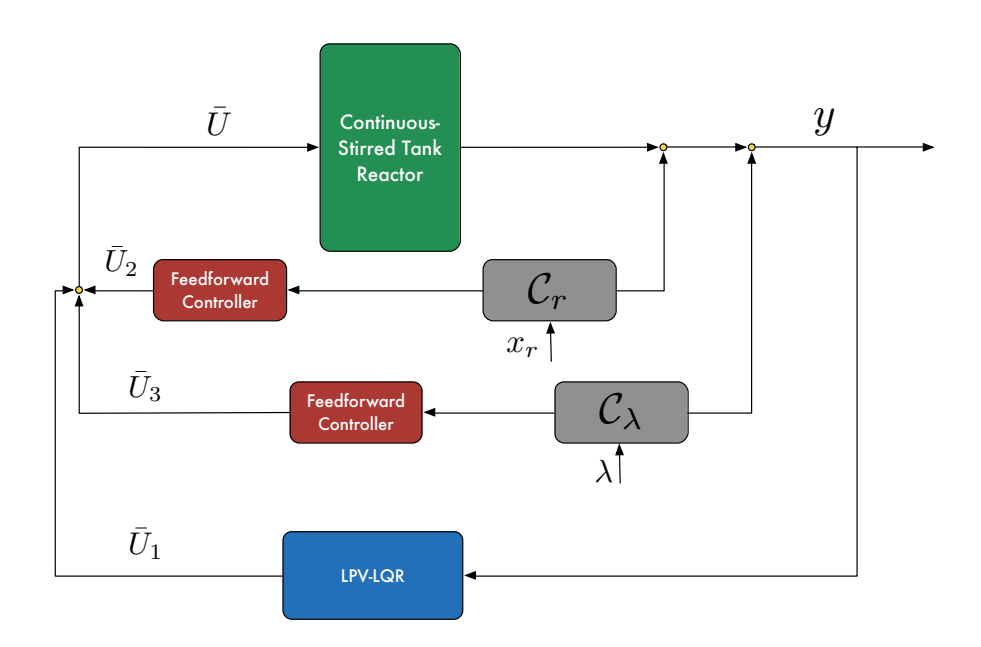


Figure 3-16: Control based on model with external disturbance

$$\begin{bmatrix} \dot{x}_{in,a} \\ \dot{x}_{in,b} \\ \dot{T} \end{bmatrix} = \mathcal{A}(\theta) \begin{bmatrix} x_{in,a} \\ x_{in,b} \\ T \end{bmatrix} + \mathcal{B}(\theta) \begin{bmatrix} u_{in,a} \\ u_{in,b} \\ Q_{in} \end{bmatrix} + \mathcal{B}_r(\theta) x_r$$

$$y = \begin{bmatrix} n_a \\ n_b \\ T \end{bmatrix} = \mathcal{C}x + \mathcal{C}_r(\theta) x_r + \mathcal{C}_{\lambda} \lambda$$

$$\dot{e} = y_{ref} - \mathcal{C}x$$

With system matrices:

$$\mathcal{A}(\theta) = \begin{bmatrix} -\frac{u_{out}(t)}{m(t)} & 0 & 0\\ 0 & -\frac{u_{out}(t)}{m(t)} & 0\\ 0 & 0 & -\frac{u_{out}(t)}{m(t)} \end{bmatrix}, \ \mathcal{B}(\theta) = \begin{bmatrix} 1 & 0 & 0\\ 0 & 1 & 0\\ \frac{C_{p_{in,a}}T_{in,a}}{m(t)C_{p_{mix}}(t)} & \frac{C_{p_{in,b}}T_{in,b}}{m(t)C_{p_{mix}}(t)} & \frac{1}{m(t)C_{p_{mix}}(t)} \end{bmatrix}$$

$$\mathcal{B}_r(\theta) = \begin{bmatrix} 0 \\ 0 \\ \frac{-\Delta H_f^{\ominus} N^{\mathsf{T}}}{\tau(t) m(t) C_{p_{mix}}(t)} \end{bmatrix}, \qquad \qquad \mathcal{C} = \begin{bmatrix} \frac{1}{M_A} & 0 & 0 \\ 0 & \frac{1}{M_B} & 0 \\ 0 & 0 & 1 \end{bmatrix}$$

$$C_r(\theta) = \begin{bmatrix} -1 \\ -1 \\ -\Delta H_f^{\ominus} N^{\mathsf{T}} \\ \overline{\tau(t) m(t) C_{P_{mix}}(t)} \end{bmatrix}, \qquad C_{\lambda} = \begin{bmatrix} n_{0_a} \\ n_{0_b} \\ 0 \end{bmatrix}$$

Now stacking the error dynamics in the states we have:

$$\begin{bmatrix} \dot{x}_{in,a} \\ \dot{x}_{in,b} \\ \dot{T} \\ \dot{e}_{n_a} \\ \dot{e}_{n_b} \\ \dot{e}_{T} \end{bmatrix} = \begin{bmatrix} \mathcal{A}(\theta) & 0_{3\times3} \\ -\mathcal{C} & 0_{3\times3} \end{bmatrix} \begin{bmatrix} x_{in,a} \\ T \\ e_{n_a} \\ e_{n_b} \\ e_{T} \end{bmatrix} + \frac{\begin{bmatrix} \mathcal{B}(\theta) \\ 0_{3\times3} \end{bmatrix}}{\begin{bmatrix} u_{in,a} \\ u_{in,b} \\ Q_{in} \end{bmatrix}} + \frac{\begin{bmatrix} \mathcal{B}_r(\theta) \\ 0_{3\times1} \end{bmatrix}}{\begin{bmatrix} u_{in,a} \\ 0_{3\times1} \end{bmatrix}} x_r + \frac{\begin{bmatrix} 0_{3\times3} \\ 1_{3\times3} \end{bmatrix}}{\begin{bmatrix} I_{3\times3} \end{bmatrix}} y_{ref}$$

$$y = \begin{bmatrix} n_a \\ n_b \\ T \end{bmatrix} = \mathcal{C}x + \mathcal{C}_r(\theta)x_r + \mathcal{C}_{\lambda}\lambda$$

$$\bar{U}_1 = \begin{bmatrix} u_{in,a} \\ u_{in,b} \\ Q_{in} \end{bmatrix} = [-k_p - k_i] \begin{bmatrix} x_{in,a} \\ x_{in,b} \\ T \\ e_{n_a} \\ e_{n_b} \\ e_{T} \end{bmatrix}$$

The parameters of the matrices $\mathcal{A}(\theta)$, $\mathcal{B}(\theta)$, $\mathcal{B}_r(\theta)$, and $\mathcal{C}_r(\theta)$ vary pointwise and assumed the inlet temperature T_0 keeps constant. Hence:

•
$$T_{in,a} = T_{in,b} = T_0 = 373 \text{ K}$$

• With
$$\theta(t) = \begin{bmatrix} u_{out}(t) \\ m(t) \\ C_{p_{mix}}(t) \end{bmatrix}$$

Choosing the LQR weighting matrices \mathbf{Q} and \mathbf{R} as follows, we can calculate \bar{U}_1 :

$$\mathbf{Q} = \begin{bmatrix} 10^2 \cdot I_{3\times3} & 0_{3\times2} & 0_{3\times1} \\ 0_{2\times3} & 2\times10^3 \cdot I_{2\times2} & 0_{2\times1} \\ 0_{1\times3} & 0_{1\times2} & 7.5\times10^2 \end{bmatrix}, \ \mathbf{R} = \operatorname{diag}(15, \ 15, \ 1.95\times10^{-3})$$

And the feedforward gains:

$$\bar{U}_2 = -\frac{\bar{G}^{\dagger}\bar{G}_r}{(0.001s+1)}\bigg|_{s=0} = \begin{bmatrix} 3.870\\ 2.065\\ 5413.44 \end{bmatrix}$$

$$\bar{U}_3 = -\frac{\bar{G}^{\dagger}G_{\lambda}}{(0.001s+1)}\bigg|_{s=0} = \begin{bmatrix} -1.935\\ -2.065\\ 3408.81 \end{bmatrix}$$

Setting the following reference changes:

$$n_a = 0.5 \text{ mol} \xrightarrow{t=50h} 1 \text{ mol}$$

 $n_b = 1 \text{ mol} \xrightarrow{t=90h} 0.75 \text{ mol}$
 $T = 373 \text{ K} \rightarrow 373 \text{ K}$

with initial conditions $n_0 = [0.5 \ 1 \ 0 \ \varepsilon = 0.0001]^{\mathsf{T}}$

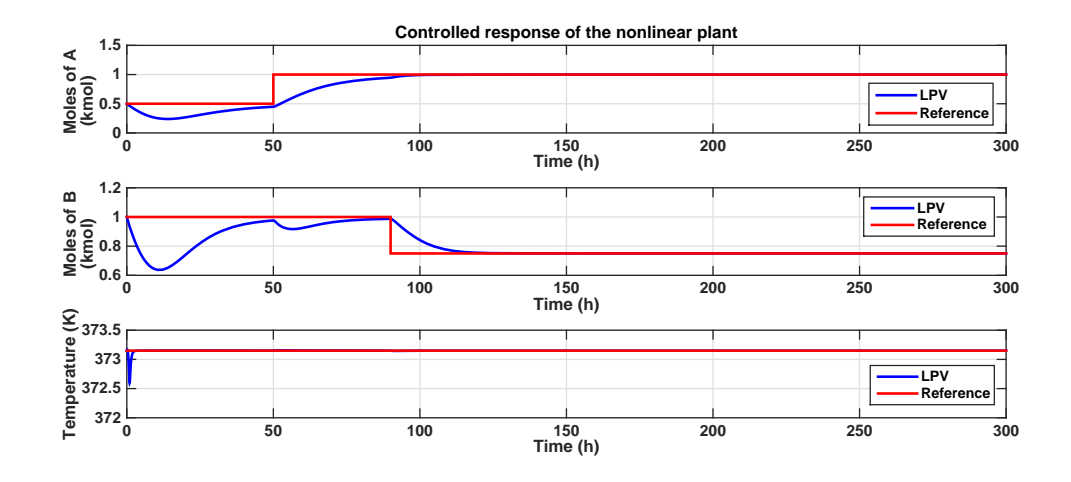


Figure 3-17: LPV-model-based LQR controllers for reference tracking

In figure 3-17, the controlled responses of the nonlinear plant with the LPV-model-based controller are displayed. It is observed that the target compositions and temperature are tracked with no steady-state error with very good settling time. However, the transient behavior reaches the reference signals with some delay due to the cancellation with the feedforward gains of the effects of x_r and λ ; these two parameters are needed for a perfect reconstruction of the moles as established in (3-26), thus, eliminating their contribution affect the unsteady-state dynamics.

In figure 3-18, the controlled actions of the LPV-model-based controller are shown. It can be seen that the mass flows remain bounded to $10~\rm kg/h$, which is a reasonable amount of mass. On the other hand, when the temperature is decreased due to the interaction of A and B in the reactor, the heat duty presents its highest value at approximately 3000 kJ to increase the temperature and regulate it around 373 K.

3-5-2 Case 2: Control with change of variable Z

Control of composition of reactants A and B

Take $n_0 = [0.5 \ 1 \ 0 \ 0.0001]^{\mathsf{T}}$ and $T_0 = 373K \approx 100^{\circ} C$. We want to control concentrations of reactants A and B and the internal temperature. The system is described by:

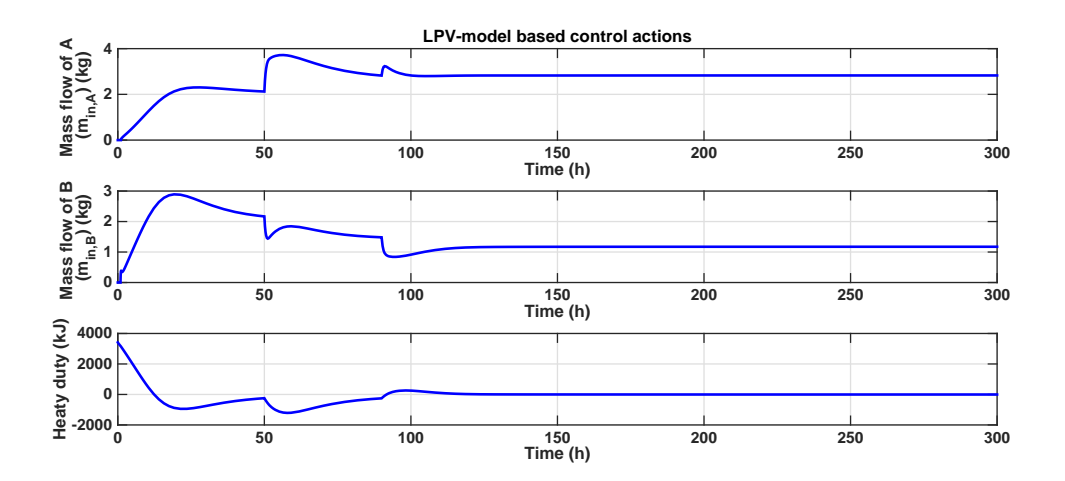


Figure 3-18: LPV-model-based LQR controllers control actions

$$\begin{bmatrix} \dot{x}_{in,a} \\ \dot{x}_{in,b} \\ \dot{\lambda} \\ \dot{Z} \end{bmatrix} = \mathcal{A}(\theta) \begin{bmatrix} x_{in,a} \\ x_{in,b} \\ \lambda \\ Z \end{bmatrix} + \mathcal{B}(\theta) \begin{bmatrix} u_{in,a} \\ u_{in,b} \\ Q_{in} \end{bmatrix}$$

$$y = \begin{bmatrix} n_a \\ n_b \\ T \end{bmatrix} = \mathcal{C}(\theta) \begin{bmatrix} x_{in,a} \\ x_{in,b} \\ \lambda \\ Z \end{bmatrix}$$

$$\dot{e} = y_{ref} - y = \begin{bmatrix} n_{a_{ref}} \\ n_{b_{ref}} \\ T_{ref} \end{bmatrix} - \begin{bmatrix} n_a \\ n_b \\ T \end{bmatrix} = y_{ref} - \mathcal{C}x$$

With system matrices:

$$\mathcal{A}(\theta) = \begin{bmatrix} -\frac{u_{out}(t)}{m(t)} & 0 & 0 & 0\\ 0 & -\frac{u_{out}(t)}{m(t)} & 0 & 0\\ 0 & 0 & -\frac{u_{out}(t)}{m(t)} & 0\\ 0 & 0 & 0 & -\frac{u_{out}(t)}{m(t)} \end{bmatrix}, \ \mathcal{B}(\theta) = \begin{bmatrix} 1 & 0 & 0\\ 0 & 1 & 0\\ 0 & 0 & 0\\ \frac{C_{p_{in,a}}T_{in,a}}{m(t)C_{p_{mix}}(t)} & \frac{C_{p_{in,b}}T_{in,b}}{m(t)C_{p_{mix}}(t)} & \frac{1}{m(t)C_{p_{mix}}(t)} \end{bmatrix}$$

$$\mathcal{C}(\theta) = \begin{bmatrix} \begin{bmatrix} \frac{1}{M_A} & 0 & n_{0_A} \\ 0 & \frac{1}{M_B} & n_{0_B} \\ 0 & 0 & 0 \end{bmatrix} \begin{bmatrix} -1 & 0 \\ -1 & 0 \\ 0 & 1 \end{bmatrix} \cdot \hat{Q} \hat{R}^{-\mathsf{T}} \end{bmatrix}$$

Now appending the error dynamics to the states, we have:

$$\begin{bmatrix} \dot{x}_{in,a} \\ \dot{x}_{in,b} \\ \dot{\lambda} \\ \dot{z} \\ e_{\dot{n}_a} \\ e_{\dot{n}_b} \\ e_{\dot{T}} \end{bmatrix} = \begin{bmatrix} \mathcal{A}(\theta) & 0_{4\times3} \\ -\mathcal{C}(\theta) & 0_{3\times3} \end{bmatrix} \begin{bmatrix} x_{in,a} \\ \lambda \\ Z \\ e_{n_a} \\ e_{n_b} \\ e_{T} \end{bmatrix} + \frac{\left[\mathcal{B}(\theta)\right]}{\left[0_{3\times3}\right]} \begin{bmatrix} u_{in,a} \\ u_{in,b} \\ Q_{in} \end{bmatrix} + \frac{\left[0_{4\times3}\right]}{\left[1_{3\times3}\right]} y_{ref}$$

$$u = \begin{bmatrix} u_{in,a} \\ u_{in,b} \\ Q_{in} \end{bmatrix} = [-k_p - k_i] \begin{bmatrix} x_{in,a} \\ x_{in,b} \\ \lambda \\ Z \\ e_{n_a} \\ e_{n_b} \\ e_{T} \end{bmatrix}$$

Choosing the LQR weighting matrices as follows, we calculate u:

$$\mathbf{Q} = \begin{bmatrix} 10^2 \cdot I_{4 \times 4} & 0_{4 \times 2} & 0_{4 \times 1} \\ 0_{2 \times 4} & 2 \times 10^3 \cdot I_{2 \times 2} & 0_{2 \times 1} \\ 0_{1 \times 4} & 0_{1 \times 2} & 7.5 \times 10^2 \end{bmatrix} \quad \mathbf{R} = \operatorname{diag}(15, 15, 1.95 \times 10^{-3})$$

Setting the following reference changes:

$$n_a = 0.5 \text{ kmol} \xrightarrow{t=50h} 1 \text{ kmol}$$

 $n_b = 1 \text{ kmol} \xrightarrow{t=90h} 0.75 \text{ kmol}$
 $T = 373 \text{ K} \rightarrow 373 \text{ K}$

In figure 3-19, the controlled responses of the nonlinear plant with the LPV-model-based controller are displayed. It is observed that the target compositions and temperature are tracked with no steady-state error with very good settling time. Notice in this case, since the variable Z takes into account the dynamics of x_r , and λ is a state of our system, the transient response is faster, allowing the controlled variables reach the reference signal. This translates into an improvement of the reference tracking performance with respect to the previous feedforward scheme, where the transient response was slower because the reaction dynamics were canceled by the action of the feedforward controllers.

In figure 3-20, the controlled actions of the LPV-model-based controller are shown. It can be seen that the mass flows remain bounded to 10 kg/h, which is a reasonable amount of mass to achieve the target composition. The heat duty is varied accordingly, without abrupt changes, to keep the temperature at the reference value.

Control of composition of product C

Take again $n_0 = [0.5 \ 1 \ 0 \ 0.0001]^{\mathsf{T}}$ and $T_0 = 373K \approx 100^{\circ} C$. This time, we want to control concentrations of product C and the internal temperature. The system is described by:

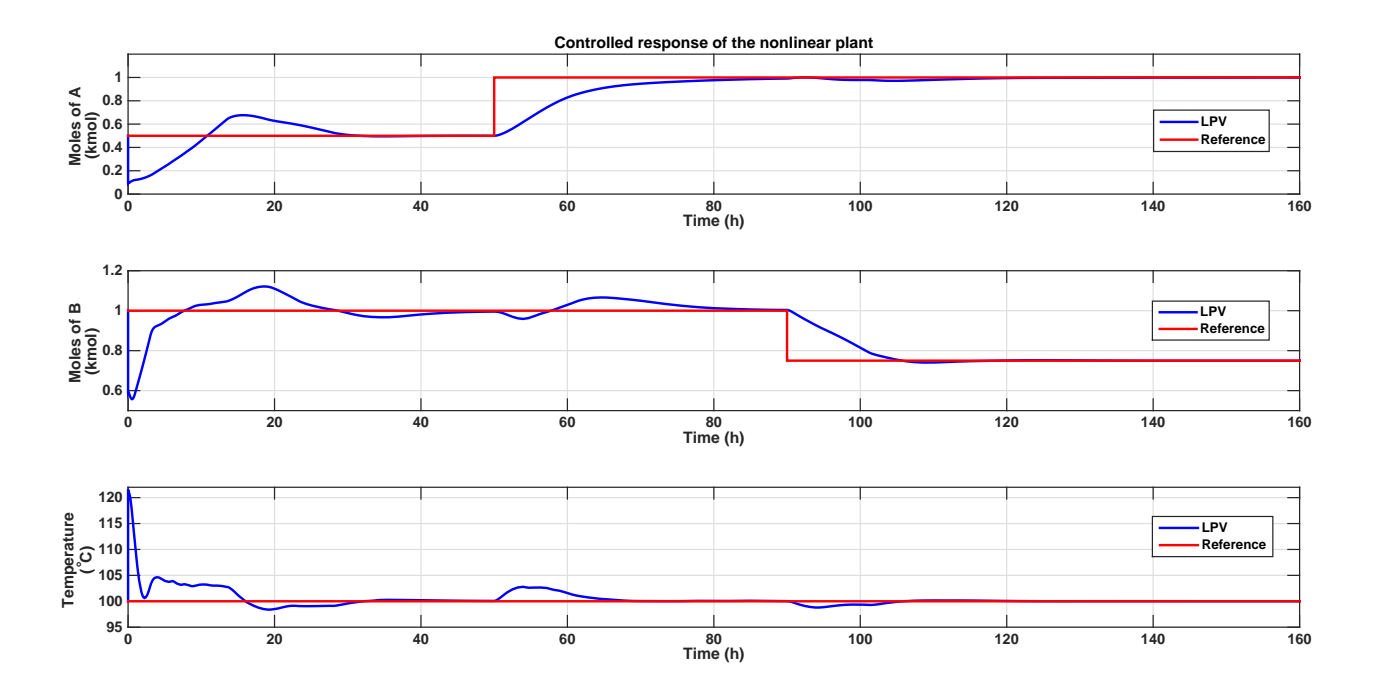


Figure 3-19: LPV-model-based LQR controllers for reference tracking

$$\begin{bmatrix} \dot{x}_{in,a} \\ \dot{x}_{in,b} \\ \dot{\lambda} \\ \dot{z} \end{bmatrix} = \mathcal{A}(\theta) \begin{bmatrix} x_{in,a} \\ x_{in,b} \\ \lambda \\ Z \end{bmatrix} + \mathcal{B}(\theta) \begin{bmatrix} u_{in,a} \\ u_{in,b} \\ Q_{in} \end{bmatrix}$$

$$y = \begin{bmatrix} n_c \\ T \end{bmatrix} = \mathcal{C}(\theta) \begin{bmatrix} x_{in,a} \\ x_{in,b} \\ \lambda \\ Z \end{bmatrix}$$

$$\dot{e} = y_{ref} - y = \begin{bmatrix} n_{c_{ref}} \\ T_{ref} \end{bmatrix} - \begin{bmatrix} n_c \\ T \end{bmatrix} = y_{ref} - \mathcal{C}x$$

With system matrices:

$$\mathcal{A}(\theta) = \begin{bmatrix} -\frac{u_{out}(t)}{m(t)} & 0 & 0 & 0 \\ 0 & -\frac{u_{out}(t)}{m(t)} & 0 & 0 \\ 0 & 0 & -\frac{u_{out}(t)}{m(t)} & 0 \\ 0 & 0 & 0 & -\frac{u_{out}(t)}{m(t)} \end{bmatrix}, \ \mathcal{B}(\theta) = \begin{bmatrix} 1 & 0 & 0 \\ 0 & 1 & 0 \\ 0 & 0 & 0 \\ \frac{C_{p_{in,a}}T_{in,a}}{m(t)C_{p_{mix}}(t)} & \frac{C_{p_{in,b}}T_{in,b}}{m(t)C_{p_{mix}}(t)} & \frac{1}{m(t)C_{p_{mix}}(t)} \end{bmatrix}$$

$$\mathcal{C}(\theta) = \begin{bmatrix} \begin{bmatrix} 0 & 0 & n_{0_C} \\ 0 & 0 & 0 \end{bmatrix} \end{bmatrix} \begin{bmatrix} 1 & 0 \\ 0 & 1 \end{bmatrix} \cdot \hat{Q} \hat{R}^{-\mathsf{T}} \end{bmatrix}$$

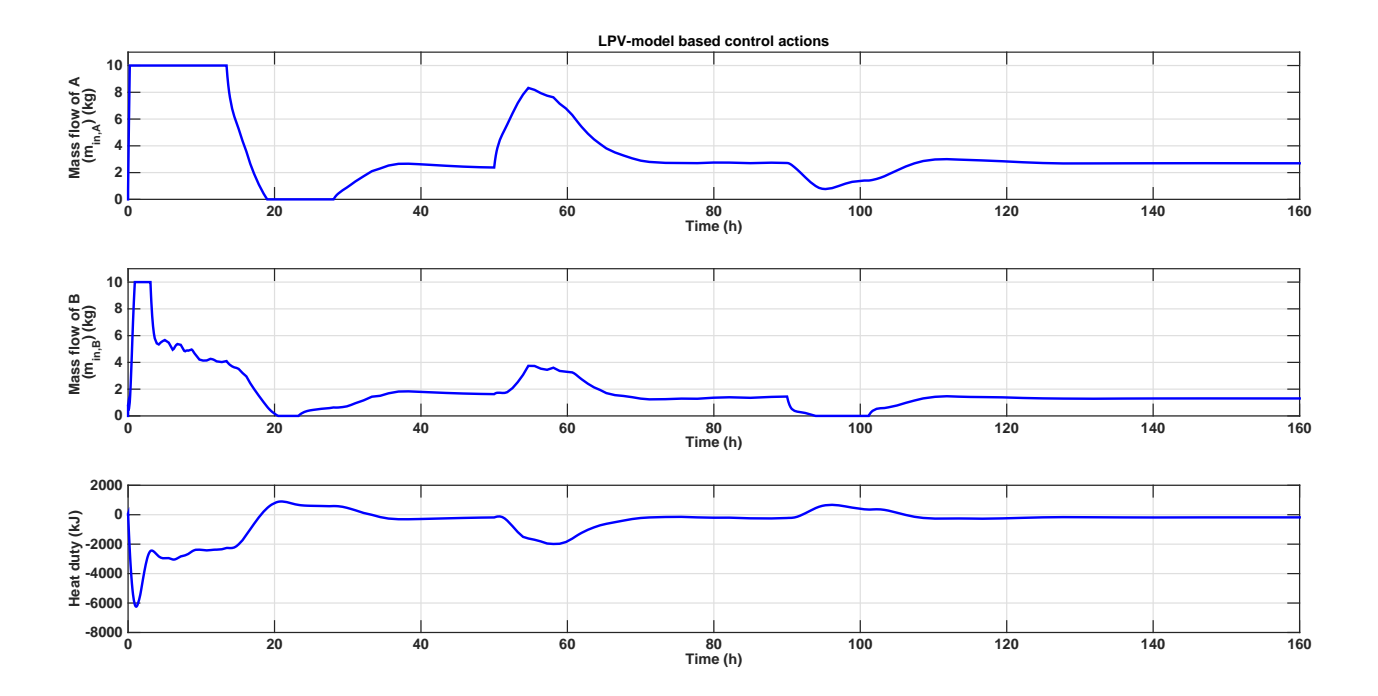


Figure 3-20: LPV-model-based LQR controllers control actions

Stacking again the error dynamics in the state vector, we have:

$$\begin{bmatrix} \dot{x}_{in,a} \\ \dot{x}_{in,b} \\ \dot{\lambda} \\ \dot{z} \\ e_{n_c} \\ \dot{e}_T \end{bmatrix} = \underbrace{\begin{bmatrix} \mathcal{A}(\theta) & 0_{4\times 2} \\ -\mathcal{C}(\theta) & 0_{2\times 2} \end{bmatrix}}_{\mathcal{A}_e} \begin{bmatrix} x_{in,a} \\ \lambda \\ Z \\ e_{n_c} \\ e_T \end{bmatrix} + \underbrace{\begin{bmatrix} \mathcal{B}(\theta) \\ 0_{2\times 3} \end{bmatrix}}_{\mathcal{B}_e} \begin{bmatrix} u_{in,a} \\ u_{in,b} \\ Q_{in} \end{bmatrix} + \underbrace{\begin{bmatrix} 0_{4\times 2} \\ I_{2\times 2} \end{bmatrix}}_{\mathbf{yref}} y_{ref}$$

$$u = \begin{bmatrix} u_{in,a} \\ u_{in,b} \\ Q_{in} \end{bmatrix} = [-k_p - k_i] \begin{bmatrix} x_{in,a} \\ \lambda \\ Z \\ e_{n_c} \\ e_T \end{bmatrix}$$

For the LQR control, let us use the same weighting matrices \mathbf{Q} and \mathbf{R} used in the control of reactants A and B, respectively.

To employ LQR, recall that two conditions must be satisfied:

- The pair (A_e, B_e) must be stabilizable.
- The pair $(\mathcal{A}_e^{\intercal}, \mathbf{Q})$ must not have uncontrollable modes on the imaginary axis.

In this case, for the control of n_c

- The pair $(\mathcal{A}_e^{\intercal}, \mathbf{Q})$ is fully controllable \checkmark
- The pair $(\mathcal{A}_e, \mathcal{B}_e)$ has an uncontrollable mode at $0 \Rightarrow \text{Not stabilizable}$.

By the extents' relation, we know:

$$n_a = \nu_a x_r + \frac{1}{M_a} x_{in_a} + n_{0_a} \lambda \tag{3-54}$$

$$n_b = \nu_b x_r + \frac{1}{M_b} x_{in_b} + n_{0_b} \lambda \tag{3-55}$$

$$n_c = \nu_c x_r \tag{3-56}$$

Adding equations (3-54) and (3-55) and solving for x_r , we obtain:

$$x_r = \frac{n_a + n_b - \left(\frac{1}{M_a}x_{in_a} + \frac{1}{M_b}x_{in_b}\right) - (n_{0_a} + n_{0_b})\lambda}{\nu_a + \nu_b}$$
(3-57)

Substituting equation (3-57) in (3-56), we can write n_c in terms of the states:

$$n_c = \frac{\nu_c}{\nu_a + \nu_b} \left(n_a + n_b - \left(\frac{1}{M_a} x_{in_a} + \frac{1}{M_b} x_{in_b} \right) - (n_{0_a} + n_{0_b}) \lambda \right)$$
(3-58)

Using (3-58), the output y can be rewritten as:

$$y = \begin{bmatrix} n_c \\ T \end{bmatrix} = \begin{bmatrix} \begin{bmatrix} -\frac{\nu_c}{M_a(\nu_a + \nu_b)} & -\frac{\nu_c}{M_b(\nu_a + \nu_b)} & -\frac{\nu_c}{\nu_a + \nu_b}(n_{0a} + n_{0b}) \end{bmatrix} \begin{bmatrix} 0 & 0 \\ 0 & 1 \end{bmatrix} \cdot \hat{Q}\hat{R}^{-\mathsf{T}} \end{bmatrix} \begin{bmatrix} x_{in_a} \\ x_{in_b} \\ \lambda \\ Z \end{bmatrix} + \underbrace{\begin{bmatrix} \frac{\nu_c}{\nu_a + \nu_b}(n_a + n_b) \\ 0 & 1 \end{bmatrix}}_{M}$$

Note that the matrix \mathcal{M} is acting as a disturbance on the output.

The recast output allows for a stabilizable pair (A_e, \mathcal{B}_e) . We can now design an LQR-based controller to control n_c and use a feed-forward scheme to get rid of the influence of \mathcal{M} as:

$$u = u_1 + u_2$$

With

$$u_1 = \begin{bmatrix} u_{in,a} \\ u_{in,b} \\ Q_{in} \end{bmatrix} = \begin{bmatrix} -k_p & -k_i \end{bmatrix} \begin{bmatrix} x_{in,a} \\ x_{in,b} \\ \lambda \\ Z \\ e_{n_c} \\ e_T \end{bmatrix} \text{ and } u_2 = (\mathcal{C}_e(sI - \mathcal{A}_e)^{-1}\mathcal{B}_e)^{\dagger} \Big|_{s=0} \mathcal{M}$$

Setting the following reference changes:

$$n_c = 0 \text{ kmol} \xrightarrow{t=10h} 2 \text{ kmol}$$

 $T = 373 \text{ K} \rightarrow 373 \text{ K}$

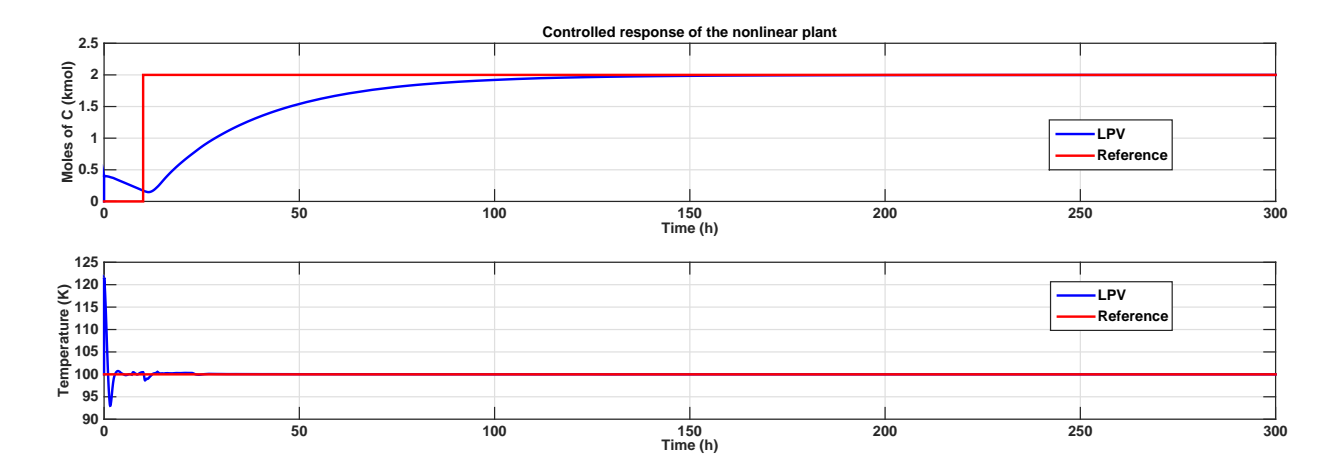


Figure 3-21: LPV-model-based LQR controllers for reference tracking

In figure 3-21, the controlled responses of the nonlinear plant with the LPV-model-based controller are displayed. It is observed that the target compositions and temperature are tracked with no steady-state error. However, the settling time is extremely slow because of the reaction kinetics. This can be improved by fine-tuning the weighting matrices $\mathcal Q$ and $\mathcal R$ from the LQR controller to achieve a better performance.

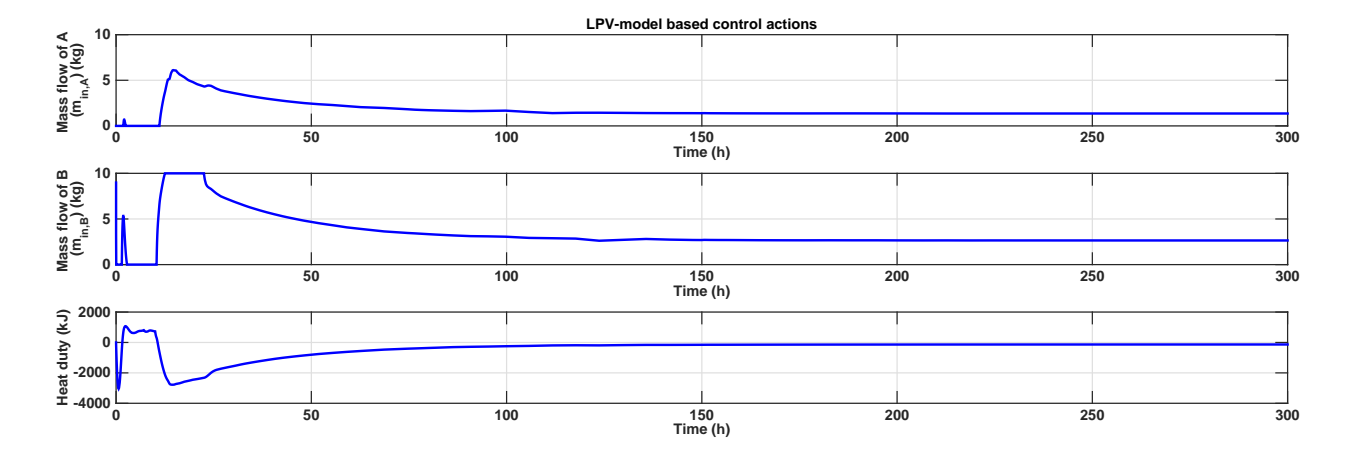


Figure 3-22: LPV-model-based LQR controllers control actions

In figure 3-22, the controlled actions of the LPV-model-based controller are shown. It can be seen that the mass flows remain bounded to 10 kg/h, which is a reasonable amount of mass to achieve the target composition. The heat duty is varied accordingly, without abrupt changes, to keep the temperature at the reference value.

Extension of the Extent Transformations to Multiphase Reaction Systems

In chapter 3, the extents transformation were introduced. This transformation decomposed the chemical species space into the reaction space, the inlet space and the invariant space. Moreover, this technique was only applied to reactors where liquid-phase reactions took place with no phase-change. Nevertheless, in a reactive batch distillation column, vaporization of the liquid is required to perform distillation, hence, the mathematical framework must be extended to this type of processes where two phases coexist. In this chapter, the extension of the extent representation to multiphase reaction system will be introduced; showing first the simplest case (continuous process) to later develop on the more complex case (batch process).

4-1 Continuous Gas-Liquid Reaction Systems

For processes where gas inlet and outlet streams are present, like in the absorption process or where there is a continuous vaporization like in the distillation process, there are more dynamics involved in the system. These dynamics correspond to the liquid and vapor phase as well as their mutual interactions. Therefore, in order to perform the decomposition into the extent representation, the liquid and vapor phase behaviors must be treated separately.

The work of Bhatt et al. (Bhatt et al., 2010) extended the application of the extent transformation to gas-liquid reactive systems. Though the approach is very similar to the original formulation of the extent transformation for CSTR's, in their extension, the authors make certain assumptions to model the process:

- The reactions only take place in the liquid phase
- The reactor has a constant total volume

- The reactor has independent gas and liquid inlets
- The mass-transfer phenomena are described by the two-film theory with no accumulation in the boundary layer.

In figure 4-1, a scheme of the process to be modeled is presented. The process according to the Bhatt et al. is modeled considering the liquid and gas phase separately with the mass transfer rates ζ_{gl} and ζ_{lg} connecting the two phases. Moreover, these aforementioned rates are combined in a single vector ζ , following the convention that the mass transfer rate from the gas phase to the liquid phase is positive, whereas the mass transfer from the liquid phase to the gas phase is negative:

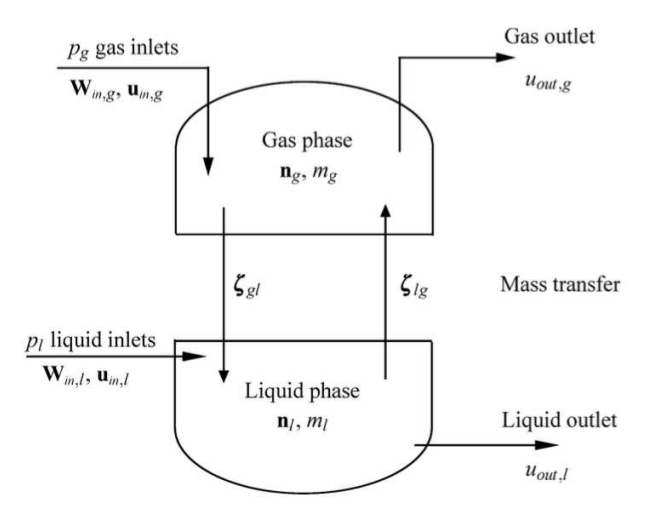


Figure 4-1: Representation of the gas-liquid reaction system (Bhatt et al., 2010)

$$\zeta = \begin{bmatrix} \zeta_{gl} \\ -\zeta_{lg} \end{bmatrix}$$

The mole balance for the gas and liquid phase is (Bhatt et al., 2010):

Gas phase

$$\dot{n}_g = W_{in,g} u_{in,g}(t) + W_{m,g} \zeta(t) - \frac{u_{out,g}(t)}{m_g(t)} n_g(t) \qquad n_g(0) = n_{g,0}$$
(4-1)

$$\implies \dot{n}_g = \begin{bmatrix} W_{in,g} & W_{m,g} \end{bmatrix} \begin{bmatrix} u_{in,g}(t) \\ \zeta(t) \end{bmatrix} - \frac{u_{out,g}(t)}{m_g(t)} n_g(t) \qquad n_g(0) = n_{g,0}$$
 (4-2)

Liquid phase

$$\dot{n}_{l} = \mathcal{V}_{l}(t)N^{\mathsf{T}}r(t) + W_{in,l}u_{in,l}(t) + W_{m,l}\zeta(t) - \frac{u_{out,l}(t)}{m_{l}(t)}n_{l}(t) \quad n_{l}(0) = n_{l,0} \quad (4-3)$$

$$\implies \dot{n}_l = \mathcal{V}_l(t) N^{\dagger} r(t) + \begin{bmatrix} W_{in,l} & W_{m,l} \end{bmatrix} \begin{bmatrix} u_{in,l}(t) \\ \zeta(t) \end{bmatrix} - \frac{u_{out,l}(t)}{m_l(t)} n_l(t) \qquad n_l(0) = n_{l,0} \quad (4\text{-}4)$$

where n_{π} is the $S_{\pi} \times 1$ vector number of moles in the π -th phase, $\pi \in \{g, l\}$, \mathcal{V} is the reaction mixture volume; r is the $R \times 1$ reaction kinetics vector; $u_{in,\pi}$ and $u_{out,\pi}$ are the inlet and outlet mass flows; m_{π} is the total mass; N is the $R \times S_{\pi}$ stoichiometric coefficient matrix, $W_{in,\pi}$ is the $S_{\pi} \times p_{\pi}$ inlet composition matrix defined as $W_{in,\pi} = M_{w,\pi}^{-1} w_{in,\pi}$; $M_{w,\pi}$ is the $S_{\pi} \times S_{\pi}$ diagonal molecular weight matrix and $w_{in,\pi}$ the $S_{\pi} \times p_{\pi}$ matrix of weight fraction; $W_{m,\pi}$ is the $S_{\pi} \times p_{m}$ mass transfer matrix defined as $W_{m,p} = M_{w,\pi}^{-1} E_{m,\pi}$; $E_{m,\pi}$ the $S_{\pi} \times p_{\pi}$ matrix with elements of 1's and 0's corresponding to the species that are transferred.

The transformation sought for the gas-liquid reactive system is (Bhatt et al., 2010):

Gas phase

$$n_g \longmapsto \begin{bmatrix} x_{in_g} \\ \lambda_g \end{bmatrix} = \underbrace{\begin{bmatrix} \mathcal{T}_{2g,0}^{\mathsf{T}} \\ \tau_{3g,0}^{\mathsf{T}} \end{bmatrix}}_{\mathcal{T}_{g,0}} n_g \tag{4-5}$$

With

$$\mathcal{T}_{2g,0}^{\mathsf{T}} = \mathcal{T}_{g,2}^{\mathsf{T}} (I_S - n_{g,0} \tau_{3_0}^{\mathsf{T}}) \text{ and } \tau_{3g,0}^{\mathsf{T}} = \frac{1_{S_l - R - p_l}^{\mathsf{T}} \mathcal{T}_{g,3}^{\mathsf{T}}}{1_{S_l - R - p_l}^{\mathsf{T}} \mathcal{T}_3^{\mathsf{T}} n_{g,0}}$$
(4-6)

Where $\mathcal{T}_{2g,0}$ is the transformation matrix of the inlet space in the gas phase, $\mathcal{T}_{3g,0}$ is the transformation matrix of the reaction and inlet invariant space in the gas phase, all with discounted initial conditions $n_{g,0}$ and $\tau_{3g,0}$ is the ratio between inlet invariant space at initial conditions $n_{g,0}$ in the liquid phase.

With this transformation, (4-2) is brought to:

$$\dot{x}_{in,g} = u_{in,g}(t) - \frac{u_{out}(t)}{m(t)} x_{in,g} \qquad x_{in,g}(0) = 0$$
 (4-7)

$$\dot{x}_{m,g} = \zeta - \frac{u_{out,g}(t)}{m_g(t)} x_{m,g}$$
 $x_{m,g}(0) = 0$ (4-8)

$$\dot{\lambda}_g = -\frac{u_{out,g}(t)}{m_g(t)} \lambda_g \qquad \lambda_g(0) = 1 \tag{4-9}$$

Liquid phase

$$n_l \longmapsto \begin{bmatrix} x_{r_l} \\ x_{in_l} \\ \lambda_l \end{bmatrix} = \underbrace{\begin{bmatrix} \mathcal{T}_{1_{l,0}}^\mathsf{T} \\ \mathcal{T}_{2_{l,0}}^\mathsf{T} \\ \tau_{3_{l,0}}^\mathsf{T} \end{bmatrix}}_{\mathcal{T}_{1,0}} n_l \tag{4-10}$$

With

$$\mathcal{T}_{1_{l,0}}^{\mathsf{T}} = \mathcal{T}_{l,1}^{\mathsf{T}}(I_S - n_{l,0}\tau_{3_{l,0}}^{\mathsf{T}}), \quad \mathcal{T}_{2_{l,0}}^{\mathsf{T}} = \mathcal{T}_{l,2}^{\mathsf{T}}(I_S - n_{l,0}\tau_{3_0}^{\mathsf{T}}) \text{ and } \tau_{3_{l,0}}^{\mathsf{T}} = \frac{1_{S_l - R - p_l}^{\mathsf{T}}\mathcal{T}_{l,3}^{\mathsf{T}}}{1_{S_l - R - p_l}^{\mathsf{T}}\mathcal{T}_3^{\mathsf{T}}n_{l,0}}$$
 (4-11)

Where $\mathcal{T}_{1_{l,0}}$ is the transformation matrix of the reaction in the liquid phase space, $\mathcal{T}_{2_{l,0}}$ is the transformation matrix of the inlet space in the liquid phase, $\mathcal{T}_{3_{l,0}}$ is the transformation matrix of the reaction and inlet invariant space in the liquid phase, all with discounted initial conditions $n_{l,0}$ and $\tau_{3_{l,0}}$ is the ratio between reaction and inlet invariant space at initial conditions $n_{l,0}$ in the liquid phase.

With this transformation, (4-4) is brought to:

$$\dot{x}_r = \mathcal{V}_l(t)r(t) - \frac{u_{out,l}(t)}{m_l(t)}x_r \qquad x_r(0) = 0$$
 (4-12)

$$\dot{x}_{in,l} = u_{in,l}(t) - \frac{u_{out,l}(t)}{m_l(t)} x_{in,l} \qquad x_{in}(0) = 0$$
(4-13)

$$\dot{x}_{m,l} = \zeta - \frac{u_{out,l}(t)}{m_l(t)} x_{m,l} \qquad x_{m,l}(0) = 0$$
 (4-14)

$$\dot{\lambda}_l = -\frac{u_{out,l}(t)}{m_l(t)} \lambda_l \qquad \lambda_l(0) = 1 \tag{4-15}$$

4-2 Batch Gas-Liquid Reaction Systems

Based on this approach introduced in the previous section, we can use its properties to decompose the reactive batch distillation process. However, note that the procedure is not as straightforward as the case presented above because of important differences:

- The volume or mass in the reactor is not constant. Part of the products are drawn out of the reactor through the distillation column.
- There is no independent gas inlet.
- The liquid inlet (liquid flow) is not independent from the gas outlet (vapor flow); the liquid flow contains the condensed species of the vapor flow.

Let us perform the mass balance in the gas and liquid phases in the reactor of the reactive reactive distillation column with R_I reactions, p inlets and v outlets:

$$\dot{n}_g = W_{m,g}\zeta(t) - n_g(t)\frac{u_{out,g}(t)}{m_g(t)} = W_{m,g}\zeta(t) - W_{out,g}(t)u_{out,g}(t), \quad n_g(0) = 0 \quad (4-16)$$

$$\dot{n}_l = \mathcal{V}_l(t) N^{\dagger} r(t) + W_{in,l}(t) u_{in,l}(t) + W_{m,l} \zeta(t), \quad n_l(0) = n_{l,0}$$
(4-17)

where $W_{out,g}$ is the $S \times v$ outlet composition matrix defined as $W_{out,g} = M_w^{-1} w_{out,g}$; $M_{w,p}$ is the $S \times S$ diagonal molecular weight matrix and $w_{out,g}$ the $S \times v$ matrix of weight fraction. Adding (4-16) and (4-17), we obtain:

$$\dot{n}_{g} + \dot{n}_{l} = \mathcal{V}_{l}(t)N^{\mathsf{T}}r(t) + W_{in,l}(t)u_{in,l}(t) + (W_{m,g} + W_{m,l})\begin{bmatrix} \zeta_{gl}(t) \\ -\zeta_{lg}(t) \end{bmatrix} - W_{out,g}(t)u_{out,g}(t) \quad (4-18)$$

Frequently in distillation processes, the accumulation of moles in the gas phase \dot{n}_g is negligible with respect to the accumulation of moles in the liquid phase \dot{n}_l for processes with operating at relative low pressure (usually less than 10 bar). (Luyben, 2012). Additionally, the mass transfer occurs among the same species, it is obvious that $\zeta_{lg} = \zeta_{gl}$ and $W_{m,l} = W_{m,g}$. Hence:

$$\dot{n}_l = \mathcal{V}_l(t) N^{\mathsf{T}} r(t) + W_{in,l}(t) u_{in,l}(t) - W_{out,q}(t) u_{out,q}(t), \quad n_l(0) = n_{l,0}$$
(4-19)

First, notice that the component mass balance of the reactor (4-19) is analogous to equation (3-10). The contributions from the reaction, the inlet flow and outlet flow are evident, but in the case of the reactive batch distillation, the outlet is a vapor flow. In general, all of the species are present in the gas phase; however, we can exploit the fact that in distillation processes species are chemically different and exhibit distinct boiling points. This allows us to simplify the model only taking the most volatile species with a matrix $\mathbb{B} \in \mathbb{R}^{S \times S}$.

 \mathbb{B} works as a selection matrix with 1's on the elements corresponding to the most volatile species and 0's elsewhere. However, note that $\mathbb{B} \in \mathbb{R}^{S \times S}$ but $\operatorname{rank}(\mathbb{B}) = e < S$, where e is the number of volatile species under the operating conditions. Moreover, its columns space is spanned by orthonormal vectors, hence, the matrix \mathbb{B} is idempotent and can be written as:

$$\mathbb{B} = \mathfrak{b}\mathfrak{b}^{\dagger} \tag{4-20}$$

where $\mathfrak{b} \in \mathbb{R}^{S \times e}$

Using (4-20), the approximation of the inlet and outlet is performed:

$$W_{in,l}(t)u_{in,l}(t) - W_{out,g}(t)u_{out,g}(t) \approx \mathbb{B}(W_{in,l}(t)u_{in,l}(t) - W_{out,g}(t)u_{out,g}(t))$$
(4-21)

$$= \mathfrak{bb}^{\dagger}(W_{in,l}(t)u_{in,l}(t) - W_{out,q}(t)u_{out,q}(t)) \tag{4-22}$$

$$= \mathfrak{b}(\mathfrak{b}^{\dagger}W_{in,l}(t)u_{in,l}(t) - \mathfrak{b}^{\dagger}W_{out,g}(t)u_{out,g}(t)) \qquad (4-23)$$

$$= b(W_{in,l}^{e}(t)u_{in,l}(t) - W_{out,g}^{e}(t)u_{out,g}(t))$$
(4-24)

where $W_{in,l}^e \in \mathbb{R}^{e \times p}$, $W_{out,g}^e \in \mathbb{R}^{e \times v}$.

Plugging (4-24) in (4-19), we can write the balance as:

$$\dot{n}_l = \mathcal{V}_l(t) N^{\dagger} r(t) + \mathfrak{b}(W^e_{in,l}(t) u_{in,l}(t) - W^e_{out,q}(t) u_{out,q}(t)), \quad n_l(0) = n_{l,0}$$
(4-25)

Again, we are looking for a linear transformation:

$$n \longmapsto \begin{bmatrix} x_r \\ x_{io} \\ x_{inv} \\ \lambda \end{bmatrix} = \underbrace{\begin{bmatrix} \mathcal{T}_{1_0}^{\mathsf{T}} \\ \mathcal{T}_{2_0}^{\mathsf{T}} \\ \mathcal{T}_{3_0}^{\mathsf{T}} \\ \tau_{0}^{\mathsf{T}} \end{bmatrix}}_{\mathcal{T}_0} n \tag{4-26}$$

Computing the matrix \mathcal{T}_0 such that:

$$\mathcal{T}_{1_0}^{\mathsf{T}} \dot{n} = \underbrace{\mathcal{T}_{1_0}^{\mathsf{T}} N^{\mathsf{T}}}_{I_R} \mathcal{V}_l(t) r(t) + \underbrace{\mathcal{T}_{1_0}^{\mathsf{T}} \mathfrak{b}}_{0_{R \times e}} \begin{bmatrix} W_{in,l}^e & -W_{out,g}^e \end{bmatrix} \begin{bmatrix} u_{in,l} \\ u_{out,g} \end{bmatrix}, \qquad \mathcal{T}_{1_0}^{\mathsf{T}} n(0) = 0 \qquad (4-27)$$

$$\mathcal{T}_{2_0}^{\mathsf{T}} \dot{n} = \underbrace{\mathcal{T}_{2_0}^{\mathsf{T}} N^{\mathsf{T}}}_{0_{e \times R}} \mathcal{V}_l(t) r(t) + \underbrace{\mathcal{T}_{2_0}^{\mathsf{T}} \mathfrak{b}}_{I_e} \begin{bmatrix} W_{in,l}^e & -W_{out,g}^e \end{bmatrix} \begin{bmatrix} u_{in,l} \\ u_{out,g} \end{bmatrix}, \qquad \mathcal{T}_{2_0}^{\mathsf{T}} n(0) = 0 \qquad (4-28)$$

$$\mathcal{T}_{2_0}^{\mathsf{T}}\dot{n} = \underbrace{\mathcal{T}_{2_0}^{\mathsf{T}}N^{\mathsf{T}}}_{0_{\mathsf{D}}\mathsf{V}_{\mathsf{E}}}\mathcal{V}_l(t)r(t) + \underbrace{\mathcal{T}_{2_0}^{\mathsf{T}}\mathfrak{b}}_{I_0} \left[W_{in,l}^e \quad -W_{out,g}^e \right] \begin{bmatrix} u_{in,l} \\ u_{out,g} \end{bmatrix}, \qquad \mathcal{T}_{2_0}^{\mathsf{T}}n(0) = 0 \quad (4\text{-}28)$$

$$\mathcal{T}_{3_0}^{\mathsf{T}}\dot{n} = \underbrace{\mathcal{T}_{3_0}^{\mathsf{T}}N^{\mathsf{T}}}_{0_{S-(R+e)\times R}} \mathcal{V}_l(t)r(t) + \underbrace{\mathcal{T}_{3_0}^{\mathsf{T}}\mathfrak{b}}_{0_{S-(R+e)\times e}} \begin{bmatrix} W_{in,l}^e & -W_{out,g}^e \end{bmatrix} \begin{bmatrix} u_{in,l} \\ u_{out,g} \end{bmatrix}, \quad \mathcal{T}_{3_0}^{\mathsf{T}}n(0) = 0 \quad (4-29)$$

$$\tau_{3_0}^{\mathsf{T}} \dot{n} = \underbrace{\tau_{3_0}^{\mathsf{T}} N^{\mathsf{T}}}_{0_{1 \times R}} \mathcal{V}_l(t) r(t) + \underbrace{\tau_{3_0}^{\mathsf{T}} \mathfrak{b}}_{0_{1 \times e}} \left[W_{in,l}^e - W_{out,g}^e \right] \begin{bmatrix} u_{in,l} \\ u_{out,g} \end{bmatrix}, \qquad \tau_{3_0}^{\mathsf{T}} n(0) = 1 \qquad (4-30)$$

The transformation must comply with the requirements described in section 3-3, which for this case will be:

- $\operatorname{rank}([N^{\intercal} \ \mathfrak{b}]) = R + e < S$
- $\operatorname{rank}([N^{\intercal} \mathfrak{b} \ n_{l,0}]) = R + e + 1$

Also, from (4-29) and (4-30) it can be inferred that $x_{inv}(0) = 0 \Longrightarrow x_{inv}(t) = 0 \ \forall t \geq 0$ and $\lambda(0) = 1 \Longrightarrow \lambda(t) = 1 \ \forall t \ge 0$

Then (4-25) is:

$$\dot{x}_r = \mathcal{V}_l(t)r(t) \qquad \qquad x_r(0) = 0 \tag{4-31}$$

$$\dot{x}_r = \mathcal{V}_l(t)r(t) \qquad x_r(0) = 0 \qquad (4-31)$$

$$\dot{x}_{io} = \begin{bmatrix} W_{in,l}^e & -W_{out,g}^e \end{bmatrix} \begin{bmatrix} u_{in,l} \\ u_{out,g} \end{bmatrix} \qquad x_{io}(0) = 0 \qquad (4-32)$$

The variable $x_{io} := x_{in} + x_{out}^{-1}$ and since these variables have physical meaning:

$$\dot{x}_{io} = \dot{x}_{in} + \dot{x}_{out} \tag{4-33}$$

$$\dot{x}_{in} = W_{in,l}^e u_{in,l}, \qquad x_{in}(0) = 0$$
 (4-34)

$$\dot{x}_{in} = W_{in,l}^e u_{in,l}, \qquad x_{in}(0) = 0$$

$$\dot{x}_{out} = -W_{out,g}^e u_{out,g}, \quad x_{out}(0) = 0$$
(4-35)

Finally, the vector of number of moles in the reaction zone can be reconstructed as:

$$n = N^{\mathsf{T}} x_r + \mathfrak{b} x_{io} \Longrightarrow n = N^{\mathsf{T}} x_r + \mathfrak{b} (x_{in} + x_{out}) \tag{4-36}$$

¹Notice that $x_{in}, x_{out} \in \mathbb{R}^{e \times 1}$, if p = v = 1 then the true extents of inlet and outlets are $\bar{x}_{in} = 1_{1 \times e}^{\intercal} x_{in}$ and $\bar{x}_{out} = 1_{1 \times e}^{\intercal} x_{out}$. If p, v > 1 then \bar{x}_{in} and \bar{x}_{out} are indistinguishable from x_{in} and x_{out} .

4-3 Case study 55

4-3 Case study

The process pertaining to this work is a reactive batch distillation column to produce a polymer and distillation of the by-product (water). The goal of the process is to separate the water from the polymer, by drawing the former at the top of the column. It is modeled with a sole reaction zone at the bottom and with a distillation zone above. This configuration is shown in figure 4-2. Moreover, it has the following characteristics:

• Number of species in the system: S = 14

• Independent reactions:
$$R_I = 7$$

Dependent reactions: $R_D = 10$ $\Longrightarrow \underbrace{R = R_I + R_D = 17}_{\text{Reactions of the system}}$

Despite the multiple sub-reactions, a general reaction scheme is described by:

Maleic Anhydride + Propylene Glycol + Water

⇒ Saturated Polymer + Water

• Mole and temperature initial conditions in the reactor:

$$M_{\text{Maleic Anhydride}}(0) = 20 \text{ kmol}$$

 $M_{\text{Propylene Glycol}}(0) = 20 \text{ kmol}$
 $M_{\text{Water}}(0) = 10 \text{ kmol}$
 $T_{\text{Reactor}}(0) = 373 \text{ K}$

- Number of stages in the process: NT = 6
- Number of actual trays: 3
- One liquid phase inlet: p = 1
- One gas phase outlet: v=1
- Reaction only occur in the reactor and in the liquid phase (no gas-phase reaction)
- Stage equilibrium approach for the distillation column
 - NRTL activity coefficient model is assumed for the liquid phase
- Vapor holdup is negligible with respect to the liquid holdup
- Process at constant atmospheric pressure
- Total condenser kept at constant temperature

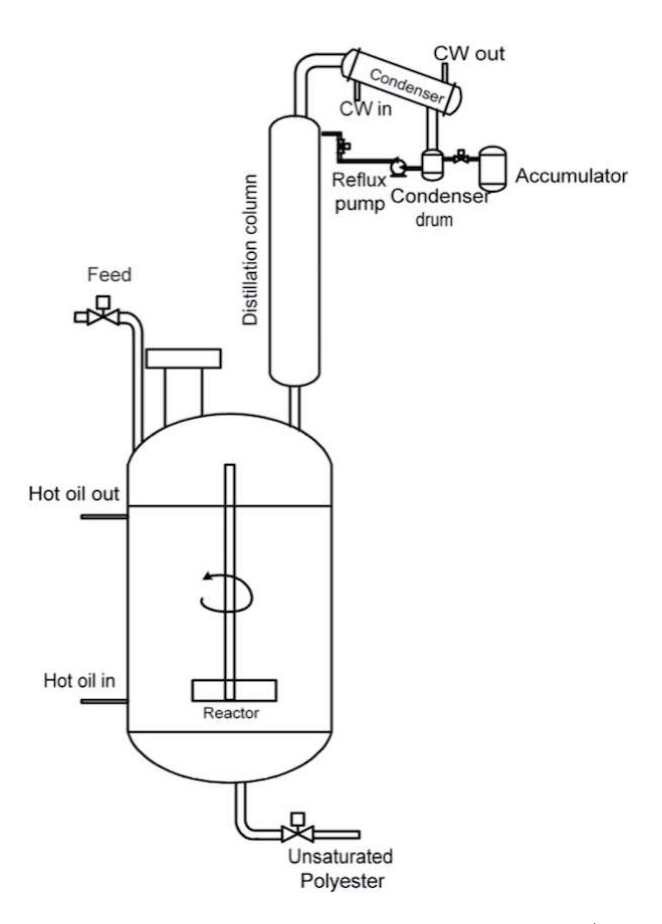


Figure 4-2: Representation of the reactive distillation column (Shah et al., 2011)

Furthermore, to keep the rigorousness of the process, the start-up of the batch process is also model and taken into account during the simulation. This will an extra difficulty to the control of the batch operation.

The mathematical model is presented with the sets of equations 4-37-4-48. The stages are numbered from top to bottom (stage 1 being the accumulator and stage NT = 6 the reactor). The model comprises the total mass balance, the component mass balance and the energy balance:

Accumulator: j = 1

Total mass balance:
$$\frac{dM_j}{dt} = L_j \tag{4-37}$$
 onent mass balance:
$$\frac{dM_j x_{j,i}}{dt} = L_j x_{j,i+1} \tag{4-38}$$
 Energy balance:
$$\frac{dM_j h_j}{dt} = L_j h_j \tag{4-39}$$

Component mass balance:
$$\frac{dM_j x_{j,i}}{dt} = L_j x_{j,i+1}$$
 (4-38)

Energy balance:
$$\frac{dM_j h_j}{dt} = L_j h_j \tag{4-39}$$

Condenser: j=2

Carlos Samuel Méndez Blanco

4-3 Case study 57

Total mass balance:
$$\frac{dM_j}{dt} = V_{j+1} - L_j \tag{4-40}$$

Component mass balance:
$$\frac{dM_j x_{j,i}}{dt} = V_{j+1} y_{j+1,i} - L_j x_{j,i}$$
 (4-41)

Energy balance:
$$\frac{dM_j h_j}{dt} = V_{j+1} H_{j+1} - L_j h_j \tag{4-42}$$

Internal stages: $j = 3, \dots, 5$

Total mass balance:
$$\frac{dM_j}{dt} = L_{j-1} + V_{j+1} - L_j - V_j$$
 (4-43)

Component mass balance:
$$\frac{dM_{j}x_{j,i}}{dt} = L_{j-1}x_{j-1,i} + V_{j+1}y_{j+1,i} - L_{j}, x_{j,i} - V_{j}y_{j,i}$$
(4-44)

Energy balance:
$$\frac{dM_jh_j}{dt} = L_{j-1}h_{j-1} + V_{j+1}H_{j+1} - L_jh_j - V_jH_j$$
 (4-45)

Reactor: j = 6

Total mass balance:
$$\frac{dM_j}{dt} = L_{j-1} - V_j \tag{4-46}$$

Component mass balance:
$$\frac{dM_j x_{j,i}}{dt} = m_l(t) N^{\mathsf{T}} r + L_{j-1} x_{j-1,i} - V_j y_{j,i} \qquad (4-47)$$

Energy balance:
$$\frac{dM_j h_j}{dt} = L_{j-1} h_{j-1} - V_j H_j - \Delta H_r + Q_{in}$$
 (4-48)

where $M_{j,i}$ is the liquid molar holdup of the *i*-th species in the *j*-th stage; $x_{j,i}$ and $y_{j,i}$ are the liquid and vapor molar composition of the *i*-th species in the *j*-th stage, respectively. h_j and H_j the liquid and vapor molar enthalpy in the *j*-th stage and L_j and V_j the liquid and vapor flows respectively.

And the internal reflux ratio \Re at the condenser stage (j=2) is

$$\mathfrak{R} = \frac{L_j}{V_{j+1}} \tag{4-49}$$

Let us focus in detail on the component mole balance in the reactor (4-47) to try to develop a simpler model:

The stoichiometric matrix $N^{\intercal} \in \mathbb{R}^{S \times R}$ but $\operatorname{rank}(N^{\intercal}) = R_I$, neither the left nor the right inverse are defined.

We perform the singular value decomposition (SVD) to obtain:

$$N^{\mathsf{T}} = \begin{bmatrix} U_{R_1} & U_{R_2} \end{bmatrix} \begin{bmatrix} \Sigma_R & 0 \\ 0 & 0 \end{bmatrix} \begin{bmatrix} V_{R_1}^{\mathsf{T}} \\ V_{R_2}^{\mathsf{T}} \end{bmatrix} \Longrightarrow N^{\mathsf{T}} = U_{R_1} \Sigma_R V_{R_1}^{\mathsf{T}}$$
(4-50)

Master of Science Thesis

Finally, making use of (4-50) and the approximation (4-24) in (4-47):

$$\frac{dM_6x_{6,i}}{dt} = m_l U_{R_1} \underbrace{\sum_{R} V_{R_1}^{\mathsf{T}} r}_{r'} + L_5 \mathfrak{b} x_{5,i}^e - V_6 \mathfrak{b} y_{6,i}^e$$
 (4-51)

$$\implies \frac{dM_6x_{6,i}}{dt} = m_l U_{R_1} r' + L_5 \mathfrak{b} x_{5,i}^e - V_6 \mathfrak{b} y_{6,i}^e$$
 (4-52)

Secondly, in the energy balance, since there is a phase change, the outlet enthalpy will have the contribution of the heat of vaporization ΔH_{vap} . Let us recast the energy balance in terms of the temperature:

$$\frac{dM_6h_6}{dt} = L_5h_5 - V_6H_6 - \Delta H_r + Q_{in} \tag{4-53}$$

$$h_6 \frac{dM_6}{dt} + M_6 \frac{dh_6}{dt} = L_5 h_5 - V_6 H_6 - \Delta H_r + Q_{in}$$
 (4-54)

But $h_j = C_{p_j}T_j$ and $H_j = C_{p_j}T_j + \Delta H_{vap}$. Assuming that C_{p_j} does not vary greatly in every stage, it can be treated as constant. Using (4-46), the energy balance results in:

$$C_{p_6}T_6(L_5 - V_6) + M_6C_{p_6}\frac{dT_6}{dt} = L_5C_{p_5}T_5 - V_6(C_{p_6}T_6 + \Delta H_{vap}) - \Delta H_r + Q_{in}$$
 (4-55)

$$M_6 C_{p_6} \frac{dT_6}{dt} = L_5 C_{p_5} T_5 - L_5 C_{p_6} T_6 - V_6 C_{p_6} T_6 + V_6 C_{p_6} T_6 - V_6 \Delta H_{vap} - \Delta H_r + Q_{in}$$
 (4-56)

Solving for $\frac{dT_6}{dt}$:

$$\frac{dT_6}{dt} = \frac{1}{M_6 C_{p_6}} \left(L_5 C_{p_5} T_5 - L_5 C_{p_6} T_6 - V_6 \Delta H_{vap} - \Delta H_r + Q_{in} \right) \tag{4-57}$$

4-3-1 Development of the model for control

Based on the reactive batch distillation process presented previously, we can apply the approximations and transformations explained in section 4-2. In this case, we have to take into account the dynamics of the water in the accumulator, measure the water composition in the condenser drum, make use of the dynamics of the reactor and the liquid flow and composition in tray 5.

The extent approach was applied in the reactor to simplify its dynamics because most the nonlinearities of the process are contained there (reaction rates and reaction heat). To control the water composition at the accumulator stage with the reflux ratio \Re , it is only necessary to measure water composition at condenser drum stage. This is possible because the liquid composition in the condenser drum is a function of the internal tray dynamic. This avoids the need to use full model of the distillation column

Accumulator:

4-3 Case study 59

$$\dot{x}_D^{\mathrm{w}} = (x_C^{\mathrm{w}}(t) - x_D^{\mathrm{w}}(t)) \frac{L_D(t)}{M_D(t)} = (x_C^{\mathrm{w}}(t) - x_D^{\mathrm{w}}(t)) \frac{V_3(t)}{M_D(t)} (1 - \Re)$$
(4-58)

where $x_D^{\mathbf{w}}(t)$ and $x_C^{\mathbf{w}}(t)$ are the composition of the water (w) in the distillate accumulator and condenser, respectively and M_D the total liquid holdup in the distillate stage.

Reactor:

$$\dot{n}_l = m_l(t)N^{\mathsf{T}}r(t) + x_5(t)L_5(t) - y_6(t)V_6(t) \approx m(t)N^{\mathsf{T}}r(t) + \mathfrak{b}(x_5^e(t)L_5(t) - y_6^e(t)V_6(t)) \tag{4-59}$$

$$\frac{dT_6}{dt} = \frac{1}{M_6(t)C_{p_6}(t)} \left(L_5(t)C_{p_5}(t)T_5(t) - L_5(t)C_{p_6}(t)T_6(t) - V_6(t)\Delta H_{vap} - \Delta H_r + Q_{in} \right)$$
(4-60)

The extent representation is:

$$\dot{x}_{r} \approx m_{l}(t)r(t) - \varepsilon x_{r}
\dot{x}_{in} \approx x_{5}^{e}(t)L_{5}(t) - \varepsilon x_{in}
\dot{x}_{out} \approx -y_{6}^{e}(t)V_{6}(t) - \varepsilon x_{out},
\Delta \dot{T}_{6} = \frac{L_{5}(t)C_{p_{5}}T_{5}}{M_{6}(t)C_{p_{6}}(t)} - \frac{L_{5}(t)T_{6}(t)}{M_{6}(t)} - \frac{V_{6}(t)\Delta H_{vap}}{M(t)C_{p_{6}}(t)} - \frac{\Delta H_{r}}{M_{6}(t)C_{p_{6}}(t)} + \frac{Q_{in}}{M_{6}(t)C_{p_{6}}(t)}, T_{6}(0) = T_{6_{0}}(4-64)$$

where x_r , x_{in} and x_{out} are the extent of reaction, inlet and outlet in the reactor in kmol/s, respectively. y_6 , y_6^e , x_5 and x_5^e are the complete and reduced vapor and liquid composition in stage 5 and the reactor stage respectively and T_6 is the liquid temperature in the reactor. Notice that a constant term ε was included here. This constant is a very small number that does not affect the real dynamics of the process; it was included as a mathematical trick to implement a similar change of variable Z as in the CSTR case.

In subsection 3-4-2, we introduced a pointwise change of variable Z that handled the nonlinearities present in x_r and T, and which at the same time, reduced the number of variables in our state space model. M_6 and C_{p_6} are assumed constant during differentiation because the term $M_6(t)C_{p_6}(t)$ does not vary greatly during the operation. Performing a similar change, define a transformation variable Z as:

$$Z = T_6 + \frac{\Delta H_f^{\ominus} N^{\mathsf{T}}}{M_6(t) C_{p_6}(t)} x_r + \frac{\Delta H_{vap} 1_{e \times 1}^{\mathsf{T}}}{M_6(t) C_{p_6}(t)} x_{out} = \underbrace{\left[1 \ \frac{\Delta H_f^{\ominus} N^{\mathsf{T}}}{M_6(t) C_{p_6}(t)} \ \frac{\Delta H_{vap} 1_{e \times 1}^{\mathsf{T}}}{M_6(t) C_{p_6}(t)} \right]}_{\mathcal{Z}} \begin{bmatrix} T_6 \\ x_r \\ x_{out} \end{bmatrix}$$
(4-65)

Differentiating with respect to time:

$$\dot{Z} = \dot{T}_6 + \frac{\Delta H_f^{\ominus} N^{\dagger}}{M_6(t) C_{p_6}(t)} \dot{x}_r + \frac{\Delta H_{vap} 1_{e \times 1}^{\dagger}}{M_6(t) C_{p_6}(t)} \dot{x}_{out}$$
(4-66)

Master of Science Thesis

Carlos Samuel Méndez Blanco

Substituting (4-61), (4-63) and (4-64) in (4-66).

$$\dot{Z} = -\frac{L_5(t)}{M_6(t)} T_6(t) - \frac{\Delta H_f^{\ominus} N^{\dagger}}{M_6(t) C_{p_6}(t)} \varepsilon x_r - \frac{\Delta H_{vap}}{M_6(t) C_{p_6}(t)} \varepsilon 1_{e \times 1}^{\dagger} x_{out}
+ \frac{L_5(t) C_{p_5(t)} T_5(t)}{M_6(t) C_{p_6}(t)} + \frac{Q_{in}}{M_6(t) C_{p_6}(t)}$$
(4-67)

Since $\frac{L_5(t)}{M_6(t)}$ and $\varepsilon \ll 1$:

$$\dot{Z} = -\left(\frac{L_5(t)}{M_6(t)} + \varepsilon\right) \left(T_6(t) + \frac{\Delta H_f^{\ominus} N^{\dagger}}{M_6(t)C_{p_6}} x_r + \frac{\Delta H_{vap}}{M_6(t)C_{p_6}(t)} \mathbf{1}_{e\times 1}^{\dagger} x_{out}\right) + \frac{L_5(t)C_{p_5(t)}T_5(t)}{M_6(t)C_{p_6}(t)} + \frac{Q_{in}}{M_6(t)C_{p_6}(t)}$$
(4-68)

From the definition of Z in (4-65):

$$\dot{Z} = -\left(\frac{L_5(t)}{M_6(t)} + \varepsilon\right) Z + \frac{L_5(t)C_{p_5(t)}T_5(t)}{M_6(t)C_{p_6}(t)} + \frac{Q_{in}}{M_6(t)C_{p_6}(t)}$$
(4-69)

In figure 4-3, the behavior of change of variable Z can be seen. Three formulations of Z are compared: The original definition as described in (4-65) and the solutions to the differential equation shown in (4-67) and (4-68).

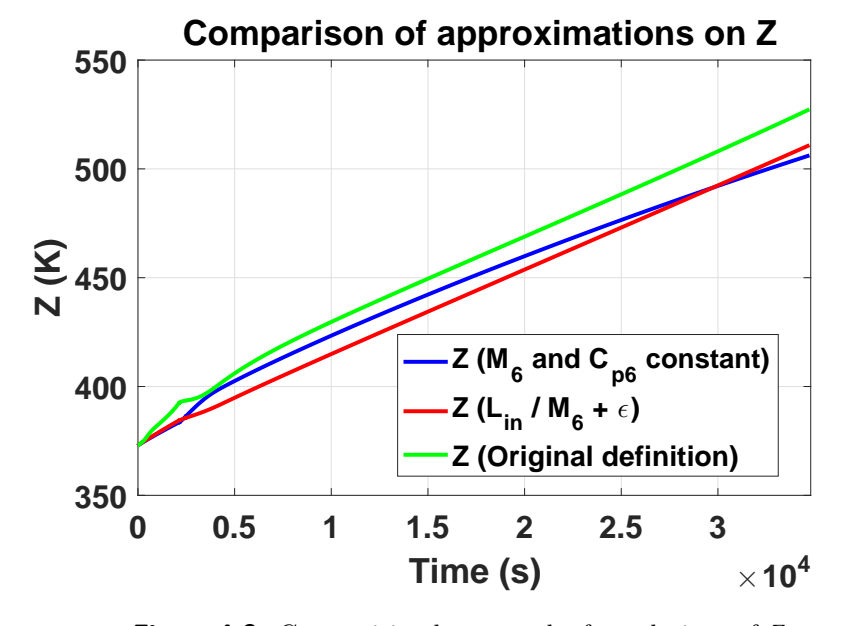


Figure 4-3: Comparision between the formulations of Z

As observed, there is an offset between these formulations and the original case. However, the behaviors of these formulations have the same tendency and magnitude. Moreover, the

goal of the change of variable Z is the construction of a linear model that can be used to represent the evolution of the temperature in time, which is described by a nonlinear model. Therefore, since we have a good approximation, the controller can be implemented with this model and eliminate the offset by means of integral action.

Finally, the model for control of the reactive batch distillation column is presented next:

• Accumulator zone:

$$\dot{x}_{D}^{w} = -(x_{D}^{w}(t) - x_{C}^{w}(t)) \frac{V_{3}(t)}{M_{D}(t)} + (x_{D}^{w}(t) - x_{C}^{w}(t)) \frac{V_{3}(t)}{M_{D}(t)} \Re, \quad x_{D}(0) = 0 (4-70)$$

$$y = x_{D}^{w} \tag{4-71}$$

• Reaction Zone

$$\dot{Z} = -\varepsilon Z - \frac{L_5(t)}{M_6(t)} Z + \frac{L_5(t) C_{p_5} T_5(t)}{M_6(t) C_{p_6}(t)} + \frac{Q_{in}}{M_6(t) C_{p_6}(t)}, \qquad Z(0) = Z_0 \quad (4-72)$$

$$y = T_6 \quad (4-73)$$

Notice that the extent of inlet x_{in} was not included in the model because its dynamics are not relevant for the measured outputs of the system. The possibility of disregard a state from our control model is an advantage that the extent transformation provides, given the nice decoupled representation obtained. Moreover, it is assumed that the composition of water in the condenser drum $x_C^{\rm w}$ can be measured.

Rewriting in compact form:

$$\begin{bmatrix}
\dot{x}_{D}^{\mathbf{w}} \\
\dot{Z}
\end{bmatrix} = \begin{bmatrix}
-\frac{V_{3}(t)}{M_{D}(t)}(x_{D}^{\mathbf{w}} - x_{C}^{\mathbf{w}}) \\
-(\frac{L_{5}(t)}{M_{6}(t)} + \varepsilon)Z
\end{bmatrix} + \begin{bmatrix}
\frac{V_{3}(t)}{M_{D}(t)}(x_{D}^{\mathbf{w}} - x_{C}^{\mathbf{w}}) & 0 \\
0 & \frac{1}{M_{6}(t)C_{p_{6}}(t)}
\end{bmatrix} \begin{bmatrix}
\mathfrak{R} \\
Q_{in}
\end{bmatrix} + \begin{bmatrix}
0 \\
C_{p_{5}}(t)T_{5}(t) \\
M_{6}(t)C_{p_{6}}(t)
\end{bmatrix} L_{5}(t) \quad (4-74)$$

$$y = \begin{bmatrix}
x_{D}^{\mathbf{w}} \\
T_{6}
\end{bmatrix} = \begin{bmatrix}
1 & 0 \\
0 & \varsigma
\end{bmatrix} \begin{bmatrix}
x_{D}^{\mathbf{w}} \\
Z
\end{bmatrix} \quad (4-75)$$

where
$$\varsigma = \begin{bmatrix} 1 & 0_{1 \times R_I + v} \end{bmatrix} \hat{Q} \hat{R}^{-\intercal} \in \mathbb{R}^1$$
.

4-3-2 State-feedback linearization

The model is described by a control-input nonaffine nonlinear system. In the accumulator model, the state $x_D^{\mathbf{w}}$ is multiplied with the input \mathfrak{R} . In the reactor, the state Z is affected by the liquid flow coming from the upper stage. However, in this latter case, the liquid flow $L_5(t)$ can be regarded as a measurable disturbance; thus, the reflux ratio \mathfrak{R} is only directly relevant to the dynamics of $x_D^{\mathbf{w}}$.

The evolution of $x_D^{\mathbf{w}}$ is described by this general model of the form:

$$\dot{w} = f(w) + g(w)u \tag{4-76a}$$

$$y = h(w) \tag{4-76b}$$

where w is any arbitrary set of states and f(w) and g(w) functions of w.

This type of representation allows for a feedback linearization. Recalling that the evolution of the composition of water in the distillate is described in (4-70), one could choose the reflux input as:

$$\Re = \frac{1}{(x_D^{\mathbf{w}}(t) - x_C^{\mathbf{w}}(t))} a + \frac{x_C^{\mathbf{w}}(t)}{x_D^{\mathbf{w}}(t) - x_C^{\mathbf{w}}(t)} \mu$$
 (4-77)

Replacing (4-77) in (4-70):

$$\dot{x}_D^{\text{w}} = \frac{V_3(t)}{M_D(t)} \underbrace{(a - x_D^{\text{w}}(t) + x_C^{\text{w}}(t))}_{+ C(t)} + \frac{V_3(t)x_C^{\text{w}}(t)}{M_D(t)} \mu$$
(4-78)

Since a is a free variable, we can equalize \star to a form of state feedback as:

$$a - x_D^{\mathbf{w}}(t) - x_C^{\mathbf{w}}(t) = -\mathbf{K}x_D^{\mathbf{w}}(t) \Longrightarrow a = (1 - \mathbf{K})x_D^{\mathbf{w}}(t) - x_C^{\mathbf{w}}(t)$$

$$(4-79)$$

Now, substituting (4-79) in (4-78), the linearized equation results in a linear affine model:

$$\dot{x}_{D}^{W} = -\frac{V_{3}(t)}{M_{D}(t)} \mathbf{K} x_{D}^{W} + \frac{V_{3}(t) x_{C}^{W}(t)}{M_{D}(t)} \mu$$
(4-80)

where **K** is the free pole location of x_D^{w} .

The plant has a pole at $-\frac{V_3(t)}{M_D(t)}$. At t=0 the distillate molar holdup $M_D(t)$ is zero. However, as division by zero is not allowed, one could think of M_D as a very small number tending to zero for purposes of dynamics analysis:

- Process start-up $(V_3(t)=0 \text{ and } M_D(t)=\delta \to 0)$: The pole $-\frac{V_3(t)}{M_D}$ is located at the origin.
- Vaporization $(V_3(t) > 0 \text{ and } M_D(t) = \delta \to 0)$: The pole $-\frac{V_3(t)}{M_D}$ is located in the left-hand side of the complex plane very far away from the origin (stable with fast dynamics).
- Distilled product formation $(V_3(t) > 0 \text{ and } M_D(t) > 0)$: The pole $-\frac{V_3(t)}{M_D}$ is located in the left-hand side of the complex plane (stable pole). Under this regime, there exist other sub-scenarios:
 - $-V_3(t) > M_D(t) \Longrightarrow -\frac{V_3(t)}{M_D(t)} < 1$: The dynamics could be fast but surely slower than in the "Vaporization" regime.

$$-V_3(t) \leq M_D(t) \Longrightarrow -\frac{V_3(t)}{M_D(t)} \geq -1$$
: The dynamics is rather slow.

Given the varying nature of the pole, a sensible choice for \mathbf{K} would be such that new model has the same pole location of the original system i.e. $\mathbf{K}=1$, so that the state-feedback-linearized model can capture the different rates of the real plant dynamics exactly where they are.

Moreover, μ lacks physical meaning, thus we need to compute the real control law. Finally, let us use the analytic value of a found in (4-79) to replace it in (4-77):

$$\Re = \frac{1 - \mathbf{K}}{x_D^{\mathbf{w}}(t) - x_C^{\mathbf{w}}(t)} x_D^{\mathbf{w}}(t) - \frac{x_C^{\mathbf{w}}(t)}{x_D^{\mathbf{w}}(t) - x_C^{\mathbf{w}}(t)} + \frac{x_C^{\mathbf{w}}(t)}{x_D^{\mathbf{w}}(t) - x_C^{\mathbf{w}}(t)} \mu$$
(4-81)

where is the free pole location of $x_D^{\mathbf{w}}$ and μ is the input derived from the feedback linearization. The model of the plant can now be recast as:

$$\begin{bmatrix} \dot{x}_{D}^{\mathbf{w}} \\ \dot{Z} \end{bmatrix} = \begin{bmatrix} -\frac{V_{3}(t)}{M_{D}(t)} & 0 \\ 0 & -\left(\frac{L_{5}(t)}{M_{6}(t)} - \varepsilon\right) \end{bmatrix} \begin{bmatrix} x_{D}^{\mathbf{w}} \\ Z \end{bmatrix} + \begin{bmatrix} \frac{V_{3}(t)x_{C}^{\mathbf{w}}(t)}{M_{D}(t)} & 0 \\ 0 & \frac{1}{M_{6}C_{p_{6}}} \end{bmatrix} \begin{bmatrix} \mu \\ Q_{in} \end{bmatrix} + \begin{bmatrix} 0 \\ \frac{C_{p_{5}}(t)T_{5}(t)}{M_{6}(t)C_{p_{6}}(t)} \end{bmatrix} L_{5}(t) - 82)$$

$$y = \begin{bmatrix} x_{D} \\ T_{6} \end{bmatrix} = \begin{bmatrix} 1 & 0 \\ 0 & \varsigma \end{bmatrix} \begin{bmatrix} x_{D} \\ Z \end{bmatrix}$$

$$(4-83)$$

In figure 4-4, it is shown a comparison between linear (LPV) model and the nonlinear plant. Although, there is some mismatch, the LPV model reproduces with sufficient accuracy the nonlinear plant. This allows to lower the complexity of the nonlinear plant and develop linear control strategies rather than more complicated nonlinear schemes.

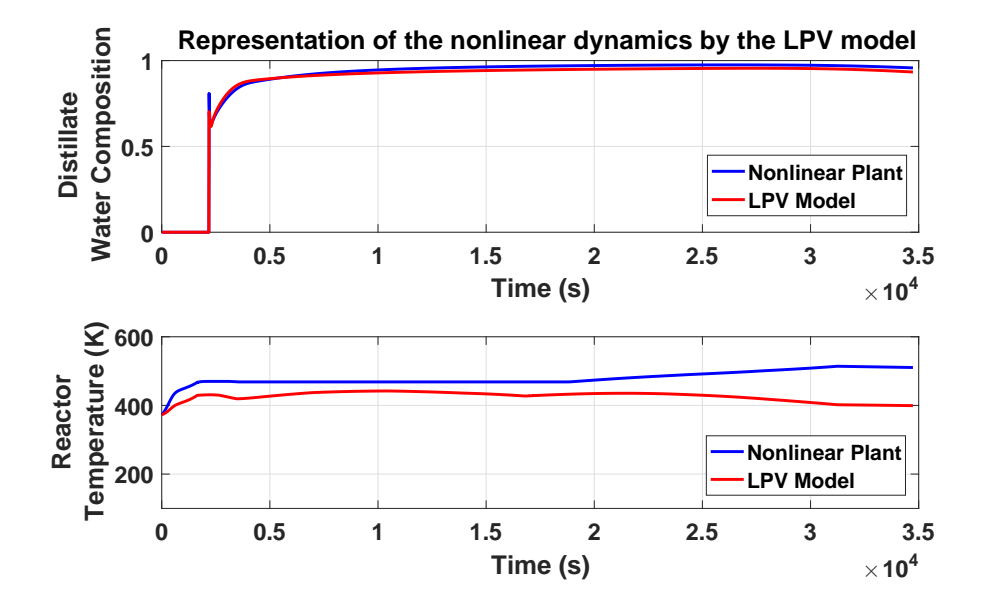


Figure 4-4: Comparision between the nonlinear plant dynamics and the reproduction done by the LPV model

4-3-3 Linear Model Predictive Control for the Reactive Batch Distillation Process

The reactive batch distillation is a process described by stiff dynamics; reaction, phase-change and flow dynamics have very different time scales in most cases. Moreover, they are strongly coupled and the batch nature of the process gives rise to a constant change of the operating point (Tyagunov, 2004). Therefore, a control scheme that can tightly control this process following a reference becomes relevant to achieve an adequate performance. Model-based strategies are very attractive for this particular type of processes; one of the most widely implemented in process industry is the model predictive control (MPC).

The MPC strategy has had an increasing acceptance in process industry for many reasons since the last two decades of the XXth century (Tyagunov, 2004):

- MPC is a model-based controller design procedure, capable of handling systems with large time delays, non-minimum phase, unstable and nonlinear dynamics.
- It is, in general, an easy-to-tune method. The tuning of the MPC is probably the less intuitive part of the design procedure.
- MPC can handle input and output constraint. These can be included in the optimization problem. The constraints play an important role in many systems, as they establish the physical limits of actuators and process variables.
- MPC can cope with structural changes, such as sensor and actuator failures, changes in the system parameters by adapting the control strategy based on the sampling of the real plant variables.

For the RBD column, we want to maximize the amount of water in the distillate; this will guarantee the separation of the polymer (desired product) and the water (by-product).

We define the following quadratic cost function:

$$\mathbf{J}_k(x(k), u(k)) = \sum_{j=1}^{N_h - 1} \mathbf{e}_y(k+j)^{\mathsf{T}} \mathbf{Q} \mathbf{e}_y(k+j) + \sum_{j=0}^{N_h} \Delta u(k+j)^{\mathsf{T}} \mathbf{R} \Delta u(k+j)$$
(4-84)

and the minimization problem:

$$\min_{\Delta u} \quad \mathbf{J}_k(x(k), u(k)) \tag{4-85a}$$

s.t.
$$\bar{x}(k+j+1) = \Phi \bar{x}(k+j) + \Theta u(k+j) + \Upsilon L(k+j)$$
 (4-85b)

$$y(k+j) = C\bar{x}(k+j) \tag{4-85c}$$

$$\Delta u_{min} \le \Delta u(k) \le \Delta u_{max} \tag{4-85d}$$

where $\mathbf{e}_{y}(k+j) = y(k+j) - y_{ref}(k+j)$, $\Phi = e^{A \cdot T_h}$, $\Theta = \int_{0}^{T_h} e^{A \cdot \tau} \mathcal{B}u(\tau) d\tau$, $\Upsilon = \int_{0}^{T_h} e^{A \cdot \tau} \mathcal{B}_{w}L(\tau) d\tau$ and T_h is the sampling time

with

$$\mathcal{A} = \begin{bmatrix} -\frac{V_3(t)}{M_D(t)} & 0 \\ 0 & -\left(\frac{L_5(t)}{M_6(t)} - \varepsilon\right) \end{bmatrix} \quad \mathcal{B} = \begin{bmatrix} \frac{V_3(t)x_C^w(t)}{M_D(t)} & 0 \\ 0 & \frac{1}{M_6(t)C_{p_6}(t)} \end{bmatrix} \quad \mathcal{C} = \begin{bmatrix} 1 & 0 \\ 0 & \varsigma \end{bmatrix} \quad \mathcal{B}_w = \begin{bmatrix} 0 \\ \frac{C_{p_5}(t)T_5(t)}{M_6(t)C_{p_6}(t)} \end{bmatrix}$$

Introducing the variables:

$$\Delta \bar{x}(k) := \bar{x}(k) - \bar{x}(k-1)$$

$$\Delta u(k) := u(k) - u(k-1)$$

$$\Delta y(k+1) := y(k+1) - y(k)$$

$$\mathbf{x}(k) = \left[\Delta \bar{x}(k)^{\mathsf{T}} \quad y(k)^{\mathsf{T}} \right]^{\mathsf{T}}$$

Using the previous definition, we obtain the following state space model using (4-85b) and (4-85c) to gain integral action by means of output and state feedback.

$$\mathbf{x}(k+j+1) = \begin{bmatrix} \Phi & 0 \\ \mathcal{C}\Phi & I \end{bmatrix} \mathbf{x}(k+j) + \begin{bmatrix} \Theta \\ \mathcal{C}\Theta \end{bmatrix} \Delta u(k+j) + \begin{bmatrix} \Upsilon \\ \mathcal{C}\Upsilon \end{bmatrix} \Delta L(k+j)^{\bullet 0}$$
(4-86)
$$y(k+j) = \begin{bmatrix} 0 & I \end{bmatrix} \mathbf{x}(k+j)$$
(4-87)

The disturbance L(k+j) can be measured and assumed that it remains constant during the prediction until new data is available. Therefore, $\Delta L(k+j) = 0$ and it does not appear in the final model.

This representation is in terms of the rate $\Delta u(k)$, which is more useful to solve the cost function **J**. Working the summations up to our prediction horizon N_h , the cost function **J** is recast in terms of matrix products:

$$\min_{\Delta \mathbf{U}_k} \quad (\mathbf{Y}_k - \mathbf{Y}_{ref})^{\mathsf{T}} \tilde{\mathbf{Q}} (\mathbf{Y}_k - \mathbf{Y}_{ref}) + \Delta \mathbf{U}_k^{\mathsf{T}} \tilde{\mathbf{R}} \Delta \mathbf{U}_k$$
 (4-88)

$$\min_{\Delta \mathbf{U}_k} \quad (\Gamma \mathbf{x}(k) - \mathbf{Y}_{ref} + \Lambda \Delta \mathbf{U}_k)^{\mathsf{T}} \tilde{\mathbf{Q}} (\Gamma \mathbf{x}(k) - \mathbf{Y}_{ref} + \Lambda \Delta \mathbf{U}_k)$$
(4-89)

(4-90)

$$\min_{\Delta \mathbf{U}_k} \quad \frac{1}{2} \Delta \mathbf{U}_k^{\mathsf{T}} \mathbf{H} \Delta \mathbf{U}_k + \mathbf{f}^{\mathsf{T}} \Delta \mathbf{U}_k + \mathbf{c}$$
 (4-91)

s.t.
$$\Delta \mathbf{U}_{k_{min}} \le \Delta \mathbf{U}_k \le \Delta \mathbf{U}_{k_{max}}$$
 (4-92)

where

$$\mathbf{Y}_{k} = \begin{bmatrix} y(k) \\ y(k+1) \\ \vdots \\ y(k+N_{h}) \end{bmatrix} \Delta \mathbf{U}_{k} = \begin{bmatrix} \Delta u(k) \\ \Delta u(k+1) \\ \vdots \\ \Delta u(k+Nh) \end{bmatrix}$$

$$\Gamma = \begin{bmatrix} \mathbf{C}\mathbf{A} \\ \mathbf{C}\mathbf{A}^{2} \\ \vdots \\ \mathbf{C}\mathbf{A}^{N_{h}} \end{bmatrix} \Lambda = \begin{bmatrix} \mathbf{C}\mathbf{B} & \mathbf{D} & 0 & \cdots & 0 \\ \mathbf{C}\mathbf{A}\mathbf{B} & \mathbf{C}\mathbf{B} & \mathbf{D} & \cdots & 0 \\ \vdots & \vdots & \ddots & \ddots & \vdots \\ \mathbf{C}\mathbf{A}^{N_{h}-1}\mathbf{B} & \mathbf{C}\mathbf{A}^{N_{h}-2}\mathbf{B} & \cdots & \mathbf{C}\mathbf{B} & \mathbf{D} \end{bmatrix}$$

$$\mathbf{A} = \begin{bmatrix} \mathcal{A} & 0 \\ \mathcal{C}\mathcal{A} & I \end{bmatrix} \mathbf{B} = \begin{bmatrix} \mathcal{B} \\ \mathcal{C}\mathcal{B} \end{bmatrix} \mathbf{C} = \begin{bmatrix} 0 & I \end{bmatrix}$$

$$\tilde{\mathbf{Q}} = \begin{bmatrix} \mathbf{Q} & & \\ \mathbf{Q} & & \\ & \ddots & \\ & & \mathbf{Q} \end{bmatrix} \qquad \tilde{\mathbf{R}} = \begin{bmatrix} \mathbf{R} & & \\ \mathbf{R} & & \\ & \ddots & \\ & & \mathbf{R} \end{bmatrix}$$

$$\frac{1}{2}\mathbf{H} = (\Lambda^{\mathsf{T}}\tilde{\mathbf{Q}}\Lambda + \tilde{\mathbf{R}}) \qquad \mathbf{f}^{\mathsf{T}} = 2[(\Gamma\mathbf{x}(k) - \mathbf{Y}_{ref})^{\mathsf{T}}\tilde{\mathbf{Q}}\Lambda - \Delta\mathbf{U}_{k_{ref}}^{\mathsf{T}}\tilde{\mathbf{R}}]$$

$$\mathbf{c} = (\Gamma\mathbf{x}(k) - \mathbf{Y}_{ref})^{\mathsf{T}}\tilde{\mathbf{Q}}(\Gamma\mathbf{x}(k) - \mathbf{Y}_{ref})$$

The cost function defined in (4-91) describes a constrained quadratic programming (QP) problem which can be efficiently solved as J is a convex function.

The QP optimization problem will minimize the vector of inputs ΔU_k . This input vector is comprised of input rate elements $\Delta u(k+j)$ at every step k up to the prediction horizon N_h . In the case of our plant, these input rates are functions of the inputs fed to the plant μ and Q_{in} . The rate constraints ΔU can be developed using (4-86):

$$u(k) = u(k-1) + \Delta u(k) (4-93)$$

$$u(k+1) = u(k-1) + \Delta u(k) + \Delta u(k+1)$$
 (4-94)

$$\div$$
 (4-95)

$$u(k+N_h-1) = u(k-1) + \sum_{j=0}^{N_h-1} \Delta u(k+j)$$
 (4-96)

Equation (4-96) can be written in vector form as:

$$U_{k} = \begin{bmatrix} I \\ I \\ \vdots \\ I \end{bmatrix} u(k-1) + \begin{bmatrix} I & 0 & 0 & \cdots & 0 \\ I & I & 0 & \cdots & 0 \\ \vdots & \vdots & \vdots & \ddots & \vdots \\ I & I & I & \cdots & I \end{bmatrix} \Delta \mathbf{U}_{k}$$

$$(4-97)$$

Generally, the input before the start of a process is zero, hence u(k-1) = 0. Under this presumption, $\Delta \mathbf{U}_k$ can be written in terms of \mathbf{U}_k . The input rate constraints is:

$$\begin{bmatrix} I & 0 & 0 & \cdots & 0 \\ I & I & 0 & \cdots & 0 \\ \vdots & \vdots & \vdots & \ddots & \vdots \\ I & I & I & \cdots & I \end{bmatrix}^{-1} \begin{pmatrix} \mathbf{U}_{k_{min}} - \begin{bmatrix} I \\ I \\ \vdots \\ I \end{bmatrix} u(k-1) \end{pmatrix} \le \Delta \mathbf{U}_{k} \le \begin{bmatrix} I & 0 & 0 & \cdots & 0 \\ I & I & 0 & \cdots & 0 \\ \vdots & \vdots & \vdots & \ddots & \vdots \\ I & I & I & \cdots & I \end{bmatrix}^{-1} \begin{pmatrix} \mathbf{U}_{k_{max}} - \begin{bmatrix} I \\ I \\ \vdots \\ I \end{bmatrix} u(k-1) \end{pmatrix}$$
(4-98)

Recall the inversion-based linearized system described in (4-80). This model depends on a control input that lacks physical meaning, therefore, one must find the relation between the bounds of \Re and those of μ .

Since \Re represents the internal reflux ratio, then $\Re \in [0,1]$. Plugging these bounds in (4-81) and setting $\mathbf{K} = 1$.

For $\Re = \Re_{max} = 1$

$$1 = -\frac{x_C^{\mathbf{w}}(t)}{x_D^{\mathbf{w}}(t) - x_C^{\mathbf{w}}(t)} + \frac{x_C^{\mathbf{w}}(t)}{x_D^{\mathbf{w}}(t) - x_C^{\mathbf{w}}(t)} \mu \Longrightarrow \mu = \mu_1 = \frac{x_D^{\mathbf{w}}(t)}{x_C^{\mathbf{w}}(t)}$$
(4-99)

For $\Re = \Re_{min} = 0$

$$0 = -\frac{x_C^{\mathbf{w}}(t)}{(x_D^{\mathbf{w}}(t) - x_C^{\mathbf{w}}(t))} + \frac{1}{(x_D^{\mathbf{w}}(t) - x_C^{\mathbf{w}}(t))} \mu \Longrightarrow \mu = \mu_2 = 1$$
 (4-100)

Notice that the bounds change depending on the values of $x_D^{\rm w}(t)$ and $x_C^{\rm w}(t)$. These changes are summarized in table 4-1

Table 4-1: Change of input bound with respect to the parameters of the plant

Condition	Bounds
$x_C^{\mathbf{w}}(t) > x_D^{\mathbf{w}}(t)$	$\mu_{max} = \mu_2$ $\mu_{min} = \mu_1$
$x_C^{\mathbf{w}}(t) = x_D^{\mathbf{w}}(t)$	$\mu_1 = \mu_2 \longrightarrow \mu_{max} = \mu_{min}$
$x_C^{\mathbf{w}}(t) < x_D^{\mathbf{w}}(t)$	$\mu_{max} = \mu_1$ $\mu_{min} = \mu_2$

These dynamic input bound are constantly calculated with information from the plant at every simulation step, and with them the optimal input μ^* is found solving the QP optimization problem.

An additional problem with batch processes is the reference to be tracked. The reference signal should be a trajectory, rather than a static point to avoid aggressive control actions by the controller. This reference trajectory allows the controller to calculate optimal inputs using the receding horizon approach, which improves the performance in terms of the error and softens the control action aggressiveness.

The reference trajectory was calculated performing an open-loop optimization where water removal from the reactor was maximized under operating conditions, i.e. composition of water at zero $(x^{w} = 0)$ in the reactor. The trajectories of the distillate composition of water and the temperature in the reactor to achieve this particular goal are shown in figure 4-5

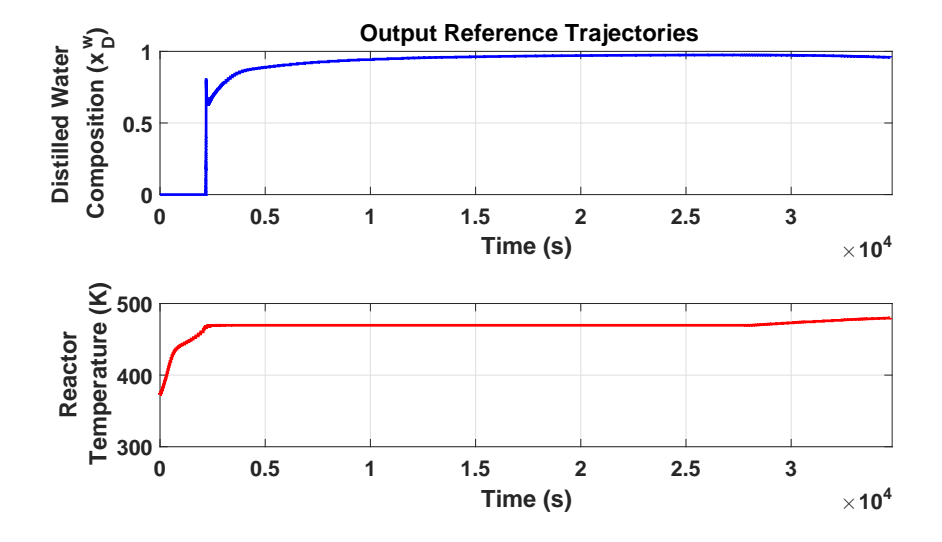


Figure 4-5: Reference trajectories of the distillate composition and reactor temperature

Based on these trajectories, the model-predictive controller was designed. The cost function defined in (4-91) subject to (4-92).

The sampling time T_h was chosen 15 seconds, because the temperature is commonly the slowest dynamics in such large processes. According to Tran (Tran, 2015), a good choice for the prediction horizon N_h is a value between 80% and 100% of the settling time of the slowest sub-process in samples. However, since batch processes do not have steady-states, the prediction horizon was chosen such that $T_h \cdot N_h = 3600$, ensuring prediction for an hour of operation; so $N_h = 240$. This choice was made because using a horizon that spans all of the batch time could not be handled by the algorithm. Finally, the following weight matrices were taken:

$$\mathbf{Q} = \begin{bmatrix} 1 & 0 \\ 0 & 1000 \end{bmatrix} \quad \mathbf{R} = \begin{bmatrix} 1 & 0 \\ 0 & 0.01 \end{bmatrix} \tag{4-101}$$

The first element on the main diagonal of \mathbf{Q} penalizes the error of the distillate water composition $x_D^{\mathbf{w}}$, whereas the second element does the same with the error of the reactor temperature. Likewise, the elements on the main diagonal of \mathbf{R} penalize the rate of μ and of the heat duty Q_{in} , respectively.

The second entry in \mathbf{Q} was chosen to give equal effort for same "badness" in the response with a high penalization on the temperature error because the plant-model mismatch is greater for the temperature dynamics.

For example: T_6 = temperature in Kelvin (K).

0.03: acceptable error in temperature
$$\longrightarrow \mathbf{q}_2 = \left(\frac{1}{0.03}\right)^2 \quad \mathbf{q}_2(\mathbf{e}_{T_6})^2 = 1 \text{ when } \mathbf{e}_{T_6} = 0.03$$

The first entry in \mathbf{Q} was set to 1 because the model of the distillate dynamics represents better the real plant behavior, so less penalization was required to achieve a good control performance.

The entries in \mathbf{R} were tuned by trial and error. A heavier penalization (0.01) was applied on Q_{in} to allow for rapid disturbance rejection. On the other hand, the penalization on \mathfrak{R} was much lower (1) due to the fact that a tight control on the composition was not required; only a similar trajectory sufficed to keep a steady removal of water from the reactor.

The bounds of μ were dynamically established by the optimization algorithm according to table 4-1. The bounds of Q_{in} were fixed to $Q_{in_{min}} = -1000$ kW and $Q_{in_{max}} = 100$ kW.

The MPC was implemented on a computer running Windows 10 software with 64-bit architecture, equipped with a 3.60 GHz Intel Core i7 processor and 32 GB of RAM memory. The controller has to track the reference trajectories presented previously. The temperature trajectory stays close to the mixture's boiling point (450 K – 470 K); therefore, it has to be efficiently tracked with the heat duty Q_{in} , because it is the variable that controls the dynamics of the evaporation within the reactor. After the vapor has reached the top of the column and condensed to liquid phase in the condenser, the reflux ratio \Re control the composition in the distillate accumulator stage.

It is worth noting that at the start-up of the process there is no manipulation of the reflux ratio ($\Re=0$) by the MPC. This situation is not ideal, because it would mean that all the material from the condenser would flow to the accumulator before the MPC takes action. Therefore, a P level controller is developed to maintain the reflux ratio high enough until the MPC starts to work on the distillate dynamics.

The P controller is of the form:

$$P_c(t) = k_p \max(\ell_{ref} - \ell(t), 0)$$
 (4-102)

where ℓ_{ref} and $\ell(t)$ are the maximum reference level of distillate before switching to the MPC and the actual level of distillate in the accumulator stage, respectively.

In figure 4-6, a block diagram of the process is shown.

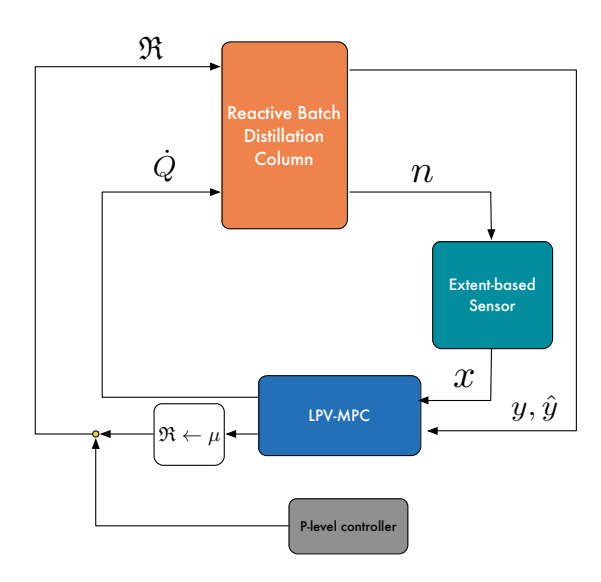


Figure 4-6: Block diagram of the reactive batch distillation column control loop

Additionally, the controlled responses of the reactor temperature and composition along with the control actions, are shown in figures 4-7, 4-8 and 4-9.

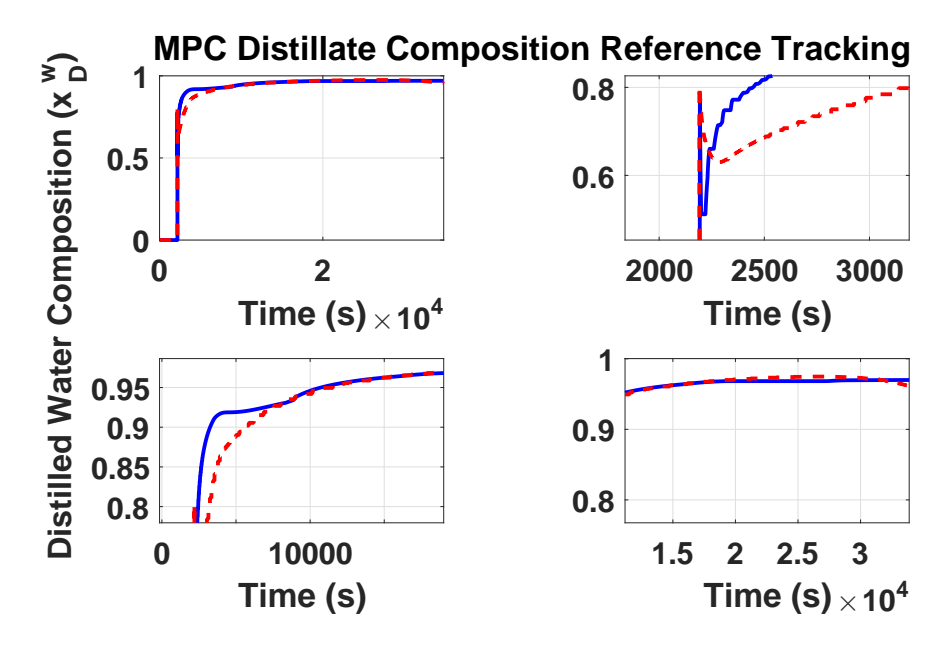


Figure 4-7: Controlled response of the distilled water composition at the accumulator stage (blue solid line) vs. Distilled water composition reference trajectory (red dashed line). Left to right: 1. Full view, 2. Transient response, 3. Tracking over optimal reference composition, 4. Final composition

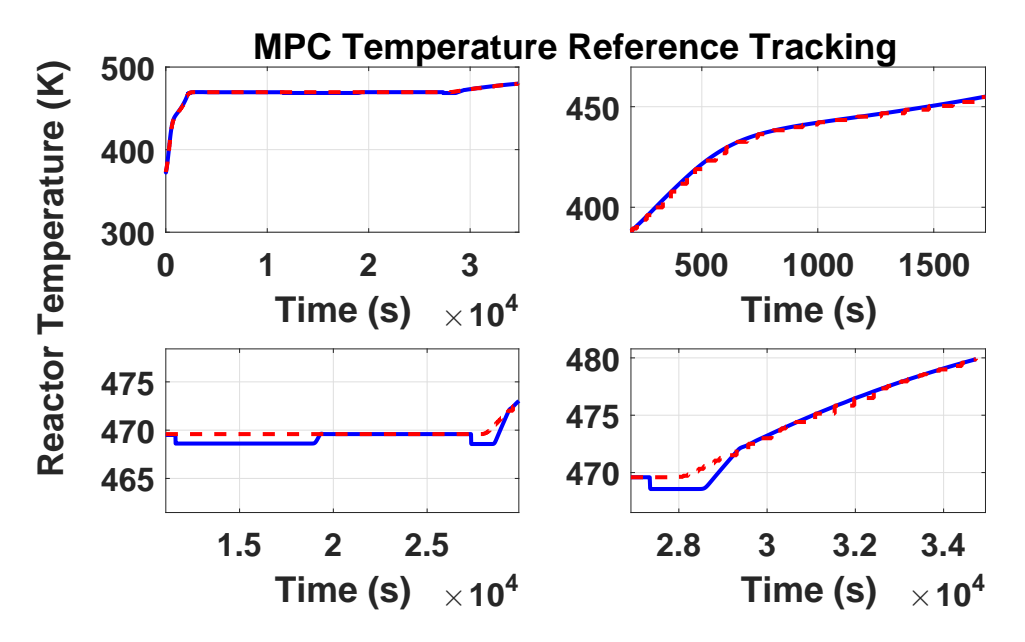


Figure 4-8: Controlled response of the reactor temperature (blue solid line) vs. Temperature reference trajectory (red dashed line). Left to right: 1. Full view, 2. Transient response, 3. Tracking over optimal reference temperature, 4. Final temperature

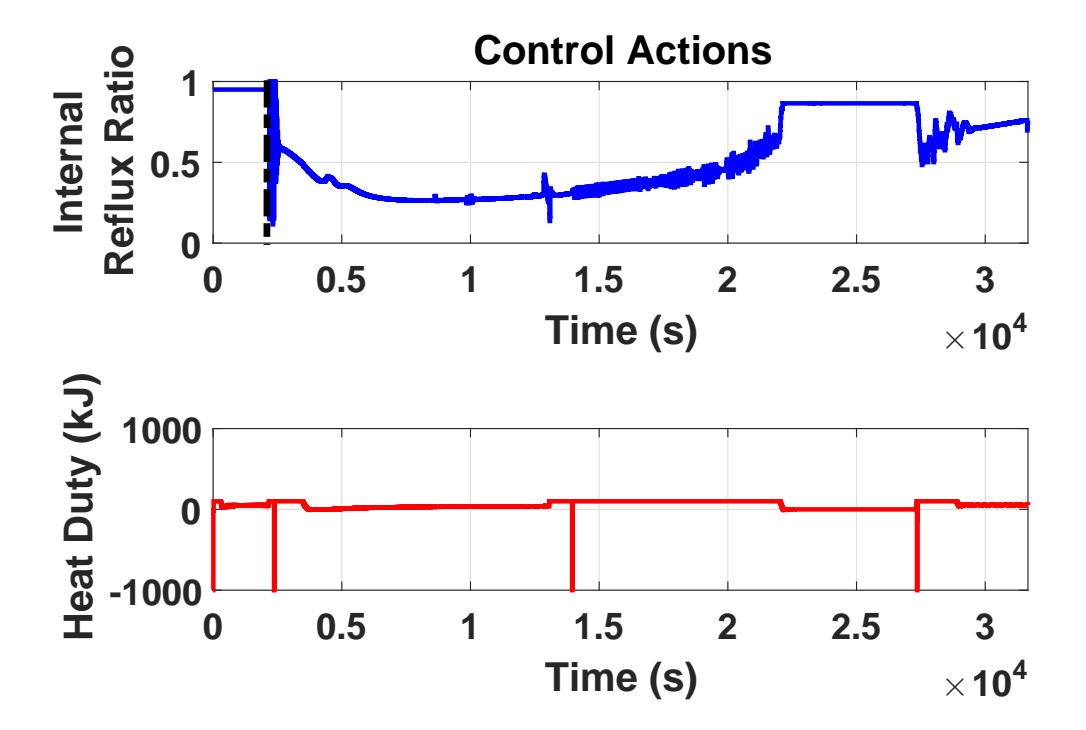


Figure 4-9: Control actions generated by the linear model-predictive controller. Left side of the dashed line: P controller action. Right side of the dashed line: MPC controller action.

As seen in figures 4-7 and 4-8 the MPC controls the process with virtually no error based

on the LPV model of the nonlinear plant. In both composition and temperature control, a lag in the response can be observed. This is induced by the controller while tracking the temperature, that takes sample every 15 seconds, therefore, the effect of the measurement delay is seen on the plant.

The reflux controller allows for tracking of the water composition in the accumulator stage. The control action can be seen in figure 4-9. At first the P-level controller keeps $\Re = 0.95$. Then, it hands over the control of the reflux ratio to the MPC, which very briefly sets \Re close to zero to increase the composition. The reflux is varied every 15 seconds (sample time) during the instances when there is a larger offset between the reference trajectory and the controlled composition. The final composition of water attained is 97% due to the presence of small amounts of propylene glycol (water and propylene glycol form an azeotrope, point at which complete separation is impossible), shown in figure 4-7.

However, the main species (polymer and water) in the reactive distillation process to be separated are chemically very different, which is why the separation attains such high values of purity. High reflux ratios favor separation, while low reflux ratios benefit the yield (Varzakas and Tzia, 2014). Note that in figure 4-9, the MPC is rather favoring the throughput of distilled water with reflux ratios mostly below 0.5, due to the good separation obtained. Towards the end of the simulation, the reflux ratio is increased to values closer to 1 to control more tightly the amount of propylene glycol flowing in the accumulator.

In figure 4-10, the moles of water and proplyene glycol are shown. Here it is clearly observed that the number of moles of water starts at 0, followed by a steady and rapid increase of the concentration of pure water. Close to the end of the process, a small amount of propylene glycol can be seen.

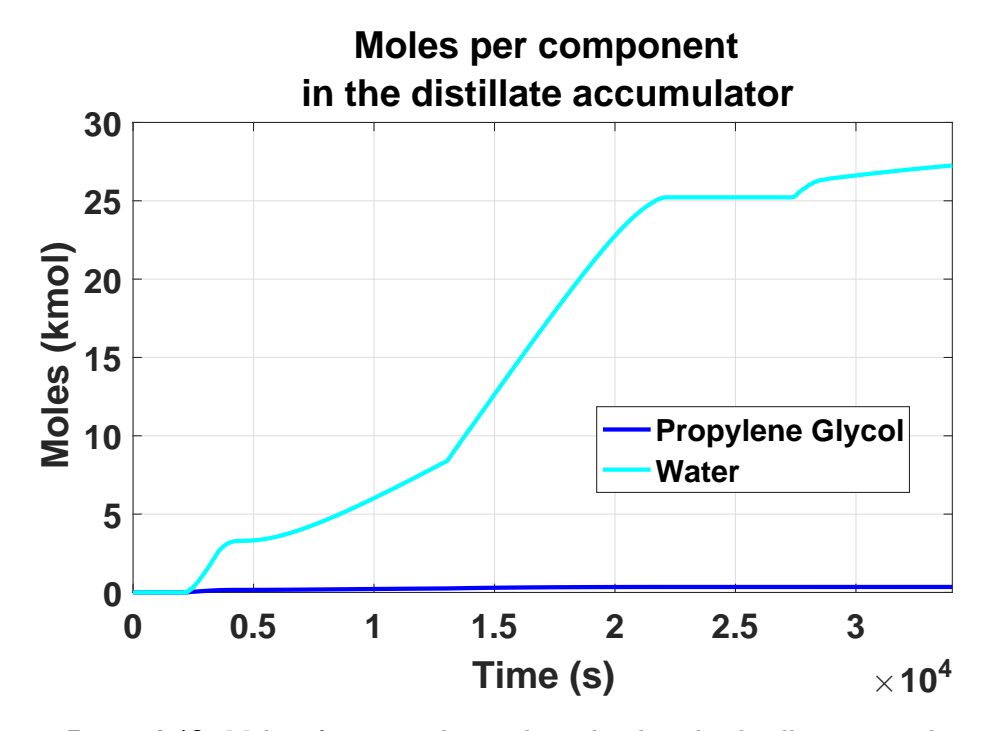


Figure 4-10: Moles of water and propylene glycol in the distillate accumulator

On the other hand, the temperature tracked in figure 4-8 with little error (= 0.1 K). This is done at the expense of a large control action (100 ~ -1000 kW). However, the heat duty of the process remains almost constant during most of the operation at 100 kW. This constant supply of heat is explained by the energetic contribution of the reaction, which provides with enough energy so that Q_{in} can be kept constant. Another reason for the low value of heat duty is the fact that the reflux ratio is set at values lower than 0.5 during great part of the process. Hence, the effect of the refluxed liquid on the reactor temperature is negligible. It only gets noticeably affected when $\Re > 0.5$, in which case, the MPC lowers the value of Q_{in} to -1000 kW to subtract heat from the reactor, tracking the temperature while rejecting any possible disturbance.

In figure 4-11, the composition of reactants water, propylene glycol and maleic anhydride, as well as products water and polymer are displayed. It can be seen that the water and the other reactants are consumed by means of the reaction. The maleic anhydride is consumed very quickly while the propylene glycol consumes more slowly. At the same time, saturated polymer and more water are generated in the reactor. Finally, the number of moles of water in the reactor decreases. The removal of water is achieved following the temperature trajectory, which stays close to the mixtures boiling point. The polymer can be extracted from the reactor and the water drew at the top of the column can be recovered to be used in a new batch run. The final number of moles of polymer is 18.05 kmol = 1481.4 kg

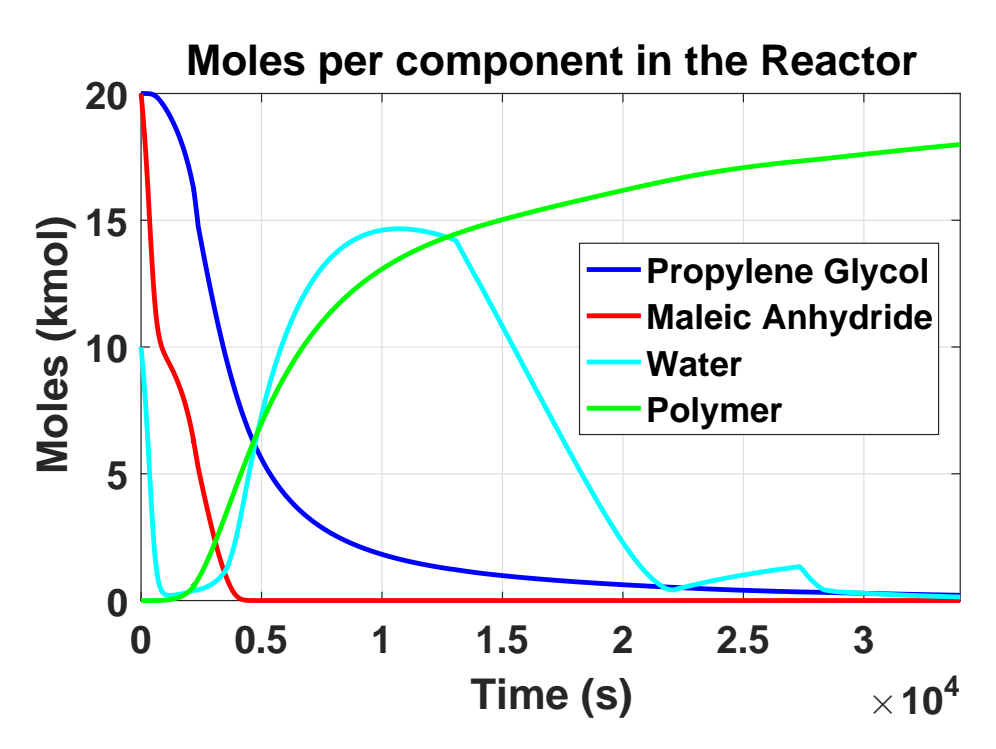


Figure 4-11: Moles of reactants and products in the reactor

It is also worth noting that the control of the distillate composition with the reflux ratio largely perturbs the controlled dynamics of the reactor temperature. Therefore, the MPC must give a higher priority to the temperature tracking while rejecting any disturbance quickly, because it is the state that governs the evaporation and removal of water from the reactor.

In general, the performance of the LPV-MPC conforms to the requirements and functions sufficiently well under the operating conditions set for the case study of the reactive batch distillation column. Additionally, the LPV-MPC takes an average of 0.95454 seconds to compute the optimum of the minimization problem.

4-3-4 Nonlinear Model Predictive Control for the Reactive Batch Distillation Process

Nonlinear model predictive control (NMPC) has gained more attention as a powerful and useful control technique, especially in process industry, due to the nonlinear and coupled nature of the dynamics involved in it. The use of nonlinear models in MPC arises by the possibility to improve forecasting quality which translates in a better control performance (Tyagunov, 2004). These nonlinear models are particularly beneficial for systems operated over large regions of the state space such as batch and semibatch processes, frequent product grade changes or processes subject to large disturbances, as they capture the detailed behavior of the plant under any operating condition. These nonlinearities are handled by NMPC, which in essence optimizes a cost function subject to a nonlinear model.

The use of nonlinear models in the MPC technique causes, in general, a loss of convexity. This makes the search and computation of a solution much more difficult, and in many cases, global optimality is not guaranteed, because the nonlinear function might have several local minima. Therefore, its practical implementation has remained very limited despite its potentiality as a control technique.

For the reactive batch distillation column discussed in our case study, a simple NMPC will be developed to compare its performance against the LPV-based MPC. This will allow the assessment of the quality of the LPV-based MPC, given its rather simple underlying model.

Consider the following objective function based on the one presented in (Allgöwer and Zheng, 2000):

$$\Phi_k = \int_{t_0}^{t_f} \mathbf{J}(x, u) dt = \int_{t_0}^{t_f} \left(||y(k+t) - y_{ref}(k+t)||_{\mathbf{Q}}^2 + ||u(k+t)||_{\mathbf{R}}^2 \right) dt$$
(4-103)

We seek the first control move $u^{\text{opt}}(t)$ of the sequence $\{u^{\text{opt}}(t_0), \dots, u^{\text{opt}}(t_f)\}$, which is a solution to the following optimization problem:

$$\min_{u^{\text{opt}}(t_0),\dots,u^{\text{opt}}(t_f)} \Phi_k \tag{4-104a}$$

s.t.
$$\dot{x} = f(x, u)$$
 (4-104b)

$$y = h(x, u) \tag{4-104c}$$

$$\frac{d\Phi}{dt} = \mathbf{J}(x, u) \tag{4-104d}$$

$$u_{min} \le u \le u_{max} \tag{4-104e}$$

where (4-104b) corresponds with the nonlinear model of the reactive batch distillation column developed in (4-37)–(4-48). The output (4-104c) corresponds with the same outputs

chosen for the LPV-based MPC, described in (4-71) and (4-73), respectively. The constraints on the input in (4-104e) were set to $u_{min} = \begin{bmatrix} \mathfrak{R}_{min} = 0 \\ Q_{in_{min}} = -1000 \text{ kJ} \end{bmatrix}$ and $u_{max} = \begin{bmatrix} \mathfrak{R}_{max} = 1 \\ Q_{in_{max}} = 100 \text{ kJ} \end{bmatrix}$.

To lower the computational complexity of the nonlinear optimization problem, the input was assumed to be piecewise constant. The process batch time was divided in n_s intervals of same length Δt . The NMPC solved the optimization problem at every Δt , implementing a precomputed constant input. In figure 4-12, a scheme of the optimization procedure is depicted.

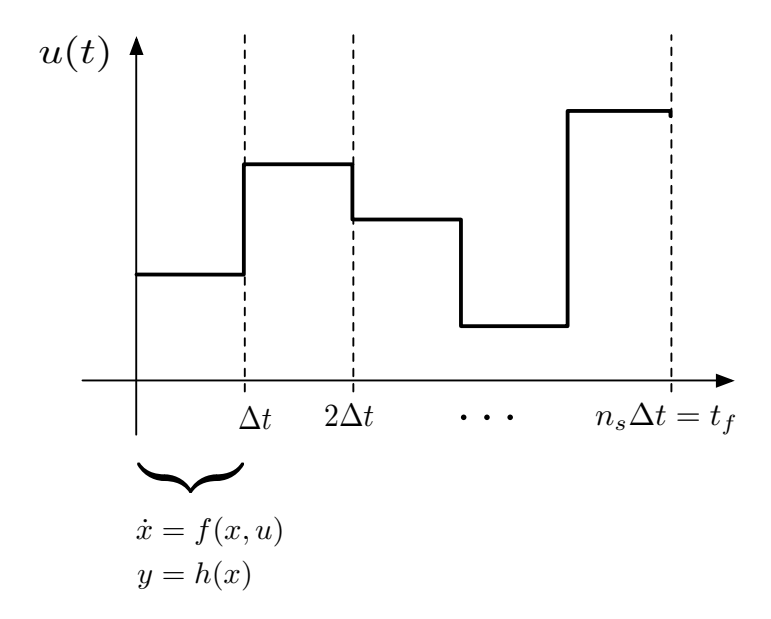


Figure 4-12: Scheme of nonlinear optimization procedure assuming piecewise constant inputs

The number of intervals was set to 10, i.e. $n_s=10$ and since $t_f\approx 35000~{\rm s}=9.7~{\rm h}$, every $\Delta t=3500~{\rm s}$. Additionally, the error is penalized with the weight matrix ${\bf Q}$. Similarly to the linear MPC case, the entries were chosen to penalize more the temperature rather than the distillate composition, because the temperature trajectory allows for the complete evaporation of the water in the reactor. Nonetheless, high penalization was not required as the NMPC was using the complete and exact model of the plant; hence there was no model-plant mismatch in this case. The matrices ${\bf Q}$ and ${\bf R}$ are:

$$\mathbf{Q} = \begin{bmatrix} 1 & 0 \\ 0 & 10 \end{bmatrix}, \ \mathbf{R} = \begin{bmatrix} 1 & 0 \\ 0 & 1 \end{bmatrix}$$

The nonlinear MPC is simulated using the whole nonlinear model of the plant for the reference tracking. It was implemented in the computer with the same characteristics described in the linear MPC. The controller achieves tracking with no virtual error because there is no the model-plant mismatch. This can be seen in figure 4-13 and 4-14. The control actions are less

varied than in the linear MPC, due to the piecewise constant assumption of the control input. Moreover, the division in the n_s intervals yields only n_s control moves along the batch time; thus, the plant is controlled with 10 input signals. This is possible because for the NMPC case, there is no model-plant mismatch. Also, the control actions taken by the nonlinear controller have less magnitude and it changes are less aggressive. The reflux ratio is above 0.5 most of the time, avoiding a rapid increase of the concentration of water in the distillate accumulator, whereas the heat input varied around $50-52~\rm kJ$ to perform reference tracking of the temperature signal. Nevertheless, this behavior is expected, as the NMPC has full knowledge of the plant model and can perform a better prediction. The control actions taken by the nonlinear model predictive controller can be seen in figure 4-15.

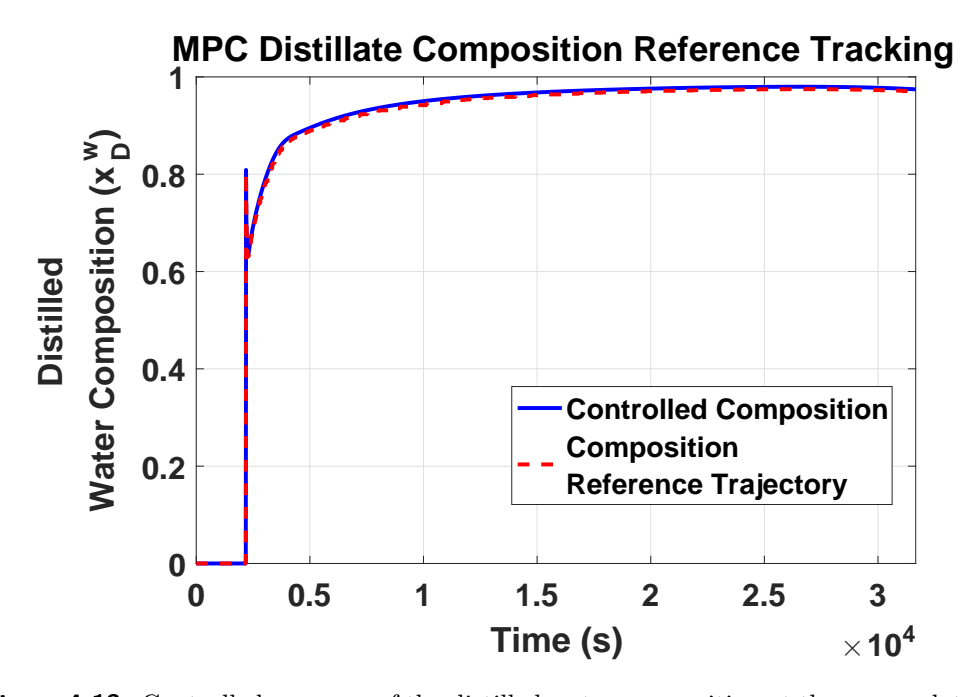


Figure 4-13: Controlled response of the distilled water composition at the accumulator stage (blue solid line) vs. Distilled water composition reference trajectory (red dashed line).

However, the time to compute the optimal input is far larger than the time consumed with the linear MPC. The nonlinear MPC takes an average of 12453 seconds to calculate the optimum of the nonlinear minimization problem given the non-convex nature of the problem. This time increases quickly if the diagonal entries in the weight matrix \mathbf{Q} were increased to values larger than 1. This amount of time is notably higher than that of the linear MPC; this evident improvement is thanks to the use of a convex function as well as the use of only the equations of the dynamics of interest.

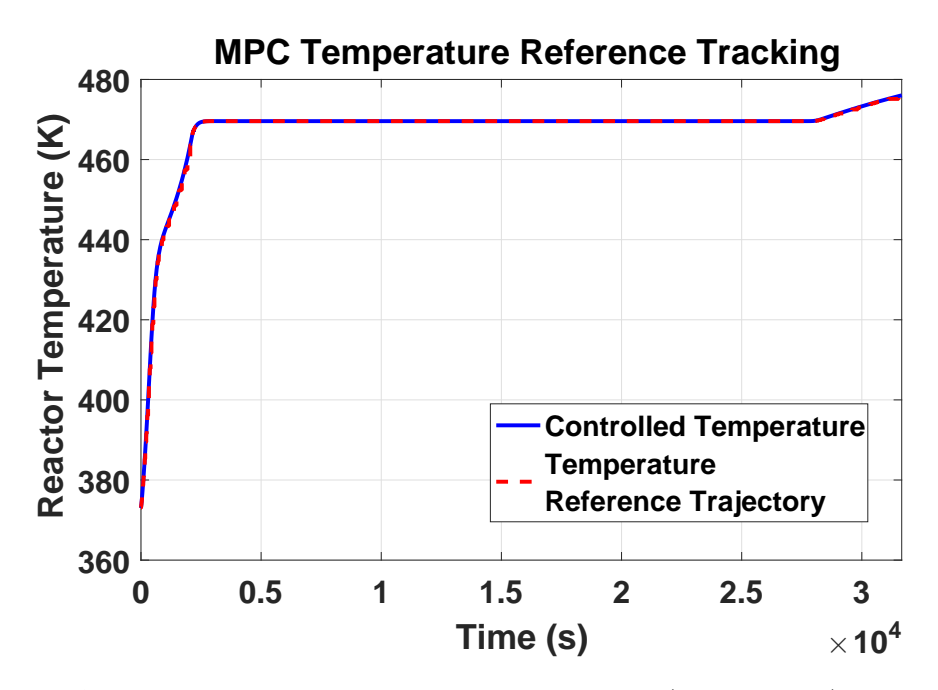


Figure 4-14: Controlled response of the reactor temperature (blue solid line) vs. Temperature reference trajectory (red dashed line).

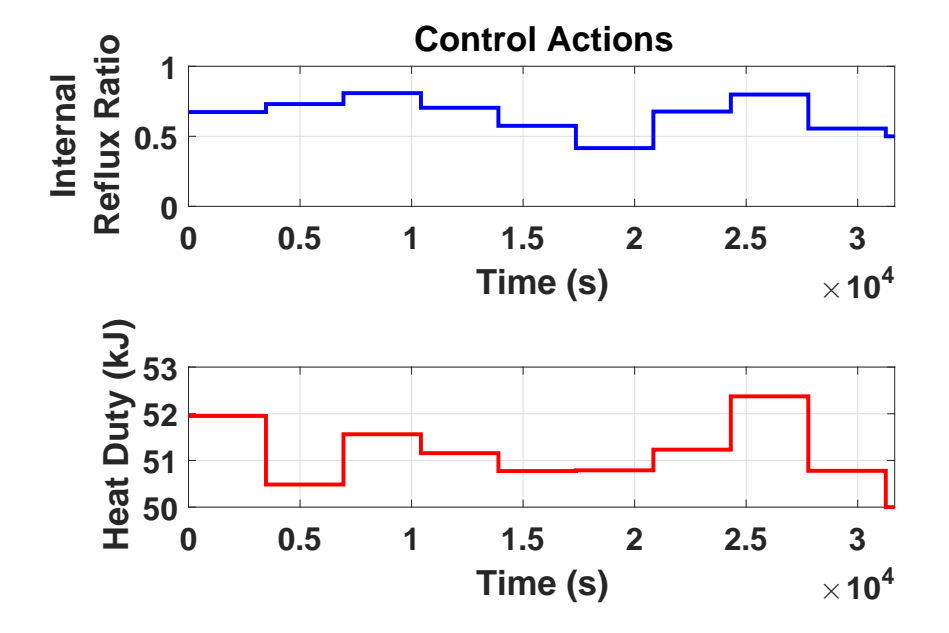


Figure 4-15: Control actions generated by the nonlinear model-predictive controller.

The evolution of moles in the reactor under the NMPC is very similar to that under the linear MPC. This can be seen in figure 4-17. However, the production of water in the reactor is much less in the nonlinear case because of the perfect tracking; this is achieved due the non-existing model-plant mismatch. This also allows for an smoother removal of water from the reactor. The small bump in the number of moles in the reactor towards the end of the batch

time seen in the linear case is not observed for the nonlinear case. The final yield of polymer with the NMPC was of 18 kmol = 14477.3 kg. In the case of the distillate accumulator under the NMPC, the evolution of moles is again similar to the linear case. Here, nevertheless, a larger accumulation of propylene glycol can be seen due to the tight control over the reactor temperature. Since the temperature is perfectly tracked, it allows for the vaporization of the water and a larger portion of the propylene glycol (azeotrope) than in the linear case. This is observed in figure 4-16.

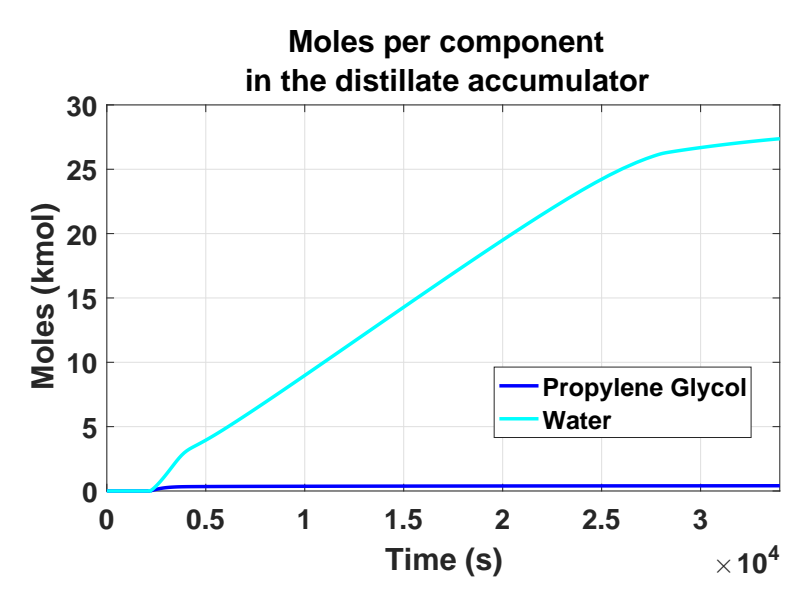


Figure 4-16: Moles of water and propylene glycol in the distillate accumulator

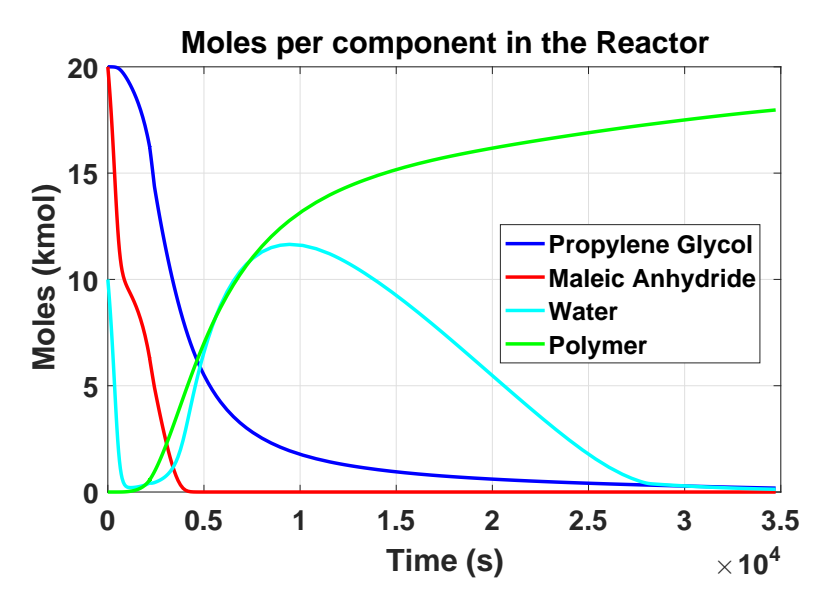


Figure 4-17: Moles of reactants and products in the reactor

Conclusions and Future Work

The extent transformation is an attractive approach to develop models for control for processes in liquid-phase where chemical reaction is involved. However, as shown in (Amrhein et al., 2010), the extent transformation can be also employed for process systems where no chemical reaction is present; only with independent inlets and outlets streams. Moreover, the theory can be utilized on systems where two phases coexist (liquid and gas) with independent inlet and outlet streams Bhatt et al. (2010). This work used these results to extend the extent transformation to a multiphase process with dependent inlet and outlet streams.

The extent transformation allows to obtain a decoupled representation of the effects or contributions in the process model. The nice feature about this transformation is that the new transformed states do have physical meaning, which could serve for process monitoring purposes. Furthermore, the plant's rigorous nonlinear model does not have to be linearized around an operating point or trajectory; hence, the transformed model preserves the information of the original one. This is of especial importance to develop accurate model-based controllers.

Moreover, splitting the dynamics of the plant gives additional freedom to combine or discard the transformed states for control purposes. For example, the reactor temperature (T_6) , the extent of reaction (x_r) and the extent of outlet (x_{out}) were combined together to compute Z, while x_{in} was discarded from the representation since it was not relevant for the control objective. Without this decoupling property of the transformation, one would have to use all the variables, resulting in nonlinear control techniques.

In the case studies presented, the extent transformation always allowed for certain mathematical manipulations (in particular when the energy balance was included) to obtain a linear parameter-varying model from the original nonlinear model. For the first case study (CSTR), given the simplicity of the process, an LQR control scheme has been developed using the obtained LPV model with satisfactory results. On the other hand, for the more complicated case study of the reactive batch distillation column, the extent transformation again, allowed for a simpler representation of the reactor temperature. This provided an advantage from the modeling and control point of view, because it is in the reactor where most of nonlinearities

are present, and the most difficult to recast in a linear-like form. For the distillate accumulator stage, a simple state-feedback linearization technique was employed. The combination of these two dynamics resulted again in an LPV system which was efficiently solved using a linear MPC, with very good results.

Despite the advantages and good capabilities of the extent transformation, it also has certain limitations. The approach uses left null spaces to compute orthogonal matrices, therefore, it requires that the matrices in the model are full-column rank and linearly independent between them, conditions that are not always possible to fulfill. These limitations can be circumvented in most cases by using matrix decomposition techniques like SVD or QR factorization responses to avoid rank-deficiency during the calculations.

Additionally, the transformation requires the availability of the number of moles in the system. This quantity, in practice, cannot always be measured; thus, its estimation is critical for the implementation of this approach. On this matter, the LPV models derived from the extent transformation, also depend of several parameters that are not always available from measurements. Hence, although it was out of the scope of this work, the model-based estimation of these varying parameters is suggested for future work, as it becomes of utmost relevance to update the model during the control strategy implementation.

The linear MPC developed with the extent-based model gives a very good performance tracking the reference trajectories imposed to the system. The capability of the extent representation in transforming the nonlinear energy balance to a linear parameter-varying equation, made possible the implementation of the linear MPC solving a convex quadratic programming problem. On the other hand, without the manipulations made possible with the extent transformation, the plant model is a set of stiff nonlinear differential equations. Hence, the NMPC must be implemented, taking into account the whole nonlinear model. Despite the reference tracking capabilities provided by both, the linear and nonlinear MPC, the NMPC is way more computationally expensive (larger calculation time) due to the non-convex nature of the optimization problem, while the linear MPC obtained almost the same performance in much lesser time.

The linear MPC based on the LPV extent representation could be a well-suited solution to combine rigorous models with linear model-based control techniques in process industry. This might also facilitate the implementation of MPC, in the quest to improve the suboptimal performance given by the PID controllers that still dominate much of the process industry scope.

Furthermore, regarding the MPC design, the reference trajectories were obtained maximizing the removal of water in the reactor stage. This can push the process to its operation limits; hence, a non-conservative choice of a control horizon N_h or weight matrices \mathbf{Q} and \mathbf{R} can rapidly make the system unstable or introduce very aggressive control to steer the system to the final state too quickly. For this reason, it is also recommended to compute the feasible and terminal sets of the MPC to improve the results presented herein.

Bibliography

- H. Ahn, K. S. Lee, M. Lee, and J. Lee. Control of a reactive batch distillation process using an iterative learning technique. *Korean Journal of Chemical Engineering*, 31(1):6–11, 2013.
- M. Al-Arfaj and W.L. Luyben. Comparison of alternative control structures for an ideal two-product reactive distillation column. *Industrial and Engineering Chemistry Research*, 39:3298–3307, 2000.
- M. Al-Arfaj and W.L. Luyben. Control of ethylene glycol reactive distillation column. *AIChE journal*, 48(4):905–908, 2002.
- M. Al-Arfaj and W.L. Luyben. Comparative control study of ideal and methyl acetate reactive distillation. *Chemical Engineering Science*, 57(24):5039–5050, 2002a.
- F. Allgöwer and A. Zheng. *Nonlinear model predictive control*, volume 26, pages 129–142. Birkhäuser, 2000.
- M. Amrhein, N. Bhatt, B. Srinivasan, and D. Bonvin. Extents of reaction and flow for homogeneous reaction systems with inlet and outlet streams. *AIChE Journal*, 56(11):2873–2886, 2010.
- S. Athimathi and T.K. Radhakrishnan. Control system design for a single feed ETBE reactive distillation column. *Chemical engineering & technology*, 29(10):1137–1154, 2006.
- L. S. Balasubramhanya and F. J. Doyle III. Nonlinear model-based control of a batch reactive distillation column. *Journal of Process Control*, 10(2–3):209–218, 2000.
- D.A. Bartlett and O.M. Wahnschafft. Dynamic simulation and control strategy evaluation for mtbe reactive distillation. *Chemical Technology Bedfordview*, pages 5–9, 1999.
- N. Bhatt, M. Amrhein, and D. Bonvin. Extents of reaction, mass transfer and flow for gasliquid reaction systems. *Industrial & Engineering Chemistry Research*, 49(17):7704–7717, 2010.
- B. H. Bisowarno, Y-C. Tian, and M. O. Tadé. Combined gain-scheduling and multimodel control of a reactive distillation column. Hong Kong, 2003. IFAC ADCHEM.

D. Bonvin. Control and optimization of batch processes. *IEEE control systems*, 26(6):34–45, 2006.

- I-L Chien, K. Chen, and C.-L. Kuo. Overall control strategy of a coupled reactor/columns process for the production of ethyl acrylate. *Journal of Process Control*, 18(3):215–231, 2008.
- S. Engell and G. Fernholz. Control of a reactive separation process. *Chemical Engineering and Processing: Process Intensification*, 42(3):201–210, 2003.
- S. Grüner and A. Kienle. Equilibrium theory and nonlinear waves for reactive distillation columns and chromatographic reactors. *Chemical Engineering Science*, 59(4):901–918, 2004.
- A. K. Jana and R. K. Adari. Nonlinear state estimation and control of a batch reactive distillation. *Chemical Engineering Journal*, 150(2–3):516–526, 2009.
- R. Kawathekar and J. Riggs. Nonlinear model predictive control of a reactive distillation column. *Control Engineering Practice*, 15(2):231–239, 2007.
- R. Khaledi and B.R. Young. Modeling and model predictive control of composition and conversion in an etbe reactive distillation column. *Industrial & engineering chemistry research*, 44(9):3134–3145, 2005.
- A. Kumar and P. Daoutidis. Modeling, analysis and control of ethylene glycol reactive distillation column. *AIChE Journal*, 45(1):51–68, 1999.
- M.V.P. Kumar and N. Kaistha. Evaluation of ratio control schemes in a two-temperature control structure for a methyl acetate reactive distillation column. *Chemical Engineering Research and Design*, 87(2):216–225, 2009.
- H-Y Lee, H-P Huang, and I-L Chien. Control of reactive distillation process for production of ethyl acetate. *Journal of Process Control*, 17(4):363–377, 2007.
- W.L. Luyben. Practical distillation control. Springer Science & Business Media, 2012.
- R. Monroy-Loperena, E. Perez-Cisneros, and J. Alvarez-Ramirez. A robust PI control configuration for a high-purity ethylene glycol reactive distillation column. *Chemical Engineering Science*, 55(21):4925–4937, 2000.
- R. Monroy-Loperena and J. Álvarez Ramírez. Output-feedback control of reactive batch distillation columns. *Industrial and Engineering Chemistry Research*, 39:378–386, 2000.
- R.H. Perry and G.W. Green, R. Perry's chemical engineers' handbook. McGraw-Hill Professional, 2008.
- K. J. Jithin Prakash, D. S. Patel, and A. K. Jana. Neuro-estimator based GMC control of a batch reactive distillation. *ISA Transactions*, 50:357–363, 2011.
- M. Sakuth, D. Reusch, and R. Janowsky. Reactive distillation. In *Ullmann's Encyclopedia of Industrial Chemistry*, volume 31. Wiley-VCH, 2008.

M. Shah, E. Zondervan, M. Oudshoorn, and A. de Haan. Reactive distillation: an attractive alternative for the synthesis of unsaturated polyester. In *Macromolecular Symposia*, volume 302, pages 46–55. Wiley Online Library, 2011.

- S. Skogestad. Chemical and energy process engineering. CRC press, 2008.
- M. G. Sneesby, M. O. Tadé, R. Datta, and T. N. Smith. ETBE synthesis via reactive distillation. 2. dynamic simulation and control aspects. *Industrial and Engineering Chemistry Research*, 36:1870–1881, 1997.
- M. G. Sneesby, M. O. Tadé, and T. N. Smith. Two-point control of a reactive distillation column for composition and conversion. *Journal of Process Control*, 9(1):19–31, 1999.
- E. Sørensen and S. Skogestad. *Batch Processing Systems Engineering*, chapter Control Strategies for a Combined Batch Reactor/Batch Distillation Process, pages 274–294. Springer Berlin Heidelberg, 1996.
- E. Sørensen, S. Macchietto, G. Stuart, and S. Skogestad. Optimal control and on-line operation of reactive batch distillation. *Computers and Chemical Engineering*, 20(12):1491–1498, 1996.
- Y-C. Tian, F. Zhao, B.H. Bisowarno, and M. O. Tadé. Pattern-based predictive control for ETBE reactive distillation. *Journal of Process Control*, 13(1):57–67, 2003.
- N.Q Tran. Tuning model-based controllers for autonomous maintenance. PhD thesis, Eindhoven University of Technology, 2015.
- R-C Tsai, J-K Cheng, H-P Huang, C-C Yu, Y-S Shen, and Y-T Chen. Design and control of the side reactor configuration for production of ethyl acetate. *Industrial & Engineering Chemistry Research*, 47(23):9472–9484, 2008.
- A. A. Tyagunov. *High-performance model predictive control for process industry*. PhD thesis, Technische Universiteit Eindhoven, 2004.
- J.E. Vandezande, D.A. Vander Griend, and R.L. DeKock. Reaction extrema: Extent of reaction in general chemistry. *Journal of Chemical Education*, 90(9):1177–1179, 2013.
- T. Varzakas and C. Tzia. Food engineering handbook: food engineering fundamentals, pages 351–352. CRC Press, 2014.
- N. Vora and P. Daoutidis. Dynamics and control of an ethyl acetate reactive distillation column. *Industrial & engineering chemistry research*, 40(3):833–849, 2001.
- S-J Wang, D-S-H Wong, and E-K Lee. Effect of interaction multiplicity on control system design for a mtbe reactive distillation column. *Journal of Process Control*, 13(6):503–515, 2003.

Glossary

List of Acronyms

ANN Artificial Neural Network

CSTR Continuous Stirred-Tank Reactor

EtAc Ethyl Acetate

ETBE Ethyl Tert-Butyl Ether

LPV Linear Parameter Varying

LQR Linear Quadratic Regulator

MGS Model Gain-Scheduling

MPC Model Predictive Control

MTBE Methyl Tert-Butyl Ether

NMPC Nonlinear Model Predictive Control

NPI Nonlinear Proportional-Integral

NRTL Non-Random Two-Liquid

PI Proportional-Integral

PID Proportional-Integral-Derivative

QP Quadratic Programming

RBD Reactive Batch Distillation

RD Reactive Distillation

Master of Science Thesis

Carlos Samuel Méndez Blanco

SISO Single-Input/Single-Output

UNIQUAC Universal QuasiChemical

VLE Vapor-Liquid Equilibrium

List of Symbols

α	Thermal Diffusivity
----------	---------------------

- γ Liquid activity coefficient
- λ Discounting factor of initial conditions in the reactor
- μ Input from feedback linearization
- $\nu_{s,r}$ Stoichiometric coefficient for the s-th species in r
- ϕ Gas fugacity coefficient
- ρ Density
- au Time constant of the system
- au_{30} Portion of the reaction and inlet invariant spaces occupied by the initial conditions
- θ Parameter vector of the LPV system
- Vapor-Liquid composition ratio
- ς Approximation of T_6 by Z
- ξ General symbol for the extent of reaction
- ζ Overall mass transfer rate
- ζ_{ql} Gas-to-liquid mass transfer rate
- ζ_{lg} Liquid-to-gas mass transfer rate
- \bar{v} Average bulk velocity
- ΔH_f^{\ominus} Standard enthalpy of formation
- ΔH_{rxn} Reaction heat
- ΔH_{vap} Enthalpy of vaporization
- $\ell(t)$ Level of distillate in the accumulator
- \hat{Q} Matrix spanning the range space of \mathcal{Z}
- B Selection matrix of the most volatile components
- Henry's coefficient
- \mathcal{I} Set of variables independent to the reaction dynamics
- \mathcal{J} Mass transfer rate
- \mathcal{R} Set of independent reactions
- \mathcal{T} Block matrix of orthogonal transformation matrices
- \mathcal{T}_0 Block matrix of orthogonal transformation matrices with discounted initial conditions
- $\mathcal{T}_1^{\mathsf{T}}$ Transformation matrix of the reaction space
- $\mathcal{T}_2^{\mathsf{T}}$ Transformation matrix of the inlet space
- $\mathcal{T}_3^{\mathsf{T}}$ Transformation matrix of the reaction and inlet invariant space

 \mathcal{T}_{1_0} Transformation matrix of the reaction space with discounted initial conditions n_0

- \mathcal{T}_{20} Transformation matrix of the inlet flow space with discounted initial conditions n_0
- \mathcal{T}_{3_0} Transformation matrix of the reaction and inlet flow invariant space with discounted initial conditions n_0
- \mathcal{V} Reaction mixture volume
- \mathcal{Z} Vector of parameters of Z
- \mathfrak{b} Generating matrix of \mathbb{B}
- Reflux ratio
- Z Change of variable
- A Vapor-Liquid molar flow ratio
- a Pole placement variable
- C_p Heat capacity
- D_x Liquid diffusion coefficient
- D_y Vapor diffusion coefficient
- E_a Activation energy of the reaction
- $E_{m,\pi}$ Selection matrix
- F Total molar flow
- f_i Molar composition in the feed of the *i*-th chemical component
- H_j Vapor enthalpy in the j-th stage
- h_i Liquid enthalpy in j-th stage
- k Chemical kinetic constant
- K_q Overall mass transfer coefficient based on the gas
- K_l Overall mass transfer coefficient based on the liquid
- k_o Preexponential factor in the Arrhenius law
- L Liquid Molar Flow
- M Total molar holdup
- m Reacting mixture mass
- M_D Total liquid holdup in the distillate stage
- $M_{w,\pi}$ Molecular weight matrix
- N Stoichiometric coefficient matrix
- n Number of moles
- n_0 Moles initial conditions
- N_h Prediction horizon
- n_s Time interval
- o* Operating point of linearization
- P Total pressure of the system
- p Number of independent inlet flows
- P_{sat_i} Saturation pressure
- Q Orthogonal matrix resulting from the QR factorization
- Q_N Matrix spanning the right null space space of \mathcal{Z}
- Q_{in} Heat flow

r	Reaction rate
R_I	Number of independent reactions
S	Number of chemical species in the reactor
T	Temperature
t	Time coordinate
T_h	Sampling Time
u_{in}	Inlet mass flow
u_{out}	Outlet mass flow
V	Vapor molar flow
v	Number of independent outlet flows
$W_{in,l}$	Inlet weight composition matrix in the liquid phase
$W_{in,l}^e$	Inlet weight composition matrix of the volatile components
$W_{m,\pi}$	Mass transfer matrix
$W_{out,g}$	Outlet weight composition matrix in the gas phase
$W^e_{out,g}$	Outlet weight composition matrix of the volatile components
x^*	Liquid molar composition at the equilibrium
x_C^{w}	Composition of the water in the condenser
x_D^{w}	Composition of the water in the distillate
x_i	Liquid molar composition of i -th chemical component
x_r	Extent of reaction
x_{inv}	Extents of reaction and inlet flow invariant dynamics
x_{in}	Extent of inlet flow
x_{io}	Combined extent of inlet and outlet
x_{out}	Extent of outlet flow
y^*	Liquid molar composition at the equilibrium
y_i	Vapor molar composition of i -th component
z	Spatial coordinate
z_r	Reaction variant
z_{inv}	Invariants of reactions and inlet flows
z_{in}	Inlet flow variant
K	Free pole location of x_D^{w}
Q	Error penalizing matrix
\mathbf{R}	Input penalizing matrix
π	Index of phase
f	Forward reaction
g	Gas phase
i	Index of the chemical component
j	Index stage of the distillation column
l	Liquid phase
r	Index of independent reaction

- $_{rev}$ Reverse reaction
- Index of the chemical species
- † Moore-Penrose pseudoinverse
- e Number of volatile species under operating conditions
- w Water